Chromatin Structure Changes During Terminal Differentiation and Cell Cycle Exit in *Drosophila melanogaster*

by

Yiqin Ma

A dissertation submitted in partial fulfillment
of the requirements for the degree of
Doctor of Philosophy
(Molecular, Cellular and Developmental Biology)
in the University of Michigan
2018

Doctoral Committee:

Associate Professor Laura Buttitta, Chair
Professor Kenneth M. Cadigan
Associate Professor Gyorgyi Csankovszki
Associate Professor Cheng-yu Lee
Associate Professor Andrzej Wierzbicki

myiqin@umich.edu

ORCID iD: 0000-0003-1083-0975

To my family and friends

For encouraging me along this journey and inspiring me in all of my pursuits.

Acknowledgements

A lot of people have accompanied me along my Ph.D. odyssey. My family, my professors and mentors, my colleagues and friends, without any of you, it would not be possible for me to finish all the work I have completed over the years. Now, as this special moment is eventually coming, I would like to take this opportunity to express my appreciation to you.

First and foremost, I owe my deepest gratitude to my advisor, Dr. Laura Buttitta. Laura is one of the most enthusiastic and energetic researchers I have ever seen. Laura has always been an inspiration and a role model for me in both research and life. Thinking of what she would do in the situation I have encountered has encouraged me to push through all of the ups and downs during these years. Being one of her first students, I am very fortunate to receive scientific training directly from her on a wide spectrum of subjects, from idea prioritization all the way to paper and grant writing. Working with Laura has always been both exciting and rewarding. She has provided me immeasurable guidance and enormous support to explore challenging topics and cutting-edge techniques for my research throughout the years. She spent countless hours helping with my presentations and editing my proposals and manuscripts. I also wish to express my sincerest thanks to Dr. Cheng-Yu Lee for sharing his rich knowledge and invaluable experience in cell biology research in *Drosophila*. I have benefited a great deal from all

the discussions and our joint lab meetings. My great thanks also go to Dr. Kenneth Cadigan, Dr. Gyorgyi Csankovszki and Dr. Andrzej Wierzbicki for providing me very insightful comments and invaluable advice on my dissertation work. In addition to my dissertation committee, I would like to thank Dr. Daniel McKay from UNC for kindly dedicating his expertise and experience in genetics and sequence analysis to my dissertation.

My sincere thanks go to my colleagues in the Buttitta Lab. I would like to specially thank Kerry Flegel, Dan “Rosaline” Sun, Kiriaki “Kiki” Kanakousaki and Olga Grushko for working closely with me since my first couple years in graduate school. As the “first cohort” of the lab, there are a lot of treasuring memories we share. My special thanks go to Shyama Nandakumar, Ajai Pulianmackal, Allison Box and Samuel Jamian-Stephan Church, working with you guys during the past few years has been amazing. I really appreciate you guys watching my back and generously providing all the assistance as I am working on my thesis. My thanks also go to all the undergrads who are working or have worked in the lab. Thank you all for all your help and laughter you’ve brought to me.

In addition, I would also like to thank the wonderful support team of our department, especially Mary Carr and Gregg Sobocinski. Thank you for being so patient and so helpful during all these years.

I would like to thank my dear friends in Ann Arbor and all around the world, with whom I have shared so much laughter and so many tears throughout my Ph.D. years.

Last but not least, my deepest gratitude goes to my family. They have provided me with their unconditional support and love throughout my life, and the best reason I can deal with all the frustrations and failures in researches is that I know there's always my family to back me up. I would like to thank my parents for doing everything possible to put me on the path to greatness. To my beloved husband Jincheng, thank you for always being there for me throughout such an unforgettable period of my life.

As it come to the end of the page, I would also want to thanks my special friends for keeping me company. Especially to Drs. Bobe, Bitao, Pangpang and Pipi, thanks for hugging my tears off during all my meltdowns.

As always, it is hard to have included everyone deserving thanks in such a short paragraph. Yet, the precious memories that we shared throughout my years in Ann Arbor are and will always be the sunshine of my life.

Table of Contents

List of Tables

List of Figures

Abstract

During development, the number of cell divisions must be precisely controlled in order to produce tissues of the correct shape, composition and size. The majority of cells complete their final cell cycle during a process called terminal differentiation, where cells acquire cell type specific characteristics. Most terminally differentiated cells will remain in a post-mitotic or G0 state permanently to carry out critical physiological functions in tissues and organs. The enforcement of cell cycle exit is thought to be critical for proper differentiation, but how these events are coordinated in most tissues remains unclear. Chromatin accessibility and organization plays a critical role in regulating gene expression during differentiation and changes in chromatin organization also occur upon entry into G0. In my thesis research I addressed how chromatin organization and accessibility changes during terminal differentiation and cell cycle exit in the *Drosophila melanogaster* (fruit fly) wing.

To examine the relationship between cell cycle exit and chromatin structure during terminal differentiation, I characterized the temporal changes in chromatin accessibility and gene expression during the process of terminal differentiation in the wing. This revealed changes in chromatin accessibility and gene expression that are coordinated with the transition from a proliferating to postmitotic state. To identify which changes are a consequence of cell cycle exit, I genetically disrupted cell cycle exit and examined the effects on chromatin accessibility and gene expression. This uncovered mutual cross-talk between a subset of genes in the wing terminal differentiation program and the cell cycle

machinery. However, most chromatin changes including those at cell cycle genes, appear to be developmentally controlled in a manner independent of cell cycling status.

Higher order chromatin organization such as the clustering of heterochromatin in the nucleus is also impacted by cell cycle exit and terminal differentiation. I found that heterochromatin clusters as cells exit the cell cycle and terminally differentiate. Heterochromatin associated modifications have been implicated in the silencing of cell cycle genes and facilitating G0. I rigorously tested this model and found that compromising heterochromatin-dependent gene silencing does not disrupt cell cycle exit. Instead, delaying or preventing cell cycle exit disrupts heterochromatin clustering and globally alters chromatin modifications, revealing that heterochromatin clustering during terminal differentiation is a consequence of cell cycle exit, rather than differentiation.

Chapter 1: Introduction[1]

Despite the vast variabilities in body size and shape, all metazoans start from a single zygotic cell. Metazoans achieve their complex and diversified body plans through coordinated amplifications in cell number and differentiation. The number of cell divisions or cell cycle is tightly controlled in order to obtain proper tissue and organ size. Terminal differentiation in most cell types is associated with a permanent exit from cell division. The coordination between cell cycle exit and terminal differentiation is crucial for proper development and organogenesis and the failure to stop dividing could result in uncontrolled proliferation, such as cancer. Therefore, it is pivotal to understand the underlying mechanisms governing cell cycle exit during terminal differentiation. In order to figure out how cell cycle exit is regulated, it is important to understand how cell cycle is regulated in actively proliferative tissues.

1.1 Cell cycle

Cell cycle is a series of ordered events where a mother cell duplicates its genetic materials, chromatin, and divides, producing two daughter cells with the same DNA content. Depending on the stages of DNA replication and separation, cell cycle can be

[1] Some of the elements from this chapter are modified from Ma, Y., Kanakousaki, K., & Buttitta, L. (2015). How the cell cycle impacts chromatin architecture and influences cell fate. *Frontiers in Genetics*, *6*, 19, doi: 10.3389/fgene.2015.00019.

further separated into 4 phases: Gap1 phase (G1), DNA synthesis phase (S), Gap2 (G2) phase and Mitosis (M). In G1, cells respond to environmental stimuli, make the decision of whether to proceed into S phase, assemble pre-replication complexes on origins where DNA replication will start and activate the expression of genes needed for subsequent S phase. In S phase, replication complexes pass through the whole genome and replicate the DNA. In G2, cells assess the integrity of replicated DNA and prepare for M phase entry by producing mitotic proteins. M phase is the final stage of cell cycle, where chromatin is condensed into chromosome and partitioned into two daughter cells by cytokinesis. The four phases of cell cycle are exquisitely regulated to ensure the faithful transmission of complete set of chromatin into daughter cells. In actively proliferating tissues such as early embryos, cells quickly go through G1-S-G2-M-G1 transitions to amplify cell populations.

1.2 Engine of the cell cycle: cyclins and Cyclin-dependent kinases

Given the periodic nature of the cell cycle, early researchers speculated that the regulators of cell cycle should also oscillate, at the time the biochemical details on cell cycle processes such as DNA replication were unknown. In 1983, Tim Hunt and his colleagues observed the gradual accumulation and abrupt disappearance of a protein during each cell division in sea urchin embryos. They named this protein cyclin [1]. The identification of the first cyclin preluded a series of important discoveries of the well conserved cell cycle regulation by cyclins and Cyclin-dependent kinases (Cdks).

Cdks are a class of specific serine/threonine kinases and their activation depends on the binding of their cognate cyclin partners. Cyclin determines Cdk substrate specificity as well as the subcellular localization of cyclin/Cdk complex. Due to the periodic degradation of cyclins, the activity of cyclin/Cdks also oscillates during the cell cycle and each cyclin/Cdk complex functions in a specific time window. The major cyclin/Cdks and their functioning periods are: CycD/Cdk4 or Cdk6 (CycD/Cdk4-6) in early G1; CycE/Cdk2 in G1-S, CycA/Cdk2 in S phase, CycA/Cdk1 in G2-M and CycB/Cdk1 in M phase (Fig. 1.1).

CycD/Cdk4-6 is activated by mitogenic signaling such as EGF/Ras and promotes G1-S transition [2–4]. The canonical model is that CycD/Cdk4-6 hypo-phosphorylates Retinoblastoma protein (RB), inhibitor of cell cycle gene transcription [5]. The phosphorylation of RB reduces its binding affinity to transcriptional factor complex E2F/DP. E2F/DP is the master transcriptional factor complex for cell cycle genes. The release of RB enables E2F/DP to activate *cycE* and *cdk2* expression, while CycE/Cdk2 can further hyper-phosphorylate RB, leading to its complete inactivation [6, 7]. This positive feedback loop between E2F/DP and CycE/Cdk2 prompts the accumulation of CycE/Cdk2 to pass the threshold required for DNA replication initiation and S phase entry.

However, in this prevailing model the role of CycD/Cdk4-6 in inactivating RB has been challenged recently. It is reported that in early G1, CycD/Cdk4-6 exclusively mono-phosphorylates RB and the mono-phosphorylated form of RB is still functional [8]. The result of this report suggests that CycD/Cdk4-6 promotes G1-S transition through alternative mechanisms instead of RB inactivation. This can be potentially achieved by

the role of CycD/Cdk4-6 in sequestering CycE/Cdk2 inhibitors p21 and p27, promoting cellular growth and directly interacting with specific transcriptional factors [9–11].

CycA is able to bind both Cdk2 and Cdk1, allowing it to function in more than one phase of the cell cycle [12]. Similar to CycE/Cdk2, CycA/Cdk2 promotes the onset of DNA replication in S phase [13]. Later in S phase CycA/Cdk1 starts to accumulate and regulates the completion of S phase by promoting late origin firing [14]. In G2, CycA/Cdk1 prevents the degradation of CycB and causes the accumulation of CycB/Cdk1 [15]. Once the level of CycB/Cdk1 passes a certain threshold, this complex promotes M phase entry by initiating nuclear envelope breakdown, chromatin condensation and mitotic spindle assembly [16–21]. The sequential activities of CycA and CycB ensure the smooth transition from G2 to M. Notably, in *Drosophila* CycA is the only essential mitotic cyclin and CycA seems to only pair with Cdk1 [15].

Cdk1 plays an essential role in M phase entry and its activity is modulated by kinase Wee, Myt1 and phosphatase Cdc25. Wee and Myt1 phosphorylate the Thr14 and Tyr15 residues of Cdk1, respectively, which inhibit Cdk1 activity [22]. The inhibitory phosphorylation on Cdk1 can be removed by phosphatase Cdc25. CycB/Cdk1 can in turn phosphorylate Wee, Myt1 to inhibit their function and also phosphorylate Cdc25 to further activate Cdc25 phosphatase function. The positive feedback loop between CycB/Cdk1 and Cdc25 eventually promotes M phase entry [23].

1.3 Antagonists of cyclin/Cdks: Cyclin-dependent kinase inhibitors

Cyclin-dependent kinase inhibitors (CKIs), as the name implies, bind and suppress cyclin/Cdk complexes. Based on their structure and targets, CKIs have been divided into two families. The INK4 (inhibitors of CDK4) family proteins exclusively bind to the monomeric form of Cdk4 and Cdk6 and constrain CycD/Cdk4-6 complex by competing with Cyclin D for Cdk binding. Four INK4 proteins have been discovered in mammals ($p16^{INK4a}$, $p15^{INK4b}$, $p18^{INK4c}$ and $p19^{INK4d}$), however, they have no homologs in *Drosophila* or yeast. The other Cip/Kip family proteins function more broadly and they suppress multiple cyclin/Cdk complexes such as CycE/Cdk2 and CycA/Cdk2. The Cip/Kip CKIs interact with both cyclins and Cdks and this family includes three members in mammalian cells ($p21^{Cip1}$, $p27^{Kip1}$ and $p57^{Kip2}$) and only one in *Drosophila* (Dacapo) [24]. Of the Cip/Kip CKI family proteins, p21 is the first and best characterized [25–27]. p21 is induced by p53 when cells are subject to γ irradiation. It suppresses CycE/Cdk2 activity and blocks G1/S transition as part of the DNA damage response [28]. The expression of p21 can also be developmentally regulated, independent of p53 [28]. p21 plays a critical role in cell cycle arrest and the deregulation of p21 has been found in multiple cancer types [29]. Although p21 suppresses CycE/Cdk2, the level of p21 can be regulated by CycE/Cdk2 in turn. CycE/Cdk2 phosphorylates p21 at Ser130, promoting its ubiquitination and subsequent degradation [30].

1.4 Proteolytic control of the cell cycle

Transitions between cell cycle phases depend on the abrupt degradation of cell cycle regulators. Most cell cycle regulators are targeted for degradation through the ubiquitin–proteasome system. Two large ubiquitin protein ligase complexes are

responsible for the proteolytic control of cyclins: SCF (Skp1/cullin/F-box protein)-related complexes and anaphase-promoting complex or cyclosome (APC/C) [31].

The SCF complex functions in multiple stages of the cell cycle and is composed of three core components: Skp1 (scaffold), Cul1 (scaffold), Rbx1 (containing RING finger and binds to ubiquitin conjugating enzyme). The substrate specificity is determined by another component called F-box protein. There are several F-box proteins, each recruiting specific set of targets and they are interchangeable in binding to the Skp1 subunit of the complex. Three F-box proteins are primarily responsible for the targeting of cell cycle regulators: Skp2, Cdt2 and Fbw7. Skp2 mediates the degradation of CycE/Cdk2 inhibitors $p21^{Cip1}$, $p27^{Kip1}$ and $p57^{Kip2}$ in the G1 phase to promote G1/S transition [31]. Cdt2 is mostly responsible for degradation in S phase and targets replication related proteins such as Cdt1 (a replication licensing factor), PCNA (DNA polymerase processivity factor), E2F and DNA polymerase η [32, 33]. The proteolytic control on these S phase regulators ensures that DNA replication only occurs once in one cell cycle [34, 35]. Fbw7 targets CycE as well as MYC, JUN and Notch for degradation [36, 37]. Due to its ability to degrade these proto-oncogenes, Fbw7 is also a tumor suppressor and is found to be mutated in numerous cancer types [37]. Notably, the efficiency of substrate ubiquitination by SCF complex is controlled by the binding affinity of F-box proteins and their substrates, which is further affected by the phosphorylation status of substrates. Typically, SCF targets are phosphorylated by Cdks, linking the proteolytic pathway with Cyclin/Cdks activity at specific cell cycle phase [34, 35].

APC/C is a giant ubiquitin-protein ligase, containing 11-13 subunits. The activator subunits are essential for the ubiquitination function of APC/C and two activators,

Cdc20/Fizzy and Cdh1/Fizzy-related are particularly important in cell cycle regulation. APC/C^{Cdc20} is responsible for the degradation of mitotic cyclins and is primarily active in mitosis. The binding of Cdc20 requires phosphorylation on multiple sites of APC/C core complex by Cdk1. Once activated, APC/C^{Cdc20} initiates the degradation of CycA and CycB. The destruction of mitotic cyclins occurs after peak Cdk1 activity, so this temporal delay prevents premature degradation of mitotic cyclins in early mitosis. In addition, when the level of Cdk1 activity drops, APC/C^{Cdc20} is deactivated and Cdc20 dissociates from APC/C core complex. Through this negative feedback loop between mitotic cyclins and APC/C^{Cdc20}, mitotic cyclins initiate their degradation, promote cells to exit from mitosis and finally deactivate APC/C^{Cdc20} [31, 38–40].

After exit from mitosis, cells need to enter G1 with low cyclin/Cdk activity so that growth factors and environmental signals can impinge on the decision to enter the next cell cycle. The low Cdk activity in early G1 is enforced by high APC/C^{Cdh1} activity [41]. Cdh1 can bind to APC/C core complex regardless of APC/C phosphorylation status. However, phosphorylation on Cdh1 itself by Cdks prevents Cdh1 from binding to APC/C. At the end of mitosis, the destruction of mitotic cyclins and dissociation of Cdc20 from APC/C enable Cdh1 to be dephosphorylated and replace Cdc20. In early G1, APC/C^{Cdh1} targets residual mitotic proteins such as Plk1 and Aurora A as well as Cdc20 to ensure a temporal gap before the next mitosis [41]. On the other hand, APC/C^{Cdh1} also targets Skp2, thus blocking the degradation of p21 and p27 to keep the level of CycE/Cdk2 activity low [41–43]. The activity of APC/C^{Cdh1} persists until G1/S transition when Cdh1 is deactivated by increasing G1 cyclin/Cdks [44].

1.5 Transcriptional control of the cell cycle

Similar to the regulation at the protein level, the transcription of cell cycle regulators also oscillates to ensure successful cell cycle progression. As briefly mentioned in the previous section, cell cycle gene expression is controlled by the interplay of transcription factor complex E2F/DP with its suppressor RB family proteins.

E2F/DP is a transcription factor complex and a master regulator of the cell cycle. It activates hundreds of cell cycle genes that execute important functions in different phases of the cell cycle, including cyclin/Cdks such as CycE, CycA, CycB, Cdk1 and Cdk2; DNA replication factors such as DNA polymerase α and proliferating cell nuclear antigen (PCNA); and also mitotic regulators such as Aurora A, Aurora B and Mad2 [45–48].

E2F/DP is a heterodimeric complex and contains one E2F family member protein and one DP family protein. In mammals, nine E2F proteins (E2F1, E2F2, E2F3a, E2F3b, E2F4-8) from eight E2F genes and three DP proteins (DP1, DP2/3, DP4) have been identified [49, 50]. All the E2F proteins share a highly conserved DNA binding domain. The high affinity binding of E2Fs to DNA requires partnering with DPs except for E2F7-8, which have an additional DNA binding domain [49]. The E2Fs can be generally divided into three groups based on their function as transcriptional activator or repressor. E2F1–E2F3a are strong transcriptional activators and are generally responsible for E2F target gene expression. Binding of RB repressor blocks their transactivation domain in the carboxy terminus of E2F, thus preventing the recruitment of basal transcription factor TFIID as well as co-activators [51]. E2F3b–E2F5 are passive repressors and the binding of RB family members can convert them into repressing E2F target gene expression. E2F

6–8 are considered as constitutive repressors of transcription and they repress gene expression independent of RB family members [49, 52].

The activity of E2F/DP transcriptional factor complex is heavily regulated by RB family members. Retinoblastoma protein (RB) is a negative regulator of the cell cycle and was the first tumor suppressor identified. This family contains two other members: p107 and p130. This family members are often referred to as pocket proteins because all three contain a conserved “pocket” domain that interacts with the LXCXE motif found in viral proteins and chromatin remodelers. The RB family proteins function as proliferation inhibitors through binding with E2F/DP and each of them preferentially associates with different subset of E2Fs: RB preferentially binds to E2F1-5 while p107 and p130 primarily associate with E2F3b-5 [49, 52].

Compared to mammals, the E2F/DP and RB families in *Drosophila melanogaster* are more streamlined. *Drosophila* has only one activator E2F (dE2F1), one repressor E2F (dE2F2), one DP and two pocket proteins, retinoblastoma family-1 (RBF1) and RBF2 [52]. Chromatin immunoprecipitation (ChIP) and genetic experiments in *Drosophila* have shown that dE2F1 and dE2F2 share almost all the binding sites on the genome, suggesting that the output of E2F target genes transcription is controlled by the interplay between dE2F1 and dE2F2 [48].

The transcriptional regulation of E2F/DP/RB on E2F target genes can be mediated by multiple chromatin modifiers or remodelers as co-factors. When free from pocket protein binding, activator E2F/DP is able to recruit histone acetyl transferase enzymes such as p300/CBP, GCN5, TRAPP and Tip60 and induce the hyper-acetylation on H3 and H4, which promotes gene expression [53–56]. When pocket protein is associated

E2F/DP, the pocket protein can recruit a variety of chromatin modifiers or remodelers to E2F target genes through the interaction between pocket domain and LXCXE motif. These co-repressors include BRM/BRG1, PcG, histone deacetylase 1 (HDAC1), PRMT5, SUV39H, HP1, mSin3B, DNMT1 and L3MBTL1 [57–68].

As mentioned earlier, the repression of RB on E2F/DP is dependent on the phosphorylation status of RB. RB protein contains 16 consensus Cdk phosphorylation sites. The unphosphorylated RB has high E2F binding affinity while hyper-phosphorylated RB cannot stably associate with E2F/DP. Individual mutation of the RB phosphorylation sites does not compromise RB's ability to block the cell cycle, suggesting that the interaction between RB and E2F is controlled at multiple sites [69, 70]. In early G1, CycD/Cdk4 mono-phosphorylates RB. Then the gradually accumulated CycE/Cdk2 hyper-phosphorylates RB, leading to the dissociation of RB from E2F/DP in late G1. The initial step of RB phosphorylation by CycD/Cdk4 is necessary because CycE/Cdk2 cannot use unphosphorylated RB as substrate [71]. Through the sequential activities of CycD/Cdk4 and CycE/Cdk2, cells are able to integrate mitogenic signaling with cell cycle decisions and constrain massive cell cycle transcription until late G1 when cells are committed to enter S phase [72]. Lastly, at the end of mitosis, protein phosphatase 1 (PP1) or PP2A dephosphorylates RB so that E2F/DP is repressed again and cells can enter G1 properly [73, 74].

1.6 Three states of G0

G0 is a cellular state where cells leave the cell cycle with G1 DNA content and rest in a post-mitotic state. Depending on the range of reversibility to re-enter the cell cycle, G0 can be divided into three states. Easily reversible G0, quiescence, is often considered as extended G1. In this state cells are temporarily arrested and readily responsive to external stimuli. It is commonly seen in nutrient starved tissue culture cells or resting stem cells. Upon mitogenic signaling such as adding back serum or wound healing stress such as tissue damage, cells will rapidly proliferate again. The irreversible G0, senescence, is permanent and not responsive to proliferative cues. This type of G0 normally occurs in aging tissues and is often referred to cellular senescence. Cellular senescence is considered to be triggered by chronic DNA damage response or telomere attrition, and is usually accompanied by morphological and metabolic changes [75, 76]. Senescence can also be induced by oncogene overexpression. By preventing proliferation senescence serves as a defense mechanism and turns the brake on during early stages of tumorigenesis [77]. The third type of G0 is prevalent during development. It occurs along with terminal differentiation and is selectively reversible. The G0 state is the final state for most differentiated cell types and in some cases is critical for cells to execute their specialized functions. The ability of terminal differentiated cells to re-enter the cell cycle is variable and dependent on both cell type and organism. For example, mammalian neurons and muscle cells have minimal, if any, proliferative potential while liver cells readily re-enter the cell cycle upon tissue damage. Some organisms possess high proliferative ability to re-enter the cell cycle in their terminally differentiated tissues, such as axolotl appendage [78] and zebrafish retina [79] while others such as most mammals do not.

1.7 Establishment of G0 through inhibiting Cdk activity

When a cell finishes mitosis, how does it decide whether to proceed with another cell cycle or enter G0? Work from tracking the proliferation-quiescence decision in single mammalian cells has provided insights that upon exit from mitosis, the cells that have higher residual level of Cdk2 activity from the previous cell cycle will commit into proliferation immediately while cells with low Cdk2 level will enter a G0-like state [80]. This work highlighted the central role of Cdk activity in determining G1 vs G0 entry and in fact, most reported G0 regulations converge towards Cdk activity control.

The level of the CKIs p21 and p27 is high in quiescent cells [80, 81]. Degradation of p21 or p27 promotes the G0 to G1 transition and cell cycle entry [80, 82, 83] while overexpression of p21 or p27 in some proliferating cells is sufficient to induce cell cycle arrest [80, 84]. p21 and p27 also contribute to G0 in terminal differentiation. For example, *p21*(-/-) mice have enhanced hippocampal neuron proliferation [85]. *p27*(-/-) mice enlarged body size with more cells in most tissues [86]. Notably, mutation of either *p21* or *p27* alone does not prevent cell cycle exit. It has been reported that even when all three Cip/Kip CKIs are compromised together, the interneurons of spinal cord still exit the cell cycle [87]. Studies in *Drosophila* also show similar results, where the loss of the sole Cip/Kip CKI, *dacapo* has minimal effects on G0 [88, 89]. These observations indicate that redundant mechanisms exist to regulate G0 in terminal differentiation.

APC/C^{Cdh1} complex has been shown to play an essential role in regulating G0 state in multiple species. CDH1 mutant yeast fail to enter quiescence during nutrients starvation,

while inactivation of APC/C subunit Apc2 in quiescent mouse hepatocytes induce cell cycle re-entry [41, 90]. In addition, Cdh1 could collaborate with other cell cycle inhibitors such as RB to promote G0 in terminal differentiation. In RB/Cdh1 double mutant *Caenorhabditis elegans*, cell cycle arrest is disrupted in the muscle cells [91]. Similar observation has been reported in *Drosophila* wings and eyes, where overexpression E2F/DP activator complex which potentially titrates away RB repressors in cdh1 mutant cells is able to bypass the robust cell cycle exit [92]. The regulation of G0 through Cdh1 may be achieved by targeting Skp2 for degradation, thus maintaining p21 and p27 level and inhibiting CycE/Cdk2 activity [41–43]. Cdh1 also targets the DNA replication complex licensing factor Cdc6 for destruction, and this perturbation of the replication complex assembly factor may contribute to G0 as well [41].

1.8 Establishment of G0 through transcriptional repression

G0 entry is accompanied by the repression of cell cycle gene expression [84, 92–94]. The RB family proteins are indispensable in silencing E2F targets and studies in mammalian cells have unveiled that RB proteins are utilized differently under different contexts. In G1, p107 and RB are abundant and associate with the E2F/DP complex to silence cell cycle genes. In quiescent cells, p130 is highly expressed while RB is maintained at very low protein levels and p107 is almost undetectable [46, 95, 96]. In mammals, the majority of E2F complexes in G0 are thus formed by p130 and E2F4. Together with several other proteins including homologs of the *C. elegans* multi-vulval class B (MuvB) gene products, they form a transcriptional repressor complex called DREAM (DP, Rb-like, E2F, and MuvB) and repress E2F target genes during G0 [7, 96].

The DREAM complex plays an important role in G0 control and perturbation of the DREAM complex disrupts G0 both in quiescent mammalian tissue culture cells and differentiated chondrocytes [96–98]. This complex is evolutionarily conserved and in *Drosophila* it consists of RBF1/RBF2, dE2F2, dDP, p55/CAF1, Myb and Myb-interacting proteins, called dREAM [52, 99] (Fig. 1.2).

1.9 Chromatin organization at multiple levels

Since the earliest observations of cells undergoing mitosis, it has been clear that there is an intimate relationship between the cell cycle and chromatin structure. Chromatin undergoes robust condensation and decondensation during the cell cycle, and transcriptional and post-transcriptional regulation of chromatin modification is controlled in a cell cycle-dependent manner. Chromatin structure is organized at multiple levels (Fig. 1.3) [100]. The smallest unit of chromatin structure, nucleosome, is formed by 147bp of DNA wrapping around a histone octamer, which consists of 2 copies each of H2A, H2B, H3 and H4. The nucleosome structure is stabilized by linker protein H1 and adjacent nucleosomes are linked by free DNA fragment. This classic “beads on a string” structure constitutes the basic 10 nm chromatin fiber. Along the chromatin fiber nucleosomes are arranged in groups with varying nucleosome number [101, 102].

Chromatin is further modified through post-translational modifications (PTMs) of histone proteins or covalent modifications of nucleotides [103–105]. These modifications on chromatin are converted into transcriptional instructions by the interplay of modification “writers,” “erasers” and “readers” residing, often together, in a multitude of chromatin

remodeling complexes that interact directly or indirectly with transcription factor complexes [106]. Based on the gene composition, expression status and enrichment of PTMs and other chromosomal proteins, chromatin is generally divided into euchromatin and heterochromatin. Euchromatin is associated with active transcription and enriched with active histone modifications such as Histone H3 trimethylation at Lysine 4 (H3K4me3) or Lysine 79 (H3K79me3). Heterochromatin is associated with gene repression and can be further divided into constitutive heterochromatin and facultative heterochromatin. Constitutive heterochromatin is commonly located at centromeres, transposons and repetitive sequences and marked by H3K9 me2/me3 and Heterochromatin Protein 1 (HP1). This type of chromatin is associated with long term and stable repression. Facultative heterochromatin is enriched in H3K27me3/Polycomb group proteins binding. Genes silenced in facultative heterochromatin are still able to be reactivated and switched into a euchromatic state.

Besides local linear interaction between neighboring nucleosomes, the chromatin fiber is also spatially packed and forms higher-order topologically associating domains (TADs) at the scale of kilobases to megabases. The level of packaging is dependent on chromatin status. For example, active chromatin region with enriched H3K4me2 or H3K79me3 is loosely packed and PcG-repressed chromatin is compact and has higher level of chromatin intermixing [107]. The compressed topology of PcG repressed heterochromatin seems to be facilitated by polycomb group proteins, which self-polymerize into clusters and contributes to long distance interaction with loci tens of Mb away [108]. In addition to the difference in folding and packaging, active chromatin and repressive chromatin seem to be mutually exclusive in spatial organization [107].

Recently studies using super resolution microscopy in human cells have revealed that a single chromosome can be segmented into two large compartments with active chromatin and inactive chromatin respectively [109]. This compartmentalization of chromatin could presumably increase the local concentration of chromatin modifiers or remodelers as well as transcriptional machinery, and enhance gene regulation efficiency.

1.10 Global chromatin restructuring during mitosis

Chromatin restructures in every round of cell cycle and the most dramatic morphology changes of chromatin occur in mitosis. To ensure the fidelity of separating identical genetic information into two daughter cells, chromatin undergoes substantial compaction into mitotic chromosomes. Mitotic chromosomes are easily recognizable based on their morphology, however, the details of their three-dimensional structure have remained enigmatic. Recent use of advanced Chromosome Conformation Capture methods such as 5C and Hi-C in human cell lines performed at timepoints across the cell cycle, have revealed that mitotic chromosomes exhibit a common structure shared in multiple cell types [110]. Mitotic chromosomes appear to be organized as a linear array of chromatin loops of variable size, which are then tightly compressed together longitudinally. The common structure of mitotic chromosomes seems striking, given the cell type-specific subdomains and features of interphase chromatin structure, such as topologically associating domains (TADs) [111]. This suggests that some cell-type specific chromatin architecture is lost during mitosis and higher-order chromatin structures form *de novo* after mitosis. This might be facilitated by the fact that many chromatin remodeling complexes and transcriptional complexes are dissociated from

chromatin during mitosis. Thus entry into G0 may be an important event in stabilizing nuclear architecture specific to cell types.

DNase sensitivity has been used to probe chromatin accessibility during different stages of the cell cycle. Somewhat surprisingly and in contrast to the Hi-C data mentioned previously, DNase sensitivity is widely preserved from interphase to mitosis [112]. During interphase, DNAse sensitivity generally corresponds to transcription factor binding sites and active gene proximal promoters. By contrast in mitosis, gene expression ceases, higher order chromatin domains are lost and many transcription factors are ejected. So why and how are most DNase sensitive regions maintained during mitosis? First to be precise, there are a few alterations to accessibility in mitosis. For example, distal regulatory elements that bind transcription factors are somewhat more likely to lose accessibility during mitosis compared to gene proximal promoters. Second, chromatin modifications and some chromatin modifiers are retained on the mitotic chromosomes and can help to preserve local chromatin structure, even if higher order structures are disrupted, as suggested by the Hi-C data.

1.11 Chromatin contribution to G0

The cell cycle impacts chromatin structure, while in turn chromatin organization and modification influences the cell cycle. As briefly mentioned in the previous section, the RB component of the G0 silencing complex DREAM is able to recruit chromatin modifiers or remodelers as co-repressors. These chromatin modifiers include histone methyltransferase SUV39H, histone deacetylase HDAC1, DNA methyltransferase

DNMT1, nucleosome remodeler BRM and nucleosome compacting factor L3MBTL1 [99]. This variety of chromatin modifiers or remodelers implies that chromatin structure can be modified at different levels to contribute to G0.

A study comparing proliferating yeast to quiescent yeast showed that quiescence entry is associated with a globally repressive chromatin structure along with a global shutoff of transcription. The histone deacetylase RPD3 is responsible for these changes and *rpd3* mutant yeasts have defects in quiescence entry and transcriptional silencing [94]. This study proposed a promising role for RPD3 in G0 control, however, the function of RPD3 in other species or in contexts of terminal differentiation is unclear. The ATPase component of SWI/SNF nucleosome remodeling complex Brm has been shown to regulate the G0 entry during skeletal myogenesis in mice, potentially through silencing *Ccnd1* [113]. Consistent observations have been reported in *C. elegans*, where compromising SWI/SNF complex disrupts the cell cycle exit in muscle precursor cells. In addition, simultaneous inactivation of SWI/SNF with other G1/S inhibitors such as RB, Cdh1 causes tumorous proliferation [114].

Histone methylation H3K27me3, H3K9me3 as well as H3K9me3 binding protein HP1 have been shown to be enriched at several Rb/E2F target genes and maintain their irreversibly repressed state during terminal differentiation in muscle [115–117]. The enrichment seems to be RB dependent. Post-mitotic removal of RB leads to de-repression of cell cycle genes, cell cycle re-entry and reduced deposition of H3K27me3 or H3K9me3/HP1 [116, 117]. However, whether these chromatin marks actively contribute to initiating G0 is still unclear. I have rigorously examined their contribution in establishing G0 during terminal differentiation in chapter 3.

1.12 *Drosophila* wings as a model system for cell cycle exit in terminal differentiation

Due to the short life cycle, conserved and simplified gene homologs system and availabilities of genetic tools to monitor and manipulate gene expression, *Drosophila melanogaster* has served as a powerful model organism for studying various biological processes.

The terminal differentiation of most *Drosophila* tissues occurs during metamorphosis, which is triggered by a discrete pulse of steroid hormone ecdysone at the third larval instar stage (L3). The attainment of critical weight of L3 animal initiates the production of ecdysone [118]. Ecdysone is produced in the prothoracic gland, then released into the haemolymph and finally converted by peripheral tissues to its active form, 20-hydroxyecdysone (20E) [119]. After binding to the heterodimer of two nuclear receptors, ecdysone receptor (EcR) and ultraspiracle (USP), 20E is able to trigger cascades of tissue specific gene expression that drive coordinated morphological and physiological changes in metamorphosis. Besides the pulse of 20E at the onset of metamorphosis, there is a second pulse with higher amplitude and longer duration in the mid-metamorphosis to further drive metamorphosis progression [120].

During metamorphosis wings undergo a series of morphogenetic changes through the temporal coordination between wing terminal differentiation program and cell cycle exit (Fig. 1.4). The major events include: pupa cuticle formation along with a temporary cell cycle arrest at G2 around 6h after puparium formation (APF); elongation and

apposition of dorsal and ventral epithelial layers with vein refinement during the synchronized final cell cycle till 24h APF; wing hair formation and deposition of adult cuticle after the permanent cell cycle arrest [121–126].

Taking advantage of the temporal and well characterized coordination between terminal differentiation and cell cycle exit in *Drosophila* wings, I examined chromatin accessibility (chapter 2) and higher order chromatin organization (chapter 3) changes during cell cycle exit under development context. My work revealed that chromatin accessibility and gene expression changes are coordinated during the transition from a proliferating to postmitotic state. I further identified the specific chromatin accessibility changes that are regulated by terminal differentiation and cell cycling status, respectively (chapter 2). I also revealed that higher order chromatin organization such as heterochromatin clusters during cell cycle exit. I rigorously tested the role of heterochromatin associated modifications in cell cycle exit and found that compromising heterochromatin mediated gene silencing does not disrupt cell cycle exit. Instead, heterochromatin clustering is a consequence of cell cycle exit (chapter 3).

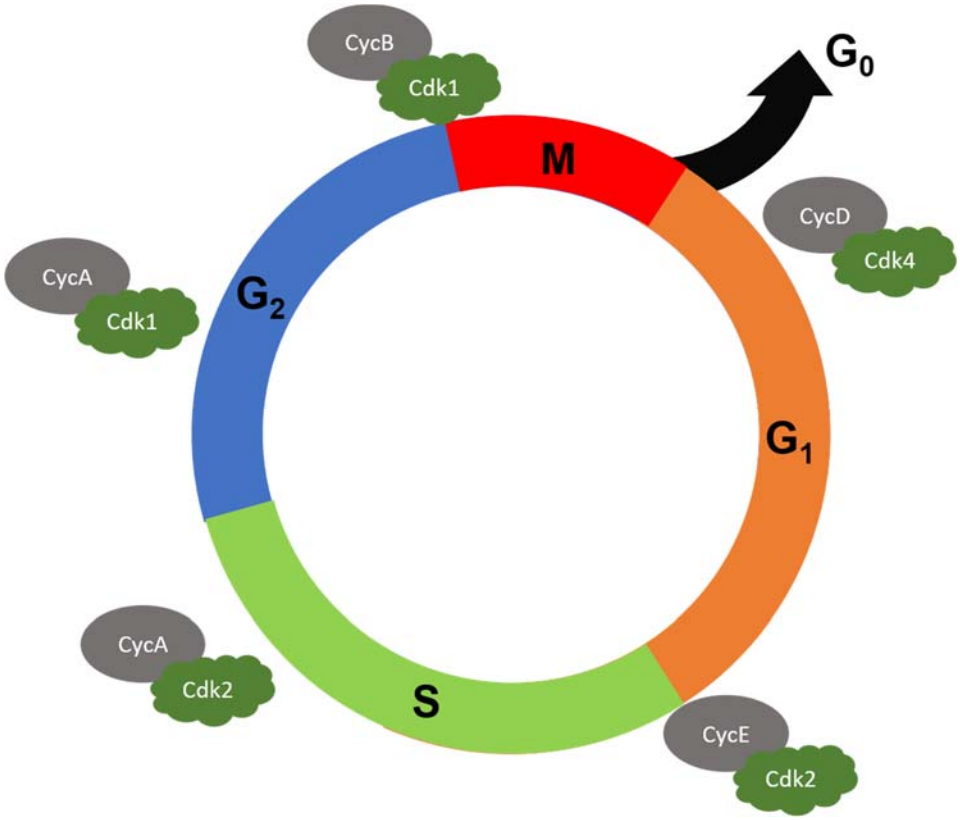

Figure 1.1 Major Cyclin/Cdks driving cell cycle progression.

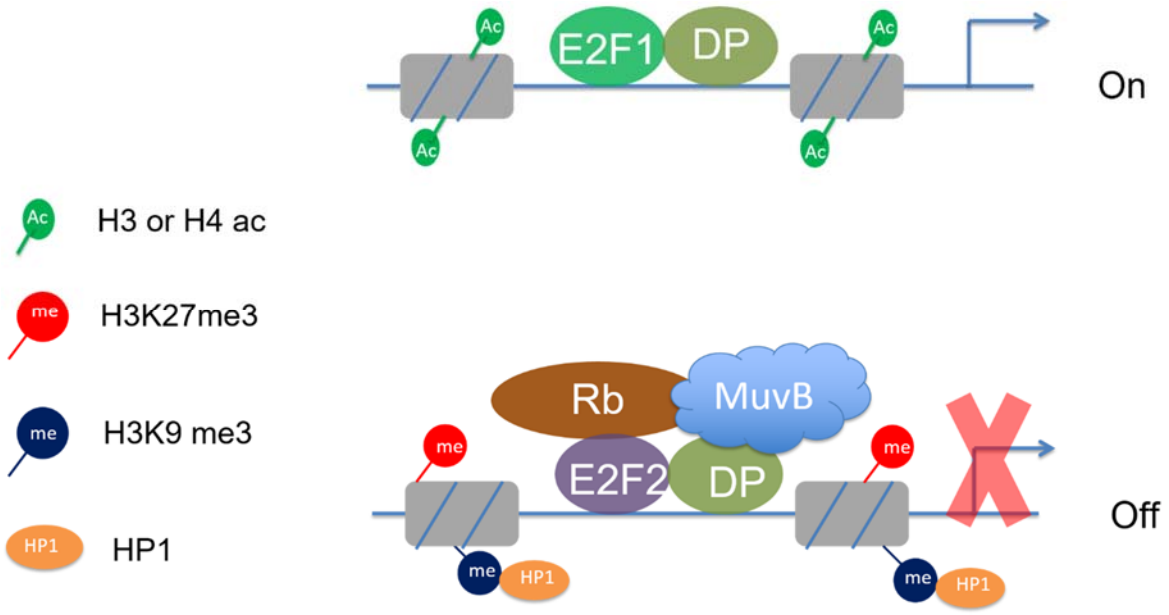

Figure 1.2 Expression of E2F target genes in G1 and G0 is controlled by the switch between E2F1/DP activator and dREAM repressor complex in *Drosophila*.

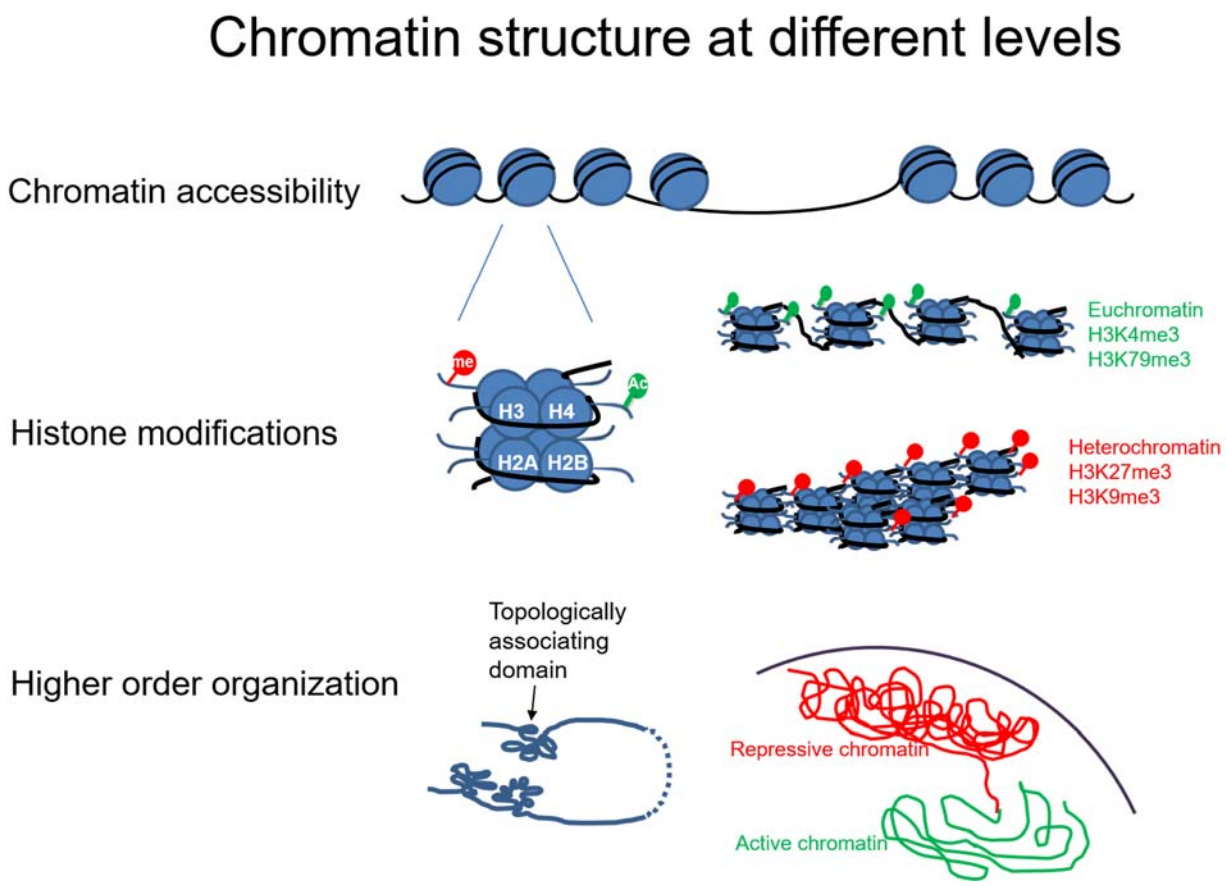

Figure 1.3 Chromatin is organized at different levels.

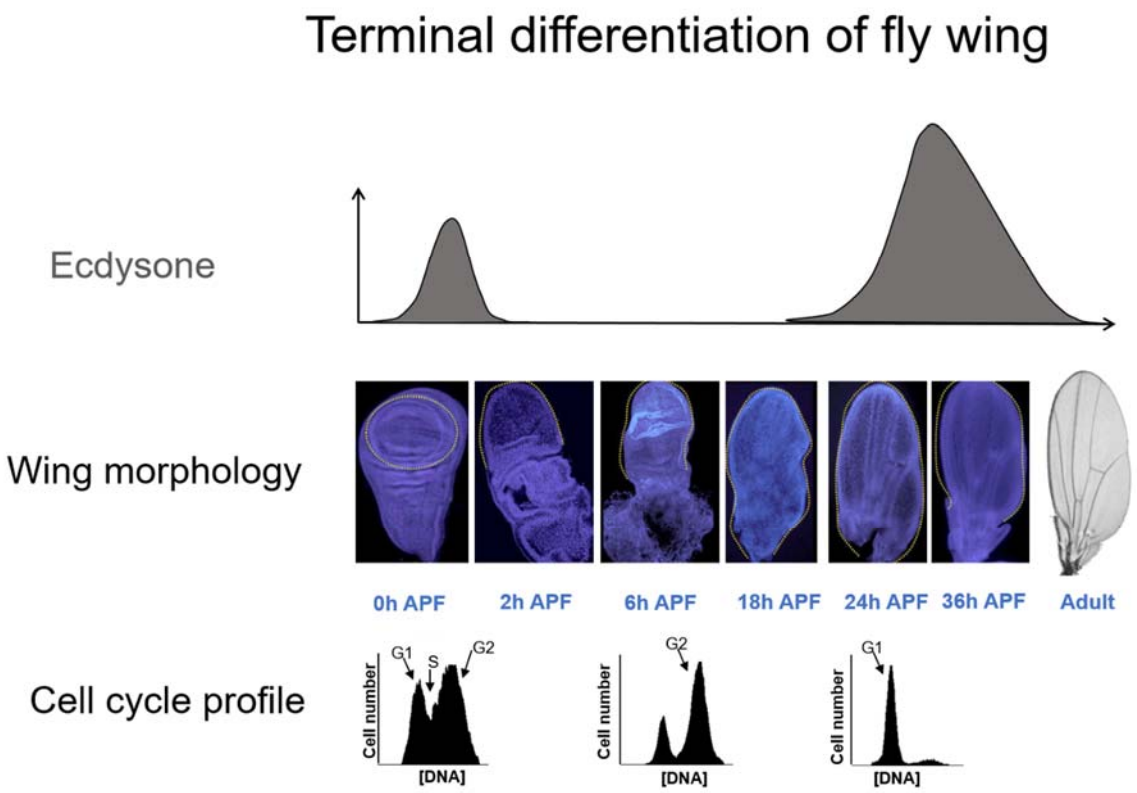

Figure 1.4 Fly wing differentiation and cell cycle activities are coordinated with the ecdysone pulses in metamorphosis.

1.13 Reference

1. Evans T, Rosenthal ET, Youngblom J, Distel D, Hunt T. Cyclin: a protein specified by maternal mRNA in sea urchin eggs that is destroyed at each cleavage division. Cell. 1983;33:389–96.

2. Filmus J, Robles AI, Shi W, Wong MJ, Colombo LL, Conti CJ. Induction of cyclin D1 overexpression by activated ras. Oncogene. 1994;9:3627–33.

3. Chang L, Karin M. Mammalian MAP kinase signalling cascades. Nature. 2001;410:37–40.

4. Roovers K, Assoian RK. Integrating the MAP kinase signal into the G1 phase cell cycle machinery. Bioessays. 2000;22:818–26.

5. Paternot S, Bockstaele L, Bisteau X, Kooken H, Coulonval K, Roger PP. Rb inactivation in cell cycle and cancer: the puzzle of highly regulated activating phosphorylation of CDK4 versus constitutively active CDK-activating kinase. Cell Cycle. 2010;9:689–99.

6. Burkhart DL, Sage J. Cellular mechanisms of tumour suppression by the retinoblastoma gene. Nat Rev Cancer. 2008;8:671–82.

7. Henley SA, Dick FA. The retinoblastoma family of proteins and their regulatory functions in the mammalian cell division cycle. Cell Div. 2012;7:10.

8. Narasimha AM, Kaulich M, Shapiro GS, Choi YJ, Sicinski P, Dowdy SF. Cyclin D activates the Rb tumor suppressor by mono-phosphorylation. Elife. 2014;3.

9. Datar SA, Jacobs HW, de la Cruz AF, Lehner CF, Edgar BA. The Drosophila cyclin D-Cdk4 complex promotes cellular growth. EMBO J. 2000;19:4543–54.

10. Coqueret O. Linking cyclins to transcriptional control. Gene. 2002;299:35–55.

11. Prall OW, Rogan EM, Musgrove EA, Watts CK, Sutherland RL. c-Myc or cyclin D1 mimics estrogen effects on cyclin E-Cdk2 activation and cell cycle reentry. Mol Cell Biol. 1998;18:4499–508.

12. Pagano M, Pepperkok R, Verde F, Ansorge W, Draetta G. Cyclin A is required at two points in the human cell cycle. EMBO J. 1992;11:961–71.

13. Girard F, Strausfeld U, Fernandez A, Lamb NJ. Cyclin A is required for the onset of DNA replication in mammalian fibroblasts. Cell. 1991;67:1169–79.

14. Katsuno Y, Suzuki A, Sugimura K, Okumura K, Zineldeen DH, Shimada M, et al. Cyclin A-Cdk1 regulates the origin firing program in mammalian cells. Proc Natl Acad Sci U S A. 2009;106:3184–9.

15. Reber A, Lehner CF, Jacobs HW. Terminal mitoses require negative regulation of Fzr/Cdh1 by Cyclin A, preventing premature degradation of mitotic cyclins and String/Cdc25. Development. 2006;133:3201–11.

16. Peter M, Nakagawa J, Dorée M, Labbé JC, Nigg EA. In vitro disassembly of the nuclear lamina and M phase-specific phosphorylation of lamins by cdc2 kinase. Cell. 1990;61:591–602.

17. Peter M, Heitlinger E, Häner M, Aebi U, Nigg EA. Disassembly of in vitro formed lamin head-to-tail polymers by CDC2 kinase. EMBO J. 1991;10:1535–44.

18. Musacchio A, Salmon ED. The spindle-assembly checkpoint in space and time. Nat Rev Mol Cell Biol. 2007;8:379–93.

19. Nigg EA. Mitotic kinases as regulators of cell division and its checkpoints. Nat Rev Mol Cell Biol. 2001;2:21–32.

20. Dephoure N, Zhou C, Villén J, Beausoleil SA, Bakalarski CE, Elledge SJ, et al. A quantitative atlas of mitotic phosphorylation. Proc Natl Acad Sci U S A. 2008;105:10762–7.

21. Roque A, Ponte I, Arrondo JLR, Suau P. Phosphorylation of the carboxy-terminal domain of histone H1: effects on secondary structure and DNA condensation. Nucleic Acids Res. 2008;36:4719–26.

22. Chow JPH, Siu WY, Ho HTB, Ma KHT, Ho CC, Poon RYC. Differential contribution of inhibitory phosphorylation of CDC2 and CDK2 for unperturbed cell cycle control and DNA integrity checkpoints. J Biol Chem. 2003;278:40815–28.

23. Lindqvist A, Rodríguez-Bravo V, Medema RH. The decision to enter mitosis: feedback and redundancy in the mitotic entry network. J Cell Biol. 2009;185:193–202.

24. Sherr CJ, Roberts JM. CDK inhibitors: positive and negative regulators of G1-phase progression. Genes Dev. 1999;13:1501–12.

25. el-Deiry WS, Tokino T, Velculescu VE, Levy DB, Parsons R, Trent JM, et al. WAF1, a potential mediator of p53 tumor suppression. Cell. 1993;75:817–25.

26. Harper JW, Adami GR, Wei N, Keyomarsi K, Elledge SJ. The p21 Cdk-interacting protein Cip1 is a potent inhibitor of G1 cyclin-dependent kinases. Cell. 1993;75:805–16.

27. Xiong Y, Hannon GJ, Zhang H, Casso D, Kobayashi R, Beach D. p21 is a universal inhibitor of cyclin kinases. Nature. 1993;366:701–4.

28. Macleod KF, Sherry N, Hannon G, Beach D, Tokino T, Kinzler K, et al. p53-dependent and independent expression of p21 during cell growth, differentiation, and DNA damage. Genes Dev. 1995;9:935–44.

29. Abbas T, Dutta A. p21 in cancer: intricate networks and multiple activities. Nat Rev Cancer. 2009;9:400–14.

30. Bornstein G, Bloom J, Sitry-Shevah D, Nakayama K, Pagano M, Hershko A. Role of the SCFSkp2 ubiquitin ligase in the degradation of p21Cip1 in S phase. J Biol Chem. 2003;278:25752–7.

31. Vodermaier HC. APC/C and SCF: controlling each other and the cell cycle. Curr Biol. 2004;14:R787-96.

32. Terai K, Abbas T, Jazaeri AA, Dutta A. CRL4(Cdt2) E3 ubiquitin ligase monoubiquitinates PCNA to promote translesion DNA synthesis. Mol Cell. 2010;37:143–9.

33. Havens CG, Walter JC. Mechanism of CRL4(Cdt2), a PCNA-dependent E3 ubiquitin ligase. Genes Dev. 2011;25:1568–82.

34. Liu E, Li X, Yan F, Zhao Q, Wu X. Cyclin-dependent kinases phosphorylate human Cdt1 and induce its degradation. J Biol Chem. 2004;279:17283–8.

35. Sugimoto N, Tatsumi Y, Tsurumi T, Matsukage A, Kiyono T, Nishitani H, et al. Cdt1 phosphorylation by cyclin A-dependent kinases negatively regulates its function without affecting geminin binding. J Biol Chem. 2004;279:19691–7.

36. Koepp DM, Schaefer LK, Ye X, Keyomarsi K, Chu C, Harper JW, et al. Phosphorylation-dependent ubiquitination of cyclin E by the SCFFbw7 ubiquitin ligase. Science. 2001;294:173–7.

37. Welcker M, Clurman BE. FBW7 ubiquitin ligase: a tumour suppressor at the crossroads of cell division, growth and differentiation. Nat Rev Cancer. 2008;8:83–93.

38. Peters J-M. The anaphase-promoting complex: proteolysis in mitosis and beyond. Mol Cell. 2002;9:931–43.

39. Harper JW, Burton JL, Solomon MJ. The anaphase-promoting complex: it's not just for mitosis any more. Genes Dev. 2002;16:2179–206.

40. Zachariae W, Nasmyth K. Whose end is destruction: cell division and the anaphase-promoting complex. Genes Dev. 1999;13:2039–58.

41. Skaar JR, Pagano M. Cdh1: a master G0/G1 regulator. Nat Cell Biol. 2008;10:755–7.

42. Bashir T, Dorrello NV, Amador V, Guardavaccaro D, Pagano M. Control of the SCF(Skp2-Cks1) ubiquitin ligase by the APC/C(Cdh1) ubiquitin ligase. Nature. 2004;428:190–3.

43. Wei W, Ayad NG, Wan Y, Zhang G-J, Kirschner MW, Kaelin WG. Degradation of the SCF component Skp2 in cell-cycle phase G1 by the anaphase-promoting complex. Nature. 2004;428:194–8.

44. Diffley JFX. Regulation of early events in chromosome replication. Curr Biol. 2004;14:R778-86.

45. Lavia P, Jansen-Dürr P. E2F target genes and cell-cycle checkpoint control. Bioessays. 1999;21:221–30.

46. Hurford RK, Cobrinik D, Lee MH, Dyson N. pRB and p107/p130 are required for the regulated expression of different sets of E2F responsive genes. Genes Dev. 1997;11:1447–63.

47. Takahashi Y, Rayman JB, Dynlacht BD. Analysis of promoter binding by the E2F and pRB families in vivo: distinct E2F proteins mediate activation and repression.

Genes Dev. 2000;14:804–16.

48. Dimova DK, Stevaux O, Frolov M V, Dyson NJ. Cell cycle-dependent and cell cycle-independent control of transcription by the Drosophila E2F/RB pathway. Genes Dev. 2003;17:2308–20.

49. DeGregori J, Johnson DG. Distinct and Overlapping Roles for E2F Family Members in Transcription, Proliferation and Apoptosis. Curr Mol Med. 2006;6:739–48.

50. Lammens T, Li J, Leone G, De Veylder L. Atypical E2Fs: new players in the E2F transcription factor family. Trends Cell Biol. 2009;19:111–8.

51. Ross JF, Liu X, Dynlacht BD. Mechanism of transcriptional repression of E2F by the retinoblastoma tumor suppressor protein. Mol Cell. 1999;3:195–205.

52. van den Heuvel S, Dyson NJ. Conserved functions of the pRB and E2F families. Nat Rev Mol Cell Biol. 2008;9:713–24.

53. Trouche D, Kouzarides T. E2F1 and E1A(12S) have a homologous activation domain regulated by RB and CBP. Proc Natl Acad Sci U S A. 1996;93:1439–42.

54. McMahon SB, Van Buskirk HA, Dugan KA, Copeland TD, Cole MD. The novel ATM-related protein TRRAP is an essential cofactor for the c-Myc and E2F oncoproteins. Cell. 1998;94:363–74.

55. Lang SE, McMahon SB, Cole MD, Hearing P. E2F transcriptional activation requires TRRAP and GCN5 cofactors. J Biol Chem. 2001;276:32627–34.

56. Taubert S, Gorrini C, Frank SR, Parisi T, Fuchs M, Chan H-M, et al. E2F-dependent histone acetylation and recruitment of the Tip60 acetyltransferase complex to chromatin in late G1. Mol Cell Biol. 2004;24:4546–56.

57. Dunaief JL, Strober BE, Guha S, Khavari PA, Alin K, Luban J, et al. The retinoblastoma protein and BRG1 form a complex and cooperate to induce cell cycle arrest. Cell. 1994;79:119–30.

58. Strober BE, Dunaief JL, Guha, Goff SP. Functional interactions between the hBRM/hBRG1 transcriptional activators and the pRB family of proteins. Mol Cell Biol. 1996;16:1576–83.

59. Dahiya A, Wong S, Gonzalo S, Gavin M, Dean DC. Linking the Rb and polycomb pathways. Mol Cell. 2001;8:557–69.

60. Luo RX, Postigo AA, Dean DC. Rb interacts with histone deacetylase to repress transcription. Cell. 1998;92:463–73.

61. Brehm A, Miska EA, McCance DJ, Reid JL, Bannister AJ, Kouzarides T. Retinoblastoma protein recruits histone deacetylase to repress transcription. Nature. 1998;391:597–601.

62. Magnaghi-Jaulin L, Groisman R, Naguibneva I, Robin P, Lorain S, Le Villain JP, et al. Retinoblastoma protein represses transcription by recruiting a histone deacetylase. Nature. 1998;391:601–5.

63. Ferreira R, Magnaghi-Jaulin L, Robin P, Harel-Bellan A, Trouche D. The three members of the pocket proteins family share the ability to repress E2F activity through recruitment of a histone deacetylase. Proc Natl Acad Sci U S A. 1998;95:10493–8.

64. Fabbrizio E, El Messaoudi S, Polanowska J, Paul C, Cook JR, Lee J-H, et al. Negative regulation of transcription by the type II arginine methyltransferase PRMT5. EMBO Rep. 2002;3:641–5.

65. Nielsen SJ, Schneider R, Bauer UM, Bannister AJ, Morrison A, O'Carroll D, et al. Rb targets histone H3 methylation and HP1 to promoters. Nature. 2001;412:561–5.

66. Rayman JB, Takahashi Y, Indjeian VB, Dannenberg J-H, Catchpole S, Watson RJ, et al. E2F mediates cell cycle-dependent transcriptional repression in vivo by recruitment of an HDAC1/mSin3B corepressor complex. Genes Dev. 2002;16:933–47.

67. Robertson KD, Ait-Si-Ali S, Yokochi T, Wade PA, Jones PL, Wolffe AP. DNMT1 forms a complex with Rb, E2F1 and HDAC1 and represses transcription from E2F-responsive promoters. Nat Genet. 2000;25:338–42.

68. Trojer P, Li G, Sims RJ, Vaquero A, Kalakonda N, Boccuni P, et al. L3MBTL1, a histone-methylation-dependent chromatin lock. Cell. 2007;129:915–28.

69. Knudsen ES, Wang JY. Dual mechanisms for the inhibition of E2F binding to RB by cyclin-dependent kinase-mediated RB phosphorylation. Mol Cell Biol. 1997;17:5771–83.

70. Brown VD, Phillips RA, Gallie BL. Cumulative effect of phosphorylation of pRB on regulation of E2F activity. Mol Cell Biol. 1999;19:3246–56.

71. Lundberg AS, Weinberg RA. Functional inactivation of the retinoblastoma protein requires sequential modification by at least two distinct cyclin-cdk complexes. Mol Cell Biol. 1998;18:753–61.

72. Yao G, Lee TJ, Mori S, Nevins JR, You L. A bistable Rb-E2F switch underlies the restriction point. Nat Cell Biol. 2008;10:476–82.

73. Nelson DA, Krucher NA, Ludlow JW. High molecular weight protein phosphatase type 1 dephosphorylates the retinoblastoma protein. J Biol Chem. 1997;272:4528–35.

74. Cicchillitti L, Fasanaro P, Biglioli P, Capogrossi MC, Martelli F. Oxidative stress induces protein phosphatase 2A-dependent dephosphorylation of the pocket proteins pRb, p107, and p130. J Biol Chem. 2003;278:19509–17.

75. Muñoz-Espín D, Serrano M. Cellular senescence: from physiology to pathology. Nat Rev Mol Cell Biol. 2014;15:482–96.

76. Hernandez-Segura A, Nehme J, Demaria M. Hallmarks of Cellular Senescence. Trends Cell Biol. 2018.

77. Collado M, Serrano M. Senescence in tumours: evidence from mice and humans. Nat Rev Cancer. 2010;10:51–7.

78. Sugiura T, Wang H, Barsacchi R, Simon A, Tanaka EM. MARCKS-like protein is an initiating molecule in axolotl appendage regeneration. Nature. 2016;531:237–40.

79. Wan J, Goldman D. Retina regeneration in zebrafish. Curr Opin Genet Dev. 2016;40:41–7.

80. Spencer SL, Cappell SD, Tsai F-C, Overton KW, Wang CL, Meyer T. The proliferation-quiescence decision is controlled by a bifurcation in CDK2 activity at mitotic exit. Cell. 2013;155:369–83.

81. Besson A, Gurian-West M, Chen X, Kelly-Spratt KS, Kemp CJ, Roberts JM. A pathway in quiescent cells that controls p27Kip1 stability, subcellular localization, and tumor suppression. Genes Dev. 2006;20:47–64.

82. Coats S, Flanagan WM, Nourse J, Roberts JM. Requirement of p27Kip1 for restriction point control of the fibroblast cell cycle. Science. 1996;272:877–80.

83. Susaki E, Nakayama K, Nakayama KI. Cyclin D2 translocates p27 out of the nucleus and promotes its degradation at the G0-G1 transition. Mol Cell Biol. 2007;27:4626–40.

84. Coller HA, Sang L, Roberts JM. A new description of cellular quiescence. PLoS Biol. 2006;4:e83.

85. Pechnick RN, Zonis S, Wawrowsky K, Pourmorady J, Chesnokova V. p21Cip1 restricts neuronal proliferation in the subgranular zone of the dentate gyrus of the hippocampus. Proc Natl Acad Sci U S A. 2008;105:1358–63.

86. Fero ML, Rivkin M, Tasch M, Porter P, Carow CE, Firpo E, et al. A syndrome of multiorgan hyperplasia with features of gigantism, tumorigenesis, and female sterility in p27(Kip1)-deficient mice. Cell. 1996;85:733–44.

87. Gui H, Li S, Matise MP. A cell-autonomous requirement for Cip/Kip cyclin-kinase inhibitors in regulating neuronal cell cycle exit but not differentiation in the developing spinal cord. Dev Biol. 2007;301:14–26.

88. Firth LC, Baker NE. Extracellular signals responsible for spatially regulated proliferation in the differentiating Drosophila eye. Dev Cell. 2005;8:541–51.

89. Buttitta LA, Katzaroff AJ, Perez CL, de la Cruz A, Edgar BA. A double-assurance mechanism controls cell cycle exit upon terminal differentiation in Drosophila. Dev Cell. 2007;12:631–43.

90. Wirth KG, Ricci R, Giménez-Abián JF, Taghybeeglu S, Kudo NR, Jochum W, et al. Loss of the anaphase-promoting complex in quiescent cells causes unscheduled hepatocyte proliferation. Genes Dev. 2004;18:88–98.

91. The I, Ruijtenberg S, Bouchet BP, Cristobal A, Prinsen MBW, van Mourik T, et al. Rb and FZR1/Cdh1 determine CDK4/6-cyclin D requirement in C. elegans and human cancer cells. Nat Commun. 2015;6:5906.

92. Buttitta LA, Katzaroff AJ, Edgar BA. A robust cell cycle control mechanism limits E2F-induced proliferation of terminally differentiated cells in vivo. J Cell Biol. 2010;189:981–96.

93. Guo Y, Flegel K, Kumar J, McKay DJ, Buttitta LA. Ecdysone signaling induces two phases of cell cycle exit in Drosophila cells. Biol Open. 2016;5:1648–61.

94. McKnight JN, Boerma JW, Breeden LL, Tsukiyama T. Global Promoter Targeting of a Conserved Lysine Deacetylase for Transcriptional Shutoff during Quiescence Entry. Mol Cell. 2015;59:732–43.

95. Moberg K, Starz MA, Lees JA. E2F-4 switches from p130 to p107 and pRB in response to cell cycle reentry. Mol Cell Biol. 1996;16:1436–49.

96. Litovchick L, Sadasivam S, Florens L, Zhu X, Swanson SK, Velmurugan S, et al. Evolutionarily conserved multisubunit RBL2/p130 and E2F4 protein complex represses human cell cycle-dependent genes in quiescence. Mol Cell. 2007;26:539–51.

97. Forristal C, Henley SA, MacDonald JI, Bush JR, Ort C, Passos DT, et al. Loss of the mammalian DREAM complex deregulates chondrocyte proliferation. Mol Cell Biol. 2014;34:2221–34.

98. Mages CF, Wintsche A, Bernhart SH, Müller GA. The DREAM complex through its subunit Lin37 cooperates with Rb to initiate quiescence. Elife. 2017;6.

99. Blais A, Dynlacht BD. E2F-associated chromatin modifiers and cell cycle control. Curr Opin Cell Biol. 2007;19:658–62.

100. Bonev B, Cavalli G. Organization and function of the 3D genome. Nat Rev Genet. 2016;17:661–78.

101. Fussner E, Strauss M, Djuric U, Li R, Ahmed K, Hart M, et al. Open and closed domains in the mouse genome are configured as 10-nm chromatin fibres. EMBO Rep. 2012;13:992–6.

102. Ricci MA, Manzo C, García-Parajo MF, Lakadamyali M, Cosma MP. Chromatin fibers are formed by heterogeneous groups of nucleosomes in vivo. Cell. 2015;160:1145–58.

103. Kharchenko P V, Alekseyenko AA, Schwartz YB, Minoda A, Riddle NC, Ernst J, et al. Comprehensive analysis of the chromatin landscape in Drosophila melanogaster. Nature. 2011;471:480–5.

104. Filion GJ, van Bemmel JG, Braunschweig U, Talhout W, Kind J, Ward LD, et al. Systematic protein location mapping reveals five principal chromatin types in Drosophila cells. Cell. 2010;143:212–24.

105. Riddle NC, Minoda A, Kharchenko P V, Alekseyenko AA, Schwartz YB, Tolstorukov MY, et al. Plasticity in patterns of histone modifications and chromosomal proteins in Drosophila heterochromatin. Genome Res. 2011;21:147–63.

106. Jenuwein T, Allis CD. Translating the Histone Code. Science (80-). 2001;293:1074–80.

107. Boettiger AN, Bintu B, Moffitt JR, Wang S, Beliveau BJ, Fudenberg G, et al. Super-resolution imaging reveals distinct chromatin folding for different epigenetic states.

Nature. 2016;529:418–22.

108. Cheutin T, Cavalli G. Polycomb silencing: from linear chromatin domains to 3D chromosome folding. Curr Opin Genet Dev. 2014;25:30–7.

109. Wang S, Su J-H, Beliveau BJ, Bintu B, Moffitt JR, Wu C, et al. Spatial organization of chromatin domains and compartments in single chromosomes. Science. 2016;353:598–602.

110. Naumova N, Imakaev M, Fudenberg G, Zhan Y, Lajoie BR, Mirny LA, et al. Organization of the Mitotic Chromosome. Science (80-). 2013;342:948–53.

111. Pope BD, Ryba T, Dileep V, Yue F, Wu W, Denas O, et al. Topologically associating domains are stable units of replication-timing regulation. Nature. 2014;515:402–5.

112. Hsiung CC-S, Morrissey CS, Udugama M, Frank CL, Keller CA, Baek S, et al. Genome accessibility is widely preserved and locally modulated during mitosis. Genome Res. 2015;25:213–25.

113. Albini S, Coutinho Toto P, Dall'Agnese A, Malecova B, Cenciarelli C, Felsani A, et al. Brahma is required for cell cycle arrest and late muscle gene expression during skeletal myogenesis. EMBO Rep. 2015;16:1037–50.

114. Ruijtenberg S, van den Heuvel S. G1/S Inhibitors and the SWI/SNF Complex Control Cell-Cycle Exit during Muscle Differentiation. Cell. 2015;162:300–13.

115. Ait-Si-Ali S, Guasconi V, Fritsch L, Yahi H, Sekhri R, Naguibneva I, et al. A Suv39h-dependent mechanism for silencing S-phase genes in differentiating but not in cycling cells. EMBO J. 2004;23:605–15.

116. Blais A, van Oevelen CJC, Margueron R, Acosta-Alvear D, Dynlacht BD. Retinoblastoma tumor suppressor protein-dependent methylation of histone H3 lysine 27 is associated with irreversible cell cycle exit. J Cell Biol. 2007;179:1399–412.

117. Sdek P, Zhao P, Wang Y, Huang C-J, Ko CY, Butler PC, et al. Rb and p130 control cell cycle gene silencing to maintain the postmitotic phenotype in cardiac myocytes. J Cell Biol. 2011;194:407–23.

118. Mirth C, Truman JW, Riddiford LM. The role of the prothoracic gland in determining critical weight for metamorphosis in Drosophila melanogaster. Curr Biol. 2005;15:1796–807.

119. Gilbert LI, Rybczynski R, Warren JT. Control and biochemical nature of the ecdysteroidogenic pathway. Annu Rev Entomol. 2002;47:883–916.

120. Ou Q, King-Jones K. What goes up must come down: transcription factors have their say in making ecdysone pulses. Curr Top Dev Biol. 2013;103:35–71.

121. Johnson SA, Milner MJ. Cuticle secretion in Drosophila wing imaginal discs in vitro: parameters of exposure to 20-hydroxy ecdysone. Int J Dev Biol. 1990;34:299–307.

122. Fristrom D, Liebrich W. The hormonal coordination of cuticulin deposition and

morphogenesis in Drosophila imaginal discs in vivo and in vitro. Dev Biol. 1986;114:1–11.

123. Uyehara CM, Nystrom SL, Niederhuber MJ, Leatham-Jensen M, Ma Y, Buttitta LA, et al. Hormone-dependent control of developmental timing through regulation of chromatin accessibility. Genes Dev. 2017;31:862–75.

124. Sobala LF, Adler PN. The Gene Expression Program for the Formation of Wing Cuticle in Drosophila. PLoS Genet. 2016;12:e1006100.

125. Taylor J, Adler PN. Cell rearrangement and cell division during the tissue level morphogenesis of evaginating Drosophila imaginal discs. Dev Biol. 2008;313:739–51.

126. Sotillos S, De Celis JF. Interactions between the Notch, EGFR, and decapentaplegic signaling pathways regulate vein differentiation during Drosophila pupal wing development. Dev Dyn. 2005;232:738–52.

Chapter 2: Crosstalk between Terminal Differentiation and Cell Cycle Exit is Mediated through the Regulation of Chromatin Accessibility

2.1 Abstract

During terminal differentiation many cells will exit the cell cycle and enter into a prolonged or permanent G0 state. Cell cycle exit is usually initiated through the repression of cell cycle gene expression by formation of a transcriptional repressor complex. However, nucleosome remodeling complexes have also been shown to contribute to stable repression of cell cycle genes and promote cell cycle exit. Here we examine the relationship between chromatin accessibility, cell cycle exit and terminal differentiation. We find that chromatin accessibility and gene expression changes are coordinated with the transition from a proliferating to postmitotic state. To identify which changes are a consequence of cell cycle exit, we genetically disrupted cell cycle exit and examined chromatin accessibility and gene expression. This uncovered mutual cross-talk between the wing terminal differentiation program and the cell cycle machinery. We find that the accessibility of important gene regulatory elements at a small group of rate-limiting cell cycle genes is developmentally controlled and enforces prolonged G0. In turn, disrupting cell cycle exit impacts gene expression and accessibility at a subset of hormone-induced transcription factors during wing

development leading to delays in the activation of a portion of the wing terminal differentiation program.

2.2 Introduction

Terminal differentiation in most cell types is accompanied by the transition of cells from a proliferative to a postmitotic state, usually accompanied by a prolonged or permanent G0. The state of G0 has been proposed to be essential for terminal differentiation through promoting the expression of late differentiation genes [1, 2]. It has been well characterized that the transition from proliferation to G0 is enforced by the silencing of cell cycle gene transcription [3]. In *Drosophila*, for example, in proliferating cells the dE2F1/dDP transcription activator complex binds to promoter proximal E2F binding motifs at hundreds of cell cycle genes, including cyclins, Cyclin-dependent kinases, replication proteins and mitotic regulators, to promote their expression. Upon entry into G0, silencing occurs through the formation of a transcriptional repressor complex consisting of dDP, RB family members Rbf1 or Rbf2, dE2F2, p55/CAF1, Myb and Myb-interacting proteins [4, 5], termed dREAM.

Formation of dREAM complex is dependent upon a reduction in cyclin/Cdk phosphorylation of RB, therefore it can be induced through developmental activation of Cyclin-dependent kinase inhibitors, developmental downregulation of Cyclins and Cdks or the upregulation of cyclin destruction through the APC/C [6–9].

Several studies have shown that the Rb component of DREAM complex can recruit chromatin remodelers to silence cell cycle genes and promote G0 [10–15]. This suggests that changes in chromatin accessibility is involved in the shutdown of cell

cycle gene expression. However, it remains unclear whether chromatin accessibility is involved in maintaining the silencing of cell cycle genes. If so, what is the contribution of differentiation pathway? In addition, it is still unclear what is the genome-wide impact of G0 perturbation in terminal differentiation, both at the transcription and chromatin level.

To address these questions, we focused our study in the terminal differentiation process of *Drosophila* wings. The terminal differentiation of most *Drosophila* tissues occurs during metamorphosis, which is driven by pulses of steroid hormone ecdysone. We characterized the genome-wide transcriptome and chromatin accessibility landscape through RNA-seq and FAIRE-seq over 6 developmental time points. We found that during wing differentiation, chromatin accessibility and gene expression changes are coordinated with the transition from a proliferating to postmitotic state. By delaying or bypassing the cell cycle exit through overexpression of cell cycle regulators, we identified a mutual crosstalk between terminal differentiation and cell cycle exit: differentiation pathway controls the accessibilities of a subset of rate-limiting cell cycle genes enhancers, while cell cycling delays the temporal response to ecdysone signaling.

2.3 Results

2.3.1 Gene expression dynamics of wing during metamorphosis

During metamorphosis wings undergo morphogenetic changes coordinated with cell cycle alterations, loss of regeneration capacity and activation of a wing terminal differentiation program [16–18]. These events are temporally coordinated by systemic hormone pulses which trigger metamorphosis and drive its progression, leading to coordinated morphogenesis and differentiation of organs [19, 20]. Although the

hormone pulses are systemic, through a combination of direct and indirect regulation they result in activation of unique gene expression programs in different tissues [19, 21–23]. For the wing, major events during metamorphosis include; eversion coordinated with a temporary cell cycle arrest in G2 and pupa cuticle formation, elongation and apposition of dorsal and ventral surfaces, coordinated with a relatively synchronized final cell cycle and vein refinement and permanent cell cycle arrest which precedes wing hair formation and deposition of adult cuticle [21, 24–27]. Underlying these processes are coordinated changes in gene expression. We and others have examined the gene expression changes in the wing during metamorphosis [3, 25]. However no previous timecourse has spanned from early metamorphosis to cuticle deposition. To fill this knowledge gap, we carried out RNA-seq experiments on wildtype Drosophila wings comparing the late wandering third instar larva stage prior to metamorphosis (L3), to stages during metamorphosis at 6h, 18h, 24h, 36h and 44h after puparium formation (APF). Over 9,000 genes exhibit dynamic expression changes during wing metamorphosis. To better identify temporal patterns of gene expression, we carried out k-means clustering based on the RNA fold changes compared to L3, and found 18 distinct clusters that best separate different expression patterns (Fig. S2.1A). Gene expression is very dynamic during metamorphosis and at almost every stage there are groups of genes reaching their peak expression. Our cluster separation is able to pull out groups of genes that are coordinately regulated. For example, RNA cluster 4 contains genes highly expressed at 6h and enriched in biological process of cuticle development from gene ontology (GO) analysis (Fig. S2.1B). The expression pattern of this gene group agrees with the formation of the pupal wing cuticle at this stage [24]. By

comparison, RNA clusters 7 and 10 are composed of genes that decrease expression after 18h, and are highly enriched in cell cycle genes. This is consistent with our previous work showing that cell cycle gene expression plummets by 24h when cells transition to a postmitotic state [3, 28].

2.3.2 Dynamics of open chromatin during metamorphosis

To examine whether the accessibility of chromatin is also dynamic during metamorphosis, we carried out Formaldehyde-Assisted Isolation of Regulatory Elements sequencing (FAIRE-seq) in parallel with our RNA-seq. We identified a total of 20,329 high-confidence open chromatin regions (peaks). We first compared the similarity of open chromatin profiles across our wing developmental time course by examining Pearson correlation coefficients. The open chromatin landscape is gradually changing during metamorphosis and early proliferative stages are distinct from late postmitotic stages in chromatin accessibility (Fig. 2.1A). By calculating the fold change in peak accessibility between stages, we found that only 5,516 peaks are static (27%) and have <2-fold changes between any two timepoints. While the remaining 14,813 peaks (73%) appear dynamic, exhibiting >2-fold changes between two or more timepoints. To further visualize their dynamics during metamorphosis, we divided the rpkm value of each FAIRE peak by its maximum rpkm value from the 6 stages, and then plotted the fraction in the form of heatmap (Fig. 2.1B). To distinguish between different dynamic patterns, we separated the peaks into 18 k-means clusters. We discovered that the dynamic peaks can be divided into 3 broad categories: a temporally sharp category that transiently opens at only one stage; a temporally broad category that

remains accessible for several sequential stages and a category of peaks that oscillate, from open to closed to reopened.

To visualize the temporal dynamics of peaks, we next compared dynamic peaks between stages to define them as opening or closing at the next sequential stage (Fig. 2.1C-D, Fig. S2.2). This revealed that most of the peaks for each stage are shared with immediately neighboring stages (Fig. S2.2A). The timepoint with the most dynamic changes is 6h while the second most dynamic is 24h. Both of these stages are associated with cell cycle arrests. We previously showed that at 6h, wings undergo a temporary G2 arrest induced by high levels of the transcription factor Broad suppressing the critical G2-M regulator cdc25c or string. This synchronizes the subsequent final cell cycle [28]. At 24h cells in the wing finish the final cell cycle in a relatively synchronized manner and enter into a postmitotic G0 state [29]. This suggests that a developmentally controlled program of coordinated chromatin accessibility changes links changes in the cell cycle with differentiation during metamorphosis.

To identify the genome location of the dynamic and static peaks, we first analyzed their distance to nearest transcription starting site (TSS) (Fig. S2.2B-C). Both dynamic and static peaks are highly enriched in 1-5 kb away from TSS. However, the next enriched category for dynamic peaks is 5-10 kb and for static peaks is 0.5 kb. To further identify the locations of peaks by gene structure, we analyzed their distribution in coding sequence (cds), introns, promoter proximal regions (-500 bp to +150 bp of the TSS), UTRs, non-coding genes (nc genes) and intergenic regions (Fig. 2.1C-D). We observed that dynamic and static peaks have similar distributions with most of them

located in introns, intergenic and promoter proximal regions. This is consistent with previous work showing that FAIRE-seq enriches for DNA regulatory elements [30, 31]. Similar to another report using FAIRE in Drosophila embryos, we find that putative regulatory elements for the wing are mostly located within introns, especially the first intron and1-5 kb upstream of the TSS. This is also consistent with the locations of *Drosophila* enhancers identified using a functional accessibility-independent approach, Starr-Seq [32].

2.3.3 Dynamic chromatin is mostly correlated with gene activation

Functional regulatory elements may become accessible to activators or repressors. To determine whether FAIRE peak dynamics correlate positively or negatively with gene expression changes, we assigned each FAIRE peak to its nearest gene and carried out pair-wise comparisons between each stage and its next two sequential stages for >2-fold changes in chromatin accessibility correlated with >2-fold gene expression changes using our RNAseq data (Fig. S2.3). When we plot peak accessibility change vs. assigned gene expression changes, we generate four quadrants: FAIRE peaks opening with corresponding gene expression increasing consistent with an activation function; FAIRE peaks opening with gene expression decreasing consistent with a repressive function; FAIRE peaks closing with gene expression increasing consistent with the loss of a repressor binding; FAIRE peaks closing and gene expression decreasing consistent with the loss of an activator binding (Fig. 2.2A).

We observed that the majority of dynamic FAIRE peaks fall into the category of peaks opening with the corresponding gene expression increasing. This suggests that the majority of gene expression changes in the differentiating wing are driven by transcriptional activators gaining access to their binding sites. The second largest group of FAIRE peaks close and are associated with loss of expression. Suggesting that loss of access for transcriptional activators also plays a major role in gene repression during terminal differentiation.

We next compared the temporal changes between RNA and FAIRE (Fig. 2.2B, Fig. S2.4 - S2.5). We first calculated the average change at a given timepoint from a specific RNA cluster and then plotted the trajectory of average RNA changes across the 6 timepoints. For comparison, we also plotted the temporal changes of FAIRE peaks that are assigned to the genes in this RNA cluster (Fig. 2.2B, Fig. S2.4). We did similar analysis to FAIRE clusters, too (Fig. S2.5). We found that the temporal changes of RNA and FAIRE can be well coordinated (Fig. 2.2B). We also noticed that there are large variations of FAIRE changes within the same RNA cluster. So we looked into the dynamic FAIRE peaks belonging to the same RNA cluster and analyzed their distributions by their original FAIRE cluster assignment (Fig. 2.2C). For the RNA clusters with dramatic and synchronized changes, their FAIRE peaks preferentially localize in one FAIRE cluster. For example, FAIRE peaks of RNA cluster 2 or 4 are enriched in FAIRE cluster 17. RNA cluster 2 and 4 are enriched in genes for cuticle development and they reach their peak expressions at 6h. While FAIRE cluster17 represents the dynamic chromatin that opens at 6h as well. Together our results suggest that the dynamic of gene expression and open chromatin is highly coordinated

and most of the dynamic regulatory elements in fly wings are associated with gene activation.

2.3.4 Regulatory elements for genes involved in wing differentiation open during metamorphosis

A major event during wing terminal differentiation is the formation of the cuticular exoskeleton. The wing cuticle is a multilayered structure and its formation requires the proper expression of cuticle proteins, cuticle deposition genes, and ZP domain proteins which link the apical surface of wing cells to the overlying cuticle [25]. When we examined cuticle formation-associated genes, we found a distinct subgroup highly expressed at 6h and 36h (Fig. 2.3B). The cuticle genes expressed at 6h are likely to be involved in the pupa cuticle formation which begins just after 6h. The cuticle genes expressed at 36h indicates an early starting point of adult wing cuticular exoskeleton formation and this extends to 44h and beyond [25]. We also noticed that different groups of cuticle genes reach their peak expression at different stages, suggesting several waves of sequential regulation may drive cuticle gene expression. The accessibilities of FAIRE peaks near cuticle genes (Fig. 2.3C) are highly accessible at 44h, 36h and 6h, consistent with the high expression at those time points. To determine whether FAIRE peaks can regulate gene expression, we examined an open chromatin region near the cuticle gene *Cpr51A* driving Gal4 expression with UAS-GFP (Fig. 2.3D). This region is highly accessible at 44h and we observed that this GFP reporter is highly expressed in almost all the wing cells at 44h. These results indicate that we are able to identify dynamic regulatory elements that drive cuticle genes expression.

2.3.5 Repression of most cell cycle genes is established and maintained through promoter proximal regulatory elements

Cells in pupal wings exit the cell cycle at 24h APF, which accompanies temporally synchronized repression of cell cycle genes [6, 28]. We examined the expression of ~300 cell cycle genes (Fig. 2.3E) and observed a temporary repression during the G2 arrest at 6h, followed by reactivation at 18h for the final cell cycle, and silencing during cell cycle exit at 24h.

We examined the chromatin accessibility profiles for these cell cycle genes and found that most of them exhibit a compact gene structure with smaller introns and relatively short intergenic upstream sequence (Fig. 2.3A). Most FAIRE peaks associated with these genes are found to be proximal to the TSS, consistent with the previously reported distribution for functional enhancers at “housekeeping” genes [33]. Surprisingly, putative regulatory elements at cell cycle genes exhibit a moderate increase in accessibility at timepoints when cells are postmitotic (24-44h) despite the temporally regulated shutoff of their associated genes at 24h.

We carried out a *de novo* motif discovery on the promoter proximal FAIRE peaks for cell cycle genes using MEME (Fig. 2.3G). The most highly enriched motifs match Motif 1, a core promoter element bound by M1BP to promote RNAPolII pausing [34, 35], the Dref-binding element DRE, a core promoter/enhancer known to be associated with cell cycle genes [3, 36] and a motif matching the binding site for the heterodimer transcription factor complex E2F/DP.

One possibility for the increase in accessibility at cell cycle genes when gene expression is silenced could be Pol II pausing via M1BP. While Pol II pausing at cell cycle genes has been reported in ESCs, in this context it poises expression to promote proliferation rather than to reduce expression [37]. Another possibility for the increase in accessibility is stable binding by a transcriptional repressor complexes. The repression of cell cycle genes in postmitotic cells requires the repressive Rb/E2F2/DP complex and multiple studies have reported that depletion of Rb leads to the partial de-repression of cell cycle genes [29, 38, 39]. However it has remained unclear whether Rb-dependent repression is required to initiate repression of cell cycle genes to promote cell cycle exit, or maintain repression in cells that have already become postmitotic. To investigate this we took advantage of a PCNA-GFP transcriptional reporter that includes known E2F binding sites contained within FAIRE peaks that remain accessible after cell cycle exit [40]. At 44h, a timepoint when the postmitotic state has been maintained for 20h, the reporter is silenced. To test whether this silencing can be reversed, we activated expression of E2F1/DP (hereafter E2F) or E2F+CycD/Cdk4 to phosphorylate and inactivate Rbf specifically after cells have already established a postmitotic state at 28h (Fig. 2.3H). Expressing either E2F or E2F/CycD/Cdk4 was able to re-induce PCNA-GFP expression in postmitotic cells, demonstrating that RB/E2F-dependent repression is required to maintain silencing of cell cycle genes in *Drosophila*.

2.3.6 Enhancers of complex cell cycle genes are dynamic

In contrast to the majority of cell cycle genes, a few key, rate-limiting cell cycle genes are controlled by long, complex regulatory elements upstream of their TSS or in

long introns. For example, *cycE*, *dacapo*, *stg* and *e2f1* fall into this group (Fig. 2.3I). We find several FAIRE peaks in regulatory regions for these genes that overlap with previously characterized functional regulatory elements [41, 42]. Here we discovered that the accessibility of these regulatory elements is temporally dynamic during metamorphosis, in a manner coordinated with the cell cycle changes. Accessibility at these elements is low during the G2 arrest at 6h, then rises at 18h and 24h and closes after 36h. To examine whether the dynamic accessibility of these elements impacts temporal gene expression, we tested regions from the *stg* and *e2f1* loci driving a Gal4/UAS-destabilized GFP to capture gene expression shutoff [43]. Our destabilized GFP reporters showed dynamic expression correlated with the accessibility of the elements. Our results suggest that dynamic chromatin accessibility at enhancers of complex cell cycle genes drives temporal expression changes during metamorphosis.

2.3.7 The closing of enhancers at complex cell cycle genes is independent of cell cycle exit

We observed that chromatin dynamics at specific cell cycle genes and their expression are coordinated with cell cycle changes during metamorphosis. However, cell cycle changes during metamorphosis are inherently coupled with the hormone signaling that drives developmental timing [28]. We therefore wondered whether the temporal changes in chromatin accessibility at complex cell cycle genes such as *cyce*, *e2f1* and *stg* are driven by cell cycle alterations or by the hormone-driven developmental timing program.

To address this question, we took advantage of conditions where cell cycle exit in the pupal wing can be either temporarily delayed or bypassed for a prolonged period without preventing metamorphosis or terminal differentiation [6, 29, 44]. In brief, overexpression of the activator E2F complex (E2F1+DP) during the final cell cycle delays cell cycle exit and causes 1 extra cell cycle during the 24-36h widow, while overexpression of E2F + CycD/Cdk4 during this same period causes multiple rounds of extra cell division and effectively bypasses cell cycle exit until well after 50h. To accomplish this we used the Gal4/UAS system in combination with a temperature-sensitive tub-Gal80 ($Gal80^{TS}$) to limit the expression of these factors from 12h -24 or 44h APF. This allows metamorphosis to initiate properly, yet still effectively delays or bypasses G0 (Fig. S2.6). We dissected 24h or 44h pupal wings under the delayed (E2F) or continued cycling (E2F+CycD) conditions and performed genomewide RNA-seq and FAIRE-seq analysis (Fig. 2.4B). Importantly, at 44h when the E2F expressing wings are postmitotic, the E2F+CycD wings are still cycling, allowing us to differentiate effects of E2F overexpression from those of cell proliferation. E2F or E2F+CycD expression was sufficient to alter the expression of several hundred genes at 24h and over 1,500 by 44h (Fig. S2.7A). Despite the dramatic changes in gene expression, there were strikingly few changes in FAIRE peak accessibility, with only a handful of peaks increasing accessibility at the 24h timepoint and up to 287 peaks increasing accessibility at the 44h timepoint (Fig. S2.7B). GO term enrichment analysis under both conditions revealed that the upregulated genes are highly enriched for those associated with the cell cycle while downregulated genes are highly enriched for genes involved in cuticle development.

Despite the upregulation of hundreds of cell cycles at both 24 and 44h (Fig. 2.4C), we observed relatively little effect on their accessibility, other than a mild decrease under E2F overexpression (Fig. 2.4D). We compared the FAIRE peak accessibility of simple cell cycle genes such as *orc6* and *pcna* to complex cell cycle genes *cyce* and *stg* when cell cycle exit was delayed or disrupted. The accessibility of the regulatory region of *pcna* and *orc6* is relatively unchanged and the closing of *cyce* and *stg* enhancers proceeds with normal timing despite the delay or bypass of cell cycle exit (Fig. 2.4E). This demonstrates that the closing of enhancers at complex cell cycle genes is developmentally controlled and independent of cell cycling status.

2.3.8 Ectopic E2F activity impacts a subset of genes involved in wing terminal differentiation

In contrast to the minimal effects on chromatin accessibility at cell cycle genes, the largest impact of delaying or disrupting cell cycle exit on chromatin was the loss of accessibility at over 1,000 genomic sites at 44h (Fig. S2.7B). This could be caused by either chromatin remodeling to close accessible sites at 44h or a failure to open sites that should become accessible. To address which of these scenarios is correct, we examined the dynamics of peaks influenced by E2F or E2F+CycD during the wildtype time-course (Fig. S2.8A). Notably, peaks that are less accessible under conditions that disrupt cell cycle exit are normally closed at 36h but highly accessible at 44h. This suggests that disrupting cell cycle exit results in a failure to open a specific subset of regulatory elements between 36h and 44h.

To determine whether this failure to open specific elements is due to ectopic E2F activity or ectopic proliferation itself, we next compared chromatin accessibility changes between E2F and E2F+CycD wings at 44h (Fig. 2.4F). While we observed differential effects on the expression levels of several hundred genes involved in the cell cycle, ribosome biogenesis and cuticle development, we observed almost no changes in chromatin accessibility between these two conditions. This is remarkable considering that wings expressing E2F at 44h are not cycling while wings expressing E2F+CycD continue to proliferate. This demonstrates that the failure to open chromatin at a subset of genes at 44h when cell cycle exit is disrupted is likely due to the ectopic E2F activity and not the ectopic proliferation.

The genes that fail to open when cell cycle exit is disrupted are enriched for roles in cuticle formation and deposition and wing terminal differentiation. Consistent with this, expression levels of genes involved in wing cuticle formation are reduced when cell cycle exit is disrupted (Fig. 2.5A), and their chromatin accessibility at potential enhancers is reduced (Fig. 2.5B, C). Together, our results indicate that ectopic E2F activity compromises the opening and activation of a portion of the wing terminal differentiation program.

To determine whether ectopic E2F activity impacts wing cuticle formation, we expressed E2F or E2F+CycD in the dorsal layer of the wing epithelium beginning at 12h APF using *Apterous*-Gal4/Gal80^{ts}. We examined the cuticle formation at 64h by transmission electron microscopy (TEM) (Fig. 2.5D). Pupal wings are normally composed of two thin monolayers of epithelial cells, and expression of E2F or E2F+CycD lead to an obvious thickening of the epithelium due to extra ectopic cells in

the dorsal side. The cuticle layer on the dorsal side of the wing was much thinner than normal, and the effect was compartment autonomous as the ventral wing cuticle was unaffected. We next examined the deposition of chitin, the key component of insect cuticle through calcofluor staining (Fig. 2.5E). Chitin staining in the dorsal wing where E2F or E2F+CycD was expressed was much weaker than the ventral. Thus, ectopic E2F expression delays and disrupts adult wing cuticle formation.

2.3.9 Disrupting cell cycle exit alters chromatin dynamics at specific ecdysone target genes

In addition to effects on wing terminal differentiation genes, we also observed that disrupting cell cycle exit impacted the expression of several ecdysone target genes. Genes such as *Blimp-1*, *Hr3* and *crol* were expressed at significantly higher levels at 44h when cell cycle exit was disrupted while the expression of *E74EF*, *E75B* and *E71CD* was reduced (Fig. 2.6A). During the normal timecourse *Blimp-1*, *Hr3* and *crol* exhibit peak expression at 36h and plummet by 44h, while *E74EF*, *E75B* and *E71CD* normally peak at 44h. Thus the disruption of cell cycle exit likely leads to a delay in the shutoff of *Blimp-1*, *Hr3* and *crol* and delayed upregulation of *E74EF*, *E75B* and *E71CD*. When we investigated chromatin accessibility at these genes, we found that specific enhancers for Blimp-1 and Hr3 failed to close at 44h when cell cycle exit was disrupted while specific enhancers at E75B and E74EF failed to open (Fig. 2.6B,C). Our results are consistent with a model where ectopic E2F activity or disrupting cell cycle exit leads to delays in chromatin remodeling at specific ecdysone target genes delaying their proper expression dynamics.

We reasoned that these alterations in transcriptional regulators downstream of ecdysone signaling could lead to the alterations in chromatin accessibility for the downstream wing terminal differentiation genes we observe when cell cycle exit is disrupted. Consistent with this, we found the Blimp-1 binding motif to be significantly enriched in FAIRE peaks that are differentially regulated under conditions that disrupt cell cycle exit (Fig. S2.8B). Several genes important for cuticle development such as *Cda5*, *Cpr50Ca*, *Cpr47Ec* and *TwdlT* harbor high scoring Blimp-1 binding sites and are potential direct Blimp-1 targets (Fig. S2.8C). However, their peaks exhibit temporal dynamics consistent with a model where Blimp-1 either binds closed chromatin at 36h and facilitates subsequent chromatin opening at 44h or where high Blimp-1 binding at 36h somehow maintains closing that is lost when Blimp-1 levels plummet at 44h (Fig. 2.6E). The temporal and spatial resolution of our FAIRE timecourse is not sufficient to distinguish between these two scenarios. Interestingly, we also found a high scoring *Blimp-1* site in E74EF, suggesting its temporal regulation is also dependent on Blimp-1.

We considered the possibility that our genetic disruption of cell cycle exit could have non-autonomous effects that might impact the timing or production of the ecdysone signal itself leading to alterations in chromatin remodeling at specific targets. We therefore tested whether our manipulations of cell cycle exit impacted ecdysone targets non-autonomously. To address this, we expressed E2F+CycD specifically in the posterior compartment of the pupa wing using the *Engrailed*-Gal4/Gal80^{ts} system and examined Blimp-1 protein levels through immunostaining (Fig. 2.6D). Blimp-1 levels normally peak at 36h and plummet by at 44h. We found that when we disrupted cell cycle exit in the posterior wing, Blimp-1 protein levels in the posterior were reduced at

36h but higher at 40-42h consistent with the delay in Blimp-1 activation we observed by RNAseq. Importantly, Blimp-1 levels were unaffected in the anterior wing, demonstrating that disrupting cell cycle exit impacts the timing of ecdysone target gene expression in a compartment-autonomous manner (Fig. 2.6D).

In summary, ectopic E2F activity and delaying cell cycle exit alters chromatin dynamics at specific ecdysone targets such as Hr3 and Blimp-1 in a cell autonomous manner. This in turn leads to delays in chromatin remodeling at their targets and altered expression dynamics of downstream wing terminal differentiation genes.

2.4 Discussion

Terminal differentiation and the transition from proliferation to cell cycle exit are usually coupled during development. In this study we comprehensively characterized the gene expression and gene regulatory mechanisms underlying these two processes by examining the transcriptome and open chromatin landscape changes during cell cycle exit. Our study reveals that during wing differentiation, chromatin accessibility and gene expression changes are coordinated. Regulatory elements can be accessible through binding of transcriptional activators or repressors, however, the relative contribution of activating vs. repressive regulation during differentiation is elusive. Here we reveal that transcriptional activation is the major contributor to dynamic gene expression changes during terminal differentiation (Fig. 2.2). The preferential usage of dynamic regulatory elements for gene activation is not Drosophila wing specific. Other differentiation contexts such as early zygotic genome activation in Drosophila embryos [45], Arabidopsis flower development [46] and human cortical neurogenesis [47] have

reported similar findings. Therefore, the preferential usage of activating gene regulatory elements may be a conserved feature of temporally regulated differentiation programs.

We discover surprising regulations of differentiation program on cell cycle genes expression both from transcription level and chromatin level. We have previously shown that the ecdysone pulse at the onset of metamorphosis temporally activates br at 6h [28]. br binds to stg upstream regulatory elements and suppresses stg expression. The low level of stg leads to the cells in the 6h APF wings to arrest in G2. This temporal arrest in G2, which synchronizes cells for the final cell cycle, is soon released at 18h when the wave of br expression goes away. Here our study reveals that the repression on stg is not only exerted by directly inhibiting the transcription, but also enforced through the closing of regulatory elements (Fig. 2.3I). In addition, we also reveal that stg is not the only cell cycle gene silenced by closing chromatin accessibility, and we observed the temporal closing of e2f1 regulatory elements as well (Fig. 2.3I), indicating a common repression on complex cell cycle genes at the chromatin level. There is also developmentally controlled repression on simple cell cycle genes. During normal cell cycle regulation such as fast proliferating L3 wings or S2 cells, transcriptional activities at G2 phase for some G2/M cell cycle genes still occur, such as aurora A, APC4 and Separase [48]. However, at the in vivo G2 arrest at 6h APF, we observed synchronized repression on almost all the cell cycle genes including aurora A, APC4 and Separase, indicating that developmental specific mechanisms are involved in regulating cell cycle genes other than conventional cell cycle regulation machineries.

Control on complex cell cycle genes at the chromatin level by developmental pathway is further manifested at the late pupal stages. The enhancers of complex cell cycle genes such as cycE, stg and e2f1 close after robust cell cycle exit at 36h (Fig. 2.3I, 2.4E). The closing of these enhancers potentially prevents the reactivation of the complex cell cycle genes and reinforce the robust cell cycle exit. We rigorously investigate whether the enhancers closing is controlled by the cell cycle exit through bypassing the G0 with E2F/CycD/Cdk4 overexpression. Surprisingly, we reveal that the accessibility of cell cycle genes enhancers is developmentally controlled and independent of cell cycling status (Fig. 2.4). Our study directly illustrates how developmental pathway can impinge on cell cycle genes at the chromatin level. It is worth to mention that although the enhancers are not accessible when we bypass cell cycle exit at 44h, ectopic E2F/CycD/Cdk4 activities are still able to utilize the regulatory sites at the open TSS and activate gene expression (Fig. 2.4C). However, the enhancers are probably required for a maximal activation and we observed reduced level of expression compared to 24h (Fig. 2.4C). In addition, there is still repressive mechanism to block cell cycle genes expression at the TSS because most of the simple cell cycle genes have reduced transcriptional activities as well. Altogether, our results reflect robust mechanisms the developmental program utilize to enforce the transition from proliferating to postmitotic state during terminal differentiation.

The developmental control on cell cycle genes is very likely to be exerted through ecdysone pathway. The level of ecdysone pathway activities has been shown to affect cell proliferation during eye development and optic lobe neurogenesis in fly and moth [49–51]. Also, we previously showed that br direct controls the stg expression at 6h.

Whether br controls the expression of other cell cycle genes is still unknow. In addition, br is only expressed at 6h and it is an unexplored question that what are the ecdysone targets that control the enhancers closing of complex cell cycle genes in the late pupal stages. Our study has shed lights on the developmental control on cell cycle program, and provided a stepping stone for future research on the interplay between differentiation and proliferation.

Remarkably, our study also demonstrates that the relationship between developmental pathway and cell cycle regulation is bi-directional and cell cycling status influences the temporal response to ecdysone induced pathways. When we simply delayed cell cycle exit from 24h to 36h or even later, we also delayed the expression of 36h ecdysone targets to 44h and the downstream ecdysone targets were further affected accordingly. The impacts of cell cycle on ecdysone target genes are both from transcriptional and chromatin level. Therefore, the correct timing for cell cycle exit is critical for the temporal activities of ecdysone pathway (Fig. 2.6). Notably, delaying cell cycle exit also compromises the acquisition of differentiation related structure such as cuticle formation (Fig. 2.5). In fact, over-proliferation has been shown to impact the proper differentiation in multiple organisms [14, 51] and the differentiation stage or differentiation grade has been served as an important parameter in histopathological classification of tumor malignancies [52]. Thus, our study provides further direct evidence for the importance of cell cycle exit during terminal differentiation.

Finally, our research proposes a potential role of Blimp-1 in regulating differentiation activities at the mid to late metamorphosis. Blimp-1, directly induced by ecdysone, is a transcriptional repressor and has been well studied in silencing ftz-f1 at

the onset of metamorphosis [53, 54]. Here we show that Blimp-1 is also highly expressed at 36h APF wings and then soon silenced afterwards. Notably, we found that dynamic chromatin regions that are opening at 44h are enriched for Blimp-1 binding sites. Some of the regions are potential regulatory elements for cuticle genes and most interestingly, E74EF (Supp. Fig. 2.8). Since these regions are closed when Blimp-1 is present and only open after Blimp-1 goes away, we propose that Blimp-1 blocks the accessibilities of the dynamic regulatory elements. Interestingly, we also identified Blimp-1 binding sites at a dynamic open region at ftz-f1 locus. This region is transiently open at 6h when Blimp-1 is absent and ftz-f1 is expressed, reminiscent of the pattern for E74EF at 44h. Future work is needed to examine the regulation of chromatin accessibilities by Blimp-1.

In summary, we characterize the crosstalk between differentiation program and cell cycle program during metamorphosis and we provide direct evidence for their mutual impacts, which are mediated through chromatin accessibilities and gene expression.

2.5 Materials and Methods

2.5.1 Fly stocks and genetics

FAIRE and RNA seq samples with genetic manipulations:

w/ y, w, hs-FLP; tub>CD2>GAL4, UAS-GFP/ +; tub-gal80TS/ +

w/ y, w, hs-FLP; tub>CD2>GAL4, UAS-GFP/ UAS-E2F1, UAS-DP; tub-gal80TS/ +

w/ y, w, hs-FLP; tub>CD2>GAL4, UAS-GFP/ UAS-CycD, UAS-Cdk4; tub-gal80TS/ UAS-E2F1, UAS-DP

Crosses were set up in 25 °C. Second instar larva (L2) were heat shocked in 37 °C for 42 min, then kept in 18 °C. White prepupal were collected and kept in 18 °C until12h APF. Then pupal were shifted to 28 °C until 24h APF or 44h APF for dissection.

TEM, chitin and Ph3 staining:

w/y, w, hs-FLP; Ap-GAL4, UAS-GFP/ +; tub-gal80TS/ +

w/y, w, hs-FLP; Ap-GAL4, UAS-GFP/ UAS-E2F1, UAS-DP; tub-gal80TS/ +

w/y, w, hs-FLP; Ap-GAL4, UAS-GFP/ UAS-CycD, UAS-Cdk4; tub-gal80TS/ UAS-E2F1, UAS-DP

Crosses were set up and kept in 18 °C. White prepupal were collected and aged to 12h APF, then shifted to 28 °C until 24h APF, 44h APF (PH3 staining) or 64h APF (TEM and chitin staining).

Blimp-1 antibody staining:

w/y, w, hs-FLP; en-GAL4, UAS-GFP/ +; tub-gal80TS/ +

w/y, w, hs-FLP; en-GAL4, UAS-GFP/ UAS-CycD, UAS-Cdk4; tub-gal80TS/ UAS-E2F1, UAS-DP

w/y, w, hs-FLP; en-GAL4, UAS-GFP/ Blimp-1^{RNAi} (BL 57479), UAS-DP; tub-gal80TS/ +

w/y, w, hs-FLP; en-GAL4, UAS-GFP/ +; tub-gal80TS/ white^{RNAi}

Crosses were set up and kept in 18 °C. White prepupal were collected and shifted to 28 °C until 36h APF or 40-42h APF for immunostaining.

PCNA reporter

PCNA-EmGFP/ y, w, hs-FLP; +; act>CD2>gal4, UAS-RFP/+

PCNA-EmGFP/ y, w, hs-FLP; UAS-E2F1, UAS-DP /+; act>CD2>gal4, UAS-RFP/+

PCNA-EmGFP/ y, w, hs-FLP; +/UAS-CycD, UAS-Cdk4; act>CD2>gal4, UAS-RFP/ UAS-E2F1, UAS-DP

Crosses were set up and kept in 25 °C, then 26h pupal were heat shocked in 37 °C for 12 min and left in 25 °C until 42h APF for dissection.

Gal4 reporters

Transgenic flies were crossed with UAS-GFP (cpr51A region, VT016704) or UAS-dsGFP (stg region, BL 45208 and e2f1 region, VT045332) in 25 °C. Then larval or staged pupal were dissected and immunostained for GFP.

2.5.2 Sample preparation and data analysis for high-throughput sequencing

FAIRE samples and RNA samples were prepared as described previously [55–57]. FAIRE-seq sequencing reads were aligned to the dm6 reference genome using Bowtie2 [58]. FAIRE-seq peak calling were performed using MACS2 [59] and PePr [60] with q-value threshold at 0.01, and only common peaks from both programs were utilized for further analysis. Z-scores were calculated using the mean and standard deviation per chromosome arm. High fidelity peaks were chosen from peaks with maximal Z-score larger than 2. FAIRE-seq line plots were generated using deepTools [61]. FAIRE-seq were visualized using Integrative Genomics Viewer [62]. DNA-binding motifs used for enrichment analysis were obtained from FlyFactorSurvey [63]. Motif de novo discovery, comparison with known motif and motif enrichment analysis were using the MEME tool, TOMTOM tool and AME tool in MEME suite [64]. Annotation of FAIRE peaks were carried out by assigning peaks to nearest TSS in R package ChIPpeakAnno [65]. RNA-seq sequencing reads were aligned to the dm6 reference genome using STAR [66], and further counted using HTSeq [67]. RPKM values of RNA-seq were calculated through Cufflinks [68]. Differentially expressed genes were defined as those having RPKM >1 in at least one stage and changing by at least twofold between pairwise time points. GO analysis was performed using DAVID (Database for

Annotation, Visualization, and Integrated Discovery) [69]. All the statistical comparisons are carried out in Deseq2 [70].

2.5.3 Immunostaining and Microscopy

Immunostaining procedures were carried out as previously described [44]. Primary antibodies used in this study include: Anti-phospho-Ser10 histone H3, 1:2000 rabbit (Millipore #06-570) or mouse (Cell Signaling #9706); Anti-GFP, 1:1000 chicken (Life Technologies A10262) or 1:1000 rabbit (Life Technologies A11122); Anti-Blimp-1, 1:500 rabbit (Active motif 61054). DNA was labeled by 1 ug/ml DAPI in 1× PBS, 0.1% Triton X for 10 min and chitin was stained by 50 ug/ml Fluorescent Brightener 28 (Sigma-Aldrich, F3543) in 1× PBS, 0.1% Triton X for 10 min. Images of were obtained using a Leica SP5 confocal (chitin staining) or Leica DMI6000B epifluorescence system.

2.5.4 Transmission electron microscopy

Tissue was incubated in Karnovski's fixative for at least 1hr at room temperature, then overnight at 4 degrees. Samples were washed with 20x volume Sorenson's buffer 3x, before post-fixing in 2% osmium tetroxide in Sorenson's buffer for 1hr at RT. Tissue was again washed 3x with 20x volume Sorenson's buffer, then dehydrated through ascending concentrations of acetone and embedded in EMbed 812 epoxy resin. Semi-thin sections were stained with toluidine blue for tissue identification. Selected regions of interest were ultra-thin sectioned 70 nm in thickness and post stained with uranyl acetate and Reynolds lead citrate. They were examined using a JEOL JEM-1400 Plus transmission electron microscope (TEM) at 80 kV.

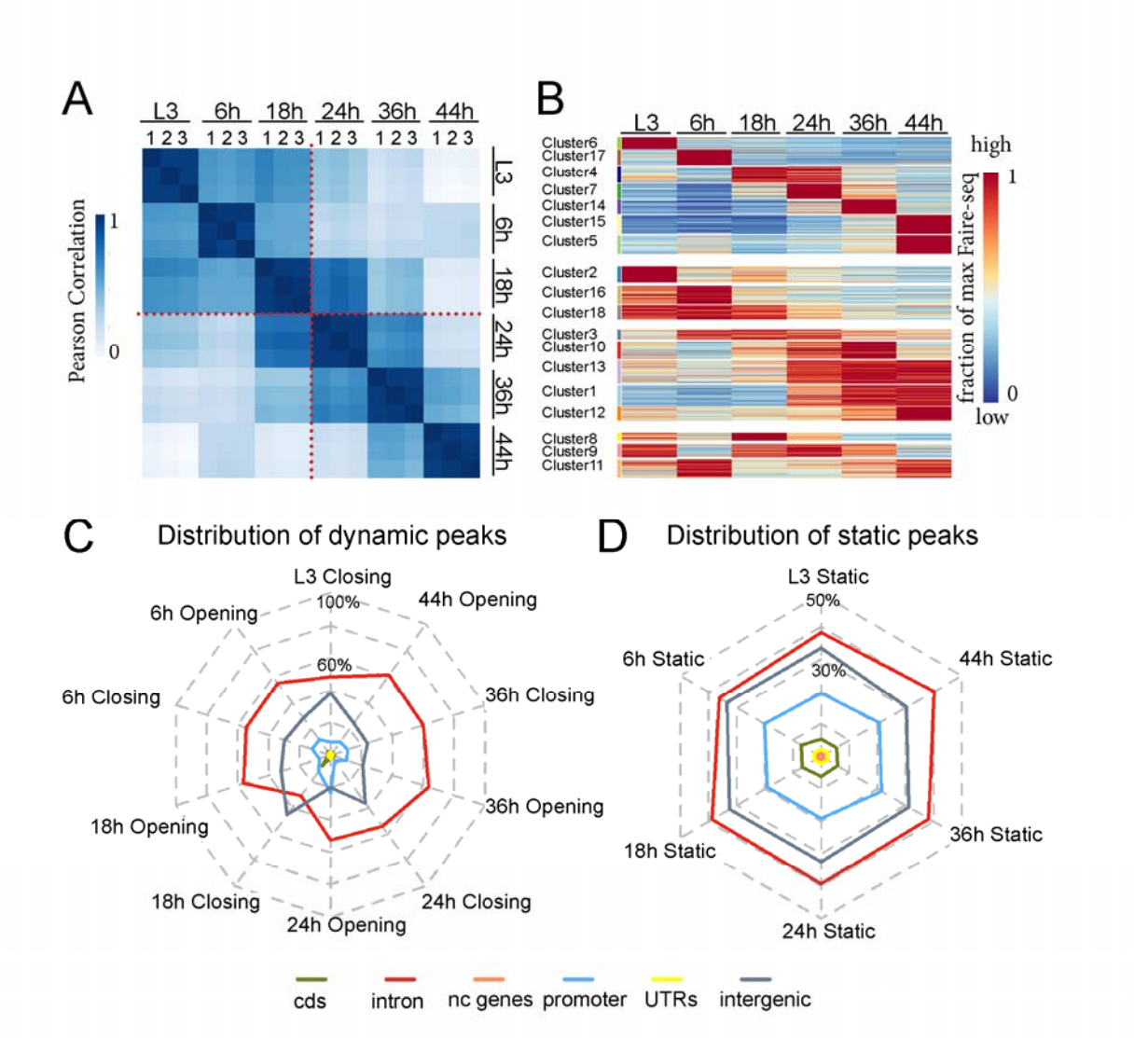

Figure 2.1 Chromatin accessibility dynamics during metamorphosis. (A) Open chromatin regions (peaks) in wings were identified by FAIRE-Seq on timepoints prior to (L3) and during metamorphosis 6h, 18h, 24h, 36h and 44h APF. Heatmaps of Pearson correlation coefficients across this timecourse reveal differences between the proliferative and postmitotic stages (red dotted line). (B) Dynamic open chromatin peaks were organized into 18 k-means clusters, displayed as a heatmap representing the fraction of the maximum FAIRE rpkm value. (C, D) Radar charts display the distribution of dynamic (C) and static (D) peaks between neighboring stages in cds, intron, non-coding genes (nc genes), proximal promoter (-500bp to 150 bp of TSS), UTRs and intergenic regions as percentages of the total peaks. For dynamic peaks, “closing” is defined as peaks that decrease in accessibility by >2-fold at the next stage, conversely “opening” indicates peaks that increase in accessibility by >2-fold at the next stage. Peaks without significant changes between subsequent timepoints were defined as “static”.

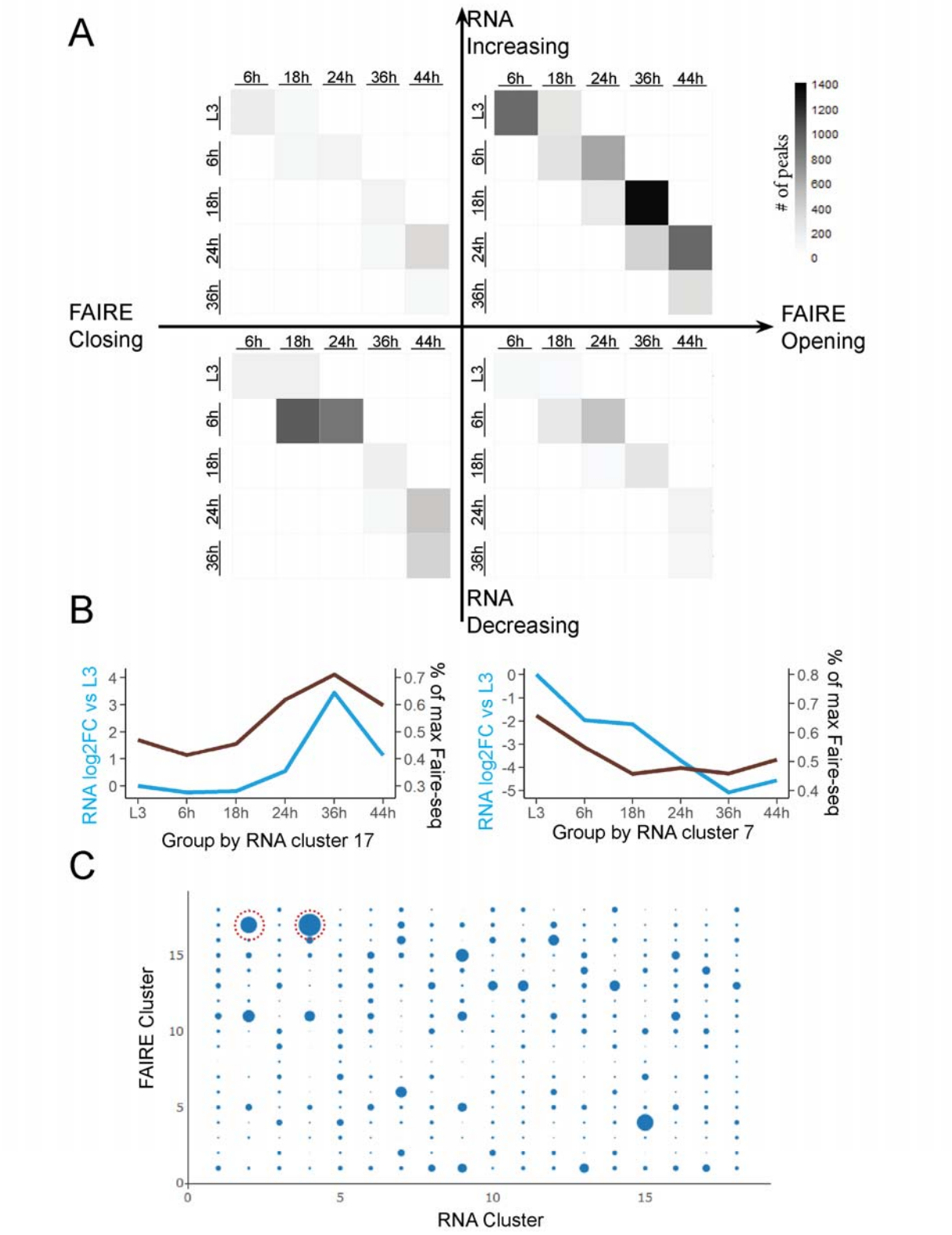
A
RNA Increasing
RNA Decreasing
FAIRE Closing
FAIRE Opening
6h
18h
24h
36h
44h
L3
# of peaks
1400
1200
1000
800
600
400
200
0
B
RNA log2FC vs L3
% of max Faire-seq
Group by RNA cluster 17
Group by RNA cluster 7
C
FAIRE Cluster
RNA Cluster

Figure 2.2 Most chromatin accessibility changes are associated with gene activation rather than repression during metamorphosis. (A) We assigned dynamic FAIRE peaks to the nearest expressed gene and correlated peak changes (opening or closing) with observed gene expression changes (increasing or decreasing) measured by RNAseq at each subsequent timepoint. This revealed four classes of FAIRE peak/RNA expression correlations; opening/increasing consistent with gene activation, closing/decreasing consistent with loss of activation; opening/decreasing consistent with binding of a repressor and closing/activation consistent with a loss of repression. We show the number of dynamic FAIRE peaks that fall into each quadrant as a heatmap. The majority of dynamic FAIRE peaks open during metamorphosis and are associated with increased expression of the nearest gene. (B) Genes were clustered based upon RNA expression patterns across metamorphosis. Two clusters showing a high positive correlation between RNA signal (average $\log_2$ fold change from L3) and accessibility of their assigned FAIRE peaks (average maximum FAIRE rpkm value) are shown. The full dataset correlating RNA expression with accessibility of their assigned FAIRE peaks for all clusters is provided in the supplement. (C) To visualize the temporal coordination between RNA expression dynamics and chromatin accessibility dynamics, we organized genes into 18 co-regulated RNAseq clusters by k-means analysis (x-axis) and plotted the distribution of FAIRE peaks assigned to each gene across the FAIRE k-means clusters (y-axis). The bubble size indicates the number of FAIRE peaks within each FAIRE cluster that are assigned to a gene within the indicated RNAseq cluster. Large bubbles show the overlap of temporally co-regulated RNAs with co-regulated chromatin accessibility changes.

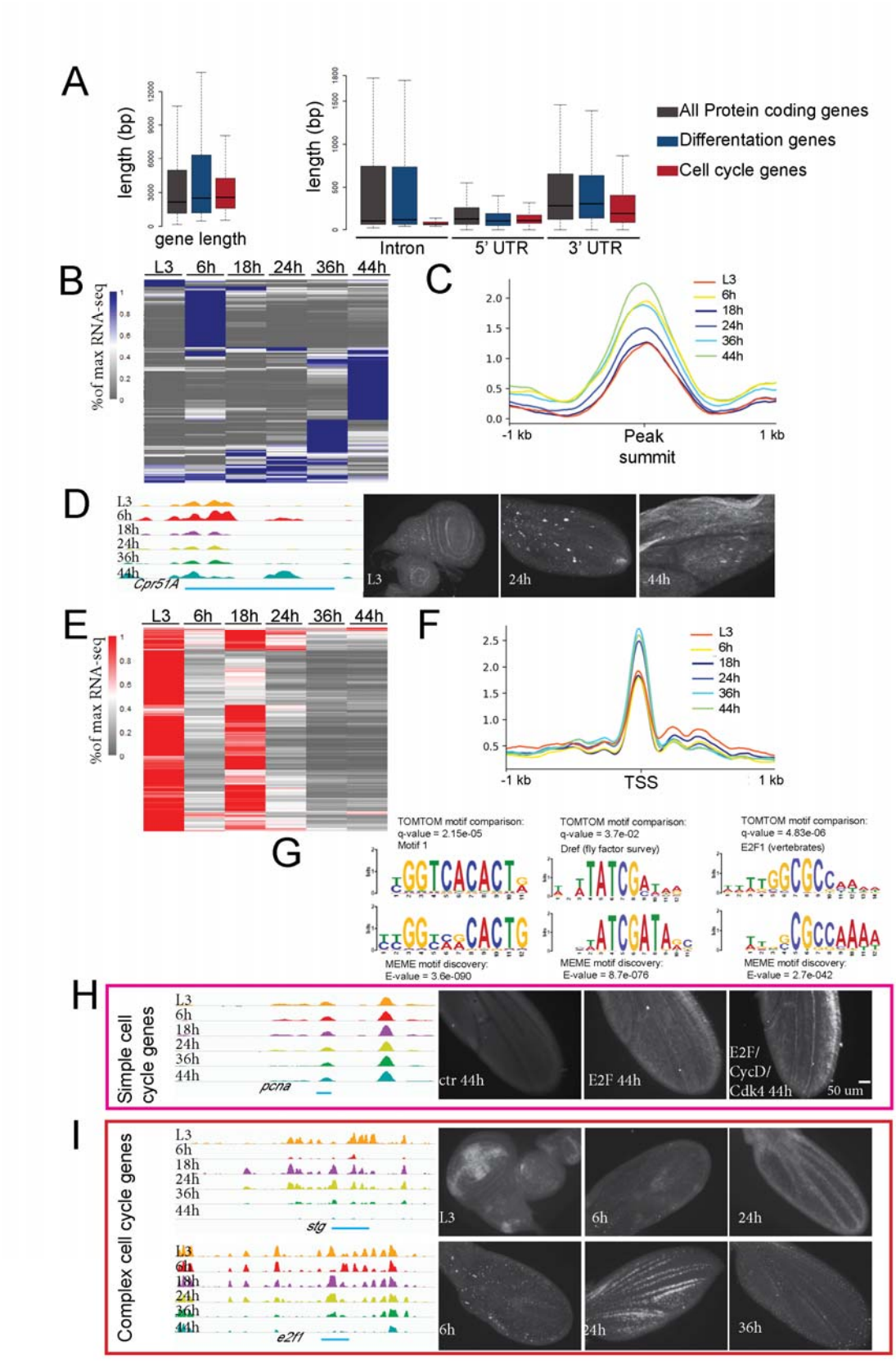
A
length (bp)
gene length
length (bp)
Intron
5' UTR
3' UTR
All Protein coding genes
Differentation genes
Cell cycle genes
B
L3 6h 18h 24h 36h 44h
%of max RNA-seq
C
L3
6h
18h
24h
36h
44h
-1 kb
Peak summit
1 kb
D
L3
6h
18h
24h
36h
44h
Cpr51A
L3
24h
44h
E
L3 6h 18h 24h 36h 44h
%of max RNA-seq
F
L3
6h
18h
24h
36h
44h
-1 kb
TSS
1 kb
G
TOMTOM motif comparison:
q-value = 2.15e-05
Motif 1
TOMTOM motif comparison:
q-value = 3.7e-02
Dref (fly factor survey)
TOMTOM motif comparison:
q-value = 4.83e-06
E2F1 (vertebrates)
MEME motif discovery:
E-value = 3.6e-090
MEME motif discovery:
E-value = 8.7e-076
MEME motif discovery:
E-value = 2.7e-042
H
Simple cell cycle genes
L3
6h
18h
24h
36h
44h
pcna
ctr 44h
E2F 44h
E2F/ CycD/ Cdk4 44h
50 um
I
Complex cell cycle genes
L3
6h
18h
24h
36h
44h
stg
e2f1
L3
6h
24h
6h
24h
36h

Figure 2.3 Temporal regulation of the wing differentiation program and cell cycle changes. (A) The length (in bp) of genes (left), introns, 5' and 3' UTRs (right) for all protein coding genes, wing differentiation genes and cell cycle genes. The majority of FAIRE peaks occur within introns (Fig. 2.1). Most cell cycle genes have a compact structure with few, short introns, while differentiation genes contain large introns, providing potential dynamic regulatory elements. (B, E) Heatmap of gene expression for differentiation genes (B) and cell cycle genes (E), plotted by the % of maximum RNA rpkm value. Both groups of genes show dynamic expression during metamorphosis. (C, F) Line plots of average FAIRE signal of the 6 stages for differentiation genes (C) and cell cycle genes (F). Differentiation genes show an increase in FAIRE peak accessibility at timepoints when gene expression is high (6, 36 and 44h). By contrast, cell cycle genes show an moderate increase in accessibility at timepoints when gene expression is repressed (24, 36, 44h) (D, I) A Gal4 reporter containing the indicated (blue line) portion of the Cpr51A regulatory region drives UAS-GFP in late wings (44h) when the regulatory elements are accessible. (G) Motif discovery was performed on FAIRE peaks for cell cycle genes using MEME and compared to known motifs using TOMTOM. Potential regulatory elements for cell cycle genes are highly enriched for E2F binding motifs, DRE promoter sequences and the PolII pausing-associated motif1. (H) A GFP reporter containing the indicated regulatory element for the simple cell cycle gene, *pcna* is silent at the postmitotic stage of 44h, but can be re-activated postmitotically when E2F or E2F+CycD/Cdk4 is expressed. *Stg* and *e2f1* are complex cell cycle genes with large dynamic regulatory regions. Gal4 reporters containing the indicated portions of their regulatory regions drives UAS-degradable-GFP to capture their regulatory dynamics. Expression correlates with accessibility for these regions.

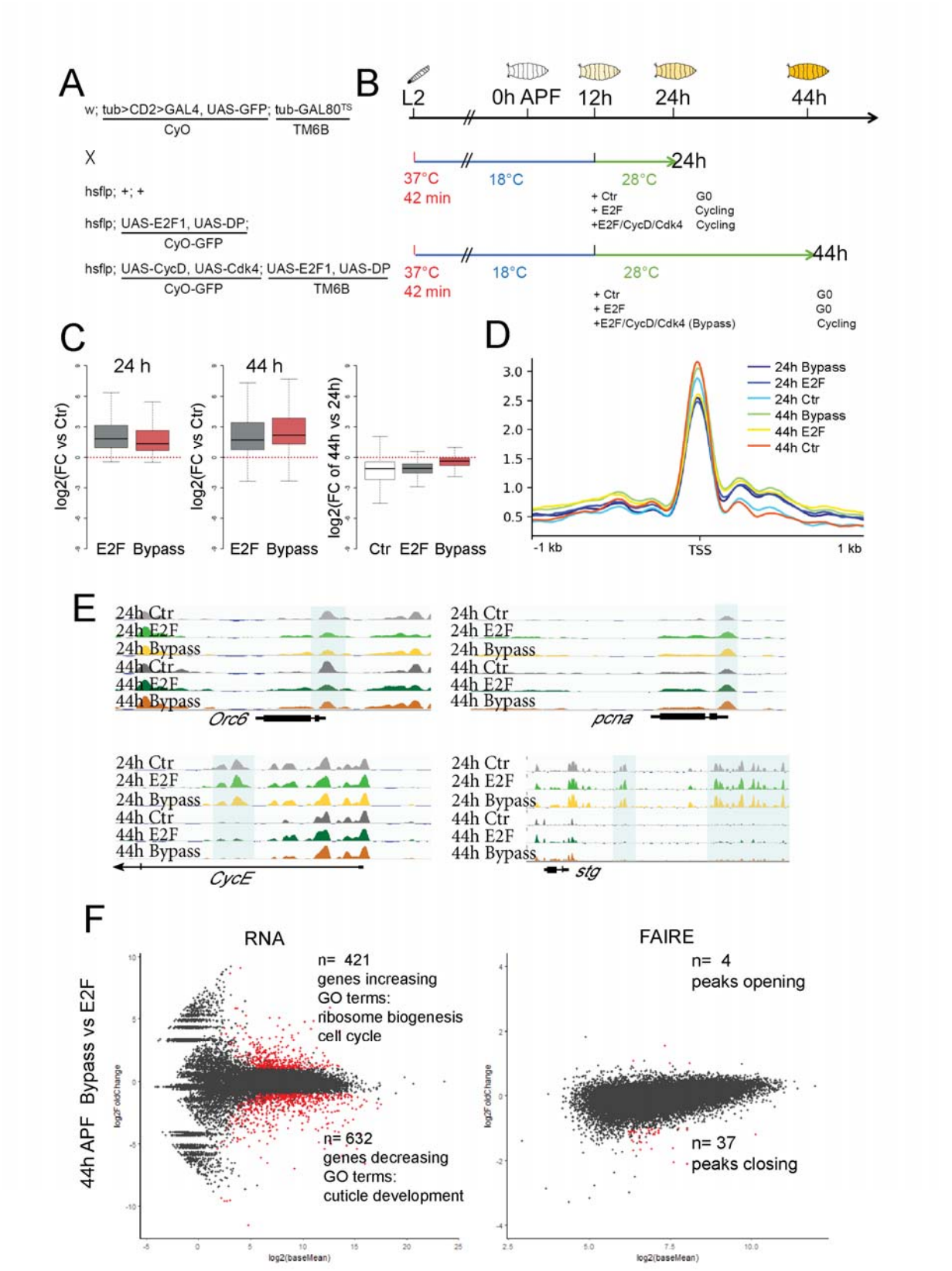
A
w; tub>CD2>GAL4, UAS-GFP; tub-GAL80TS
CyO
TM6B
X
hsflp; +; +
hsflp; UAS-E2F1, UAS-DP;
CyO-GFP
hsflp; UAS-CycD, UAS-Cdk4; UAS-E2F1, UAS-DP
CyO-GFP
TM6B
B
L2
0h APF
12h
24h
44h
37°C
42 min
18°C
28°C
+ Ctr
+ E2F
+E2F/CycD/Cdk4
G0
Cycling
Cycling
24h
44h
+ Ctr
+ E2F
+E2F/CycD/Cdk4 (Bypass)
G0
G0
Cycling
C
24 h
44 h
log2(FC vs Ctr)
log2(FC of 44h vs 24h)
E2F Bypass
E2F Bypass
Ctr E2F Bypass
D
24h Bypass
24h E2F
24h Ctr
44h Bypass
44h E2F
44h Ctr
-1 kb
TSS
1 kb
E
24h Ctr
24h E2F
24h Bypass
44h Ctr
44h E2F
44h Bypass
Orc6
pcna
CycE
stg
F
RNA
FAIRE
44h APF Bypass vs E2F
n= 421
genes increasing
GO terms:
ribosome biogenesis
cell cycle
n= 632
genes decreasing
GO terms:
cuticle development
n= 4
peaks opening
n= 37
peaks closing
log2(baseMean)

Figure 2.4 Enhancer accessibility of complex cell cycle genes is developmentally controlled and independent of cell cycling status. (A, B) Genotype and scheme of experiments to disrupt cell cycle exit during metamorphosis. E2F activation delays cell cycle exit to 36h while E2F+CycD/Cdk4 bypasses cell cycle exit until after 50h. (C) Expression of cell cycle genes is increased when we delay or bypass cell cycle exit (log2 fold change for cell cycle genes vs. controls expressing GFP). (D) Line plots of average FAIRE signal for cell cycle genes. Accessibility at most cell cycle genes is slightly decreased when cell cycle exit is delayed or bypassed. (E) Regulatory elements for simple cell cycle genes (*orc6*, *pcna*) remain accessible independent of cycling status. Complex cell cycle genes (*cyce*, *stg*) lose accessibility at regulatory regions independent of cycling status. (F) MA-plots of RNA and FAIRE changes between conditions that delayed cell cycle exit (E2F) and those that bypass exit (E2F+CycD/cdk4) at 44h. Abundant changes in expression of cell cycle genes, ribosome biogenesis and cuticle formation genes are observed, while chromatin accessibility is nearly identical between conditions where cells enter a delayed G0 vs continue cycling.

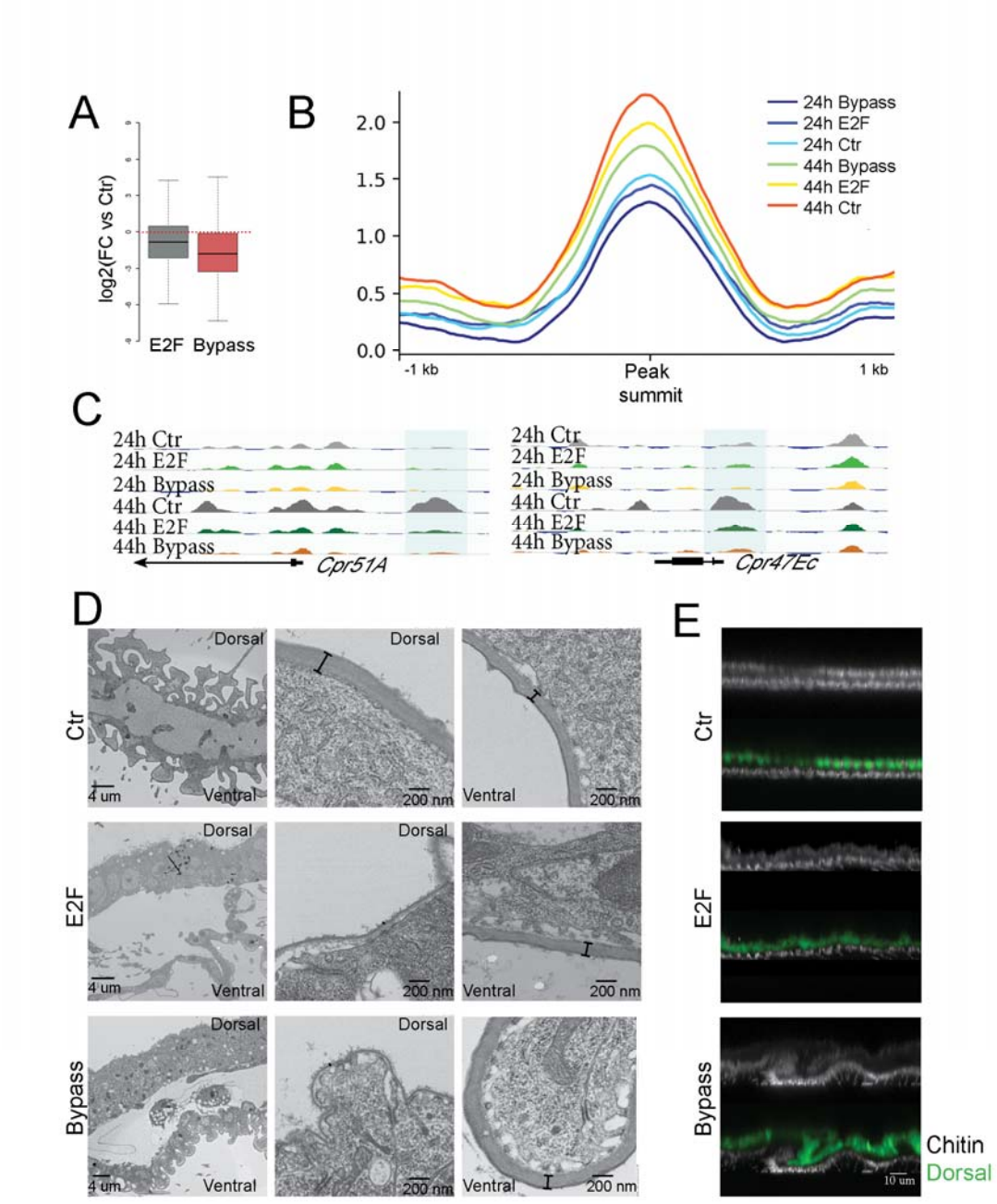

Figure 2.5 Compromising cell cycle exit impacts chromatin accessibility and gene expression at a subset of wing terminal differentiation genes. (A) log2 fold changes in RNA and (B) line plots of average FAIRE signal for genes involved in cuticle formation and differentiation. Delaying or preventing cell cycle exit reduces their expression and chromatin accessibility. (C) Selected cuticle protein genes exhibiting a failure to open potential regulatory elements at 44h when cell cycle exit is delayed or bypassed. (D, E) TEM (D) and chitin staining (E) of 64h wings that delayed or bypass cell cycle exit in the dorsal wing epithelium using *Apterous*-Gal4/Gal80^{ts} to activate E2F or E2F+CycD/Cdk4 expression during the final cell cycle. Extra cellular matrix formation and chitin deposition are disrupted when cell cycle exit is compromised.

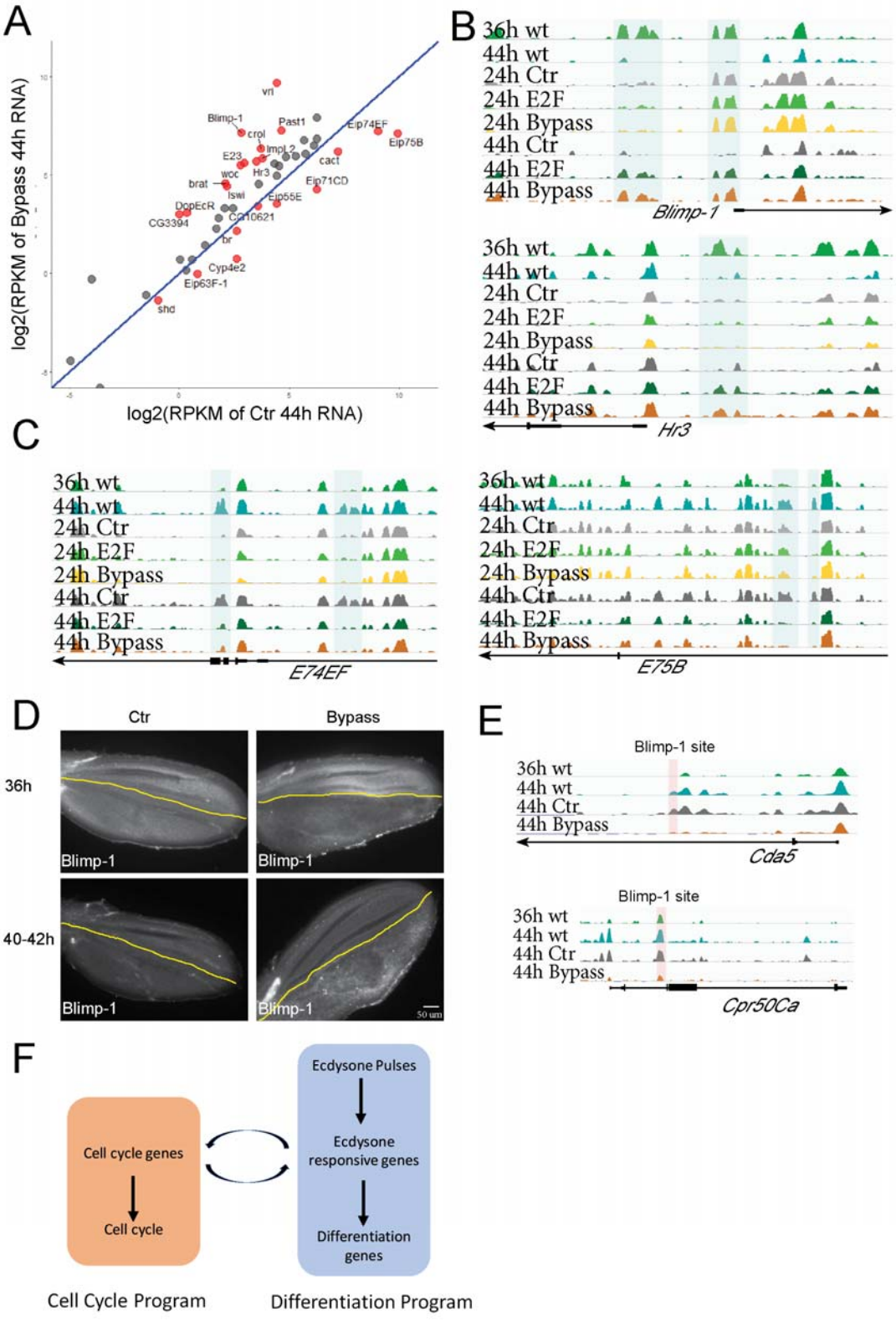
A
log2(RPKM of Bypass 44h RNA)
log2(RPKM of Ctr 44h RNA)
vri
Blimp-1
Past1
Eip74EF
Eip75B
crol
Impl2
E23
cact
Hr3
woc
brat
Eip71CD
Iswi
Eip55E
DopEcR
CG10621
CG3394
br
Cyp4e2
Eip63F-1
shd
B
36h wt
44h wt
24h Ctr
24h E2F
24h Bypass
44h Ctr
44h E2F
44h Bypass
Blimp-1
Hr3
C
E74EF
E75B
D
Ctr
Bypass
36h
40-42h
Blimp-1
50 um
E
Blimp-1 site
Cda5
Cpr50Ca
F
Cell cycle genes
Cell cycle
Ecdysone Pulses
Ecdysone responsive genes
Differentiation genes
Cell Cycle Program
Differentiation Program

Figure 2.6 Bypassing cell cycle exit disrupts chromatin dynamics at ecdysone target genes and alters their expression. (A) Scatterplot of ecdysone responsive genes in 44h wings under conditions that bypass cell cycle exit vs. controls with normal exit. Genes with significant changes in expression are labeled in red. (B, C) Chromatin regions of *Blimp-1*, *Hr3*, *E74* and *E75* fail to close or open at 44h when cell cycle exit is compromised. (D) Blimp-1 antibody staining of wings at 36h and 40-42h wings with normal cell cycle exit (Ctr) or bypassed cell cycle exit in the posterior (using *engrailed*-Gal4/Gal80^{ts}). Compromising cell cycle exit delays the activation of Blimp-1 in a compartment autonomous manner. (E) Peaks that fail to open at 44h from selective cuticle development genes harbor high scoring Blimp-1 binding sites, suggesting them as potential direct Blimp-1 targets. (F) Model of the crosstalk between cell cycle program and differentiation program.

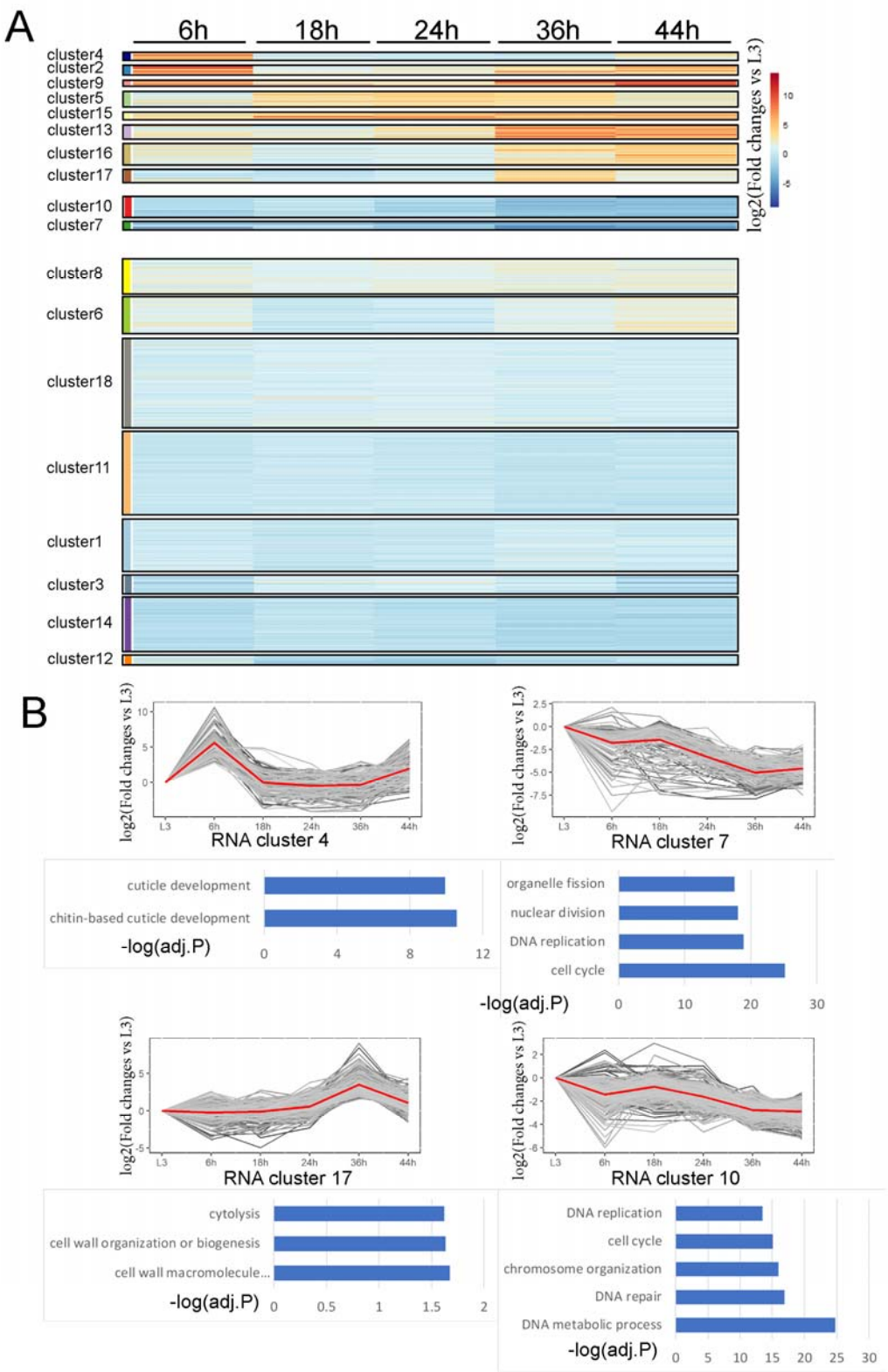
A
6h
18h
24h
36h
44h
cluster4
cluster2
cluster9
cluster5
cluster15
cluster13
cluster16
cluster17
cluster10
cluster7
cluster8
cluster6
cluster18
cluster11
cluster1
cluster3
cluster14
cluster12
log2(Fold changes vs L3)
B
RNA cluster 4
RNA cluster 7
cuticle development
chitin-based cuticle development
-log(adj.P)
organelle fission
nuclear division
DNA replication
cell cycle
RNA cluster 17
RNA cluster 10
cytolysis
cell wall organization or biogenesis
cell wall macromolecule...
DNA repair
DNA metabolic process
chromosome organization

Figure S2.1 Gene expression is dynamic during metamorphosis. (A) Heatmap of RNA log2 fold change vs L3 for the indicated stages. The pattern of RNA changes during metamorphosis is separated into 18 k-means clusters. (B) Line plots of the log2 fold change vs L3 for the indicated RNA clusters. Each gene is represented by a single gray line and the average of all genes for the given cluster is plotted in red line. GO term enrichments are also shown along with their adjust P-values. During metamorphosis differentiation related genes such as cuticle development are activated while cell cycle genes are repressed.

Figure S2.2 Open chromatins are enriched in regions of 1-5 kb to TSS and most of the open chromatins are shared between immediately neighboring stages. (A) Pie charts of the proportion of dynamic peaks and static peaks for each stage. (B, C) Radar charts display the distribution of dynamic (B) and static (C) peaks between neighboring stages in different distances to TSS as percentages of the total peaks.

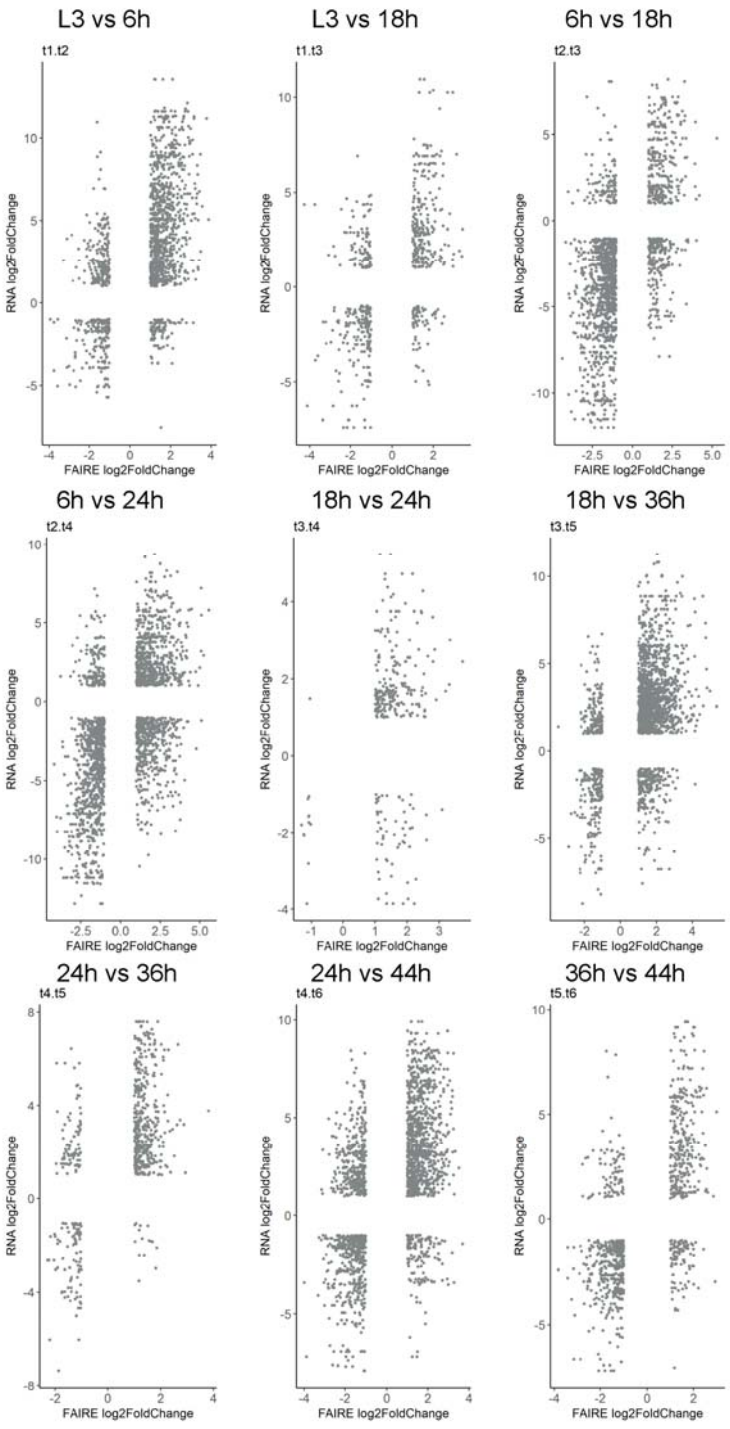

Figure S2.3 The majority of dynamic open chromatin is associated with gene activation rather than gene repression. Scatterplots of FAIRE peaks and corresponding genes with significant changes between 2 sequential stages. Significance is defined by 2-fold changes and adjust P-value less than 0.05.

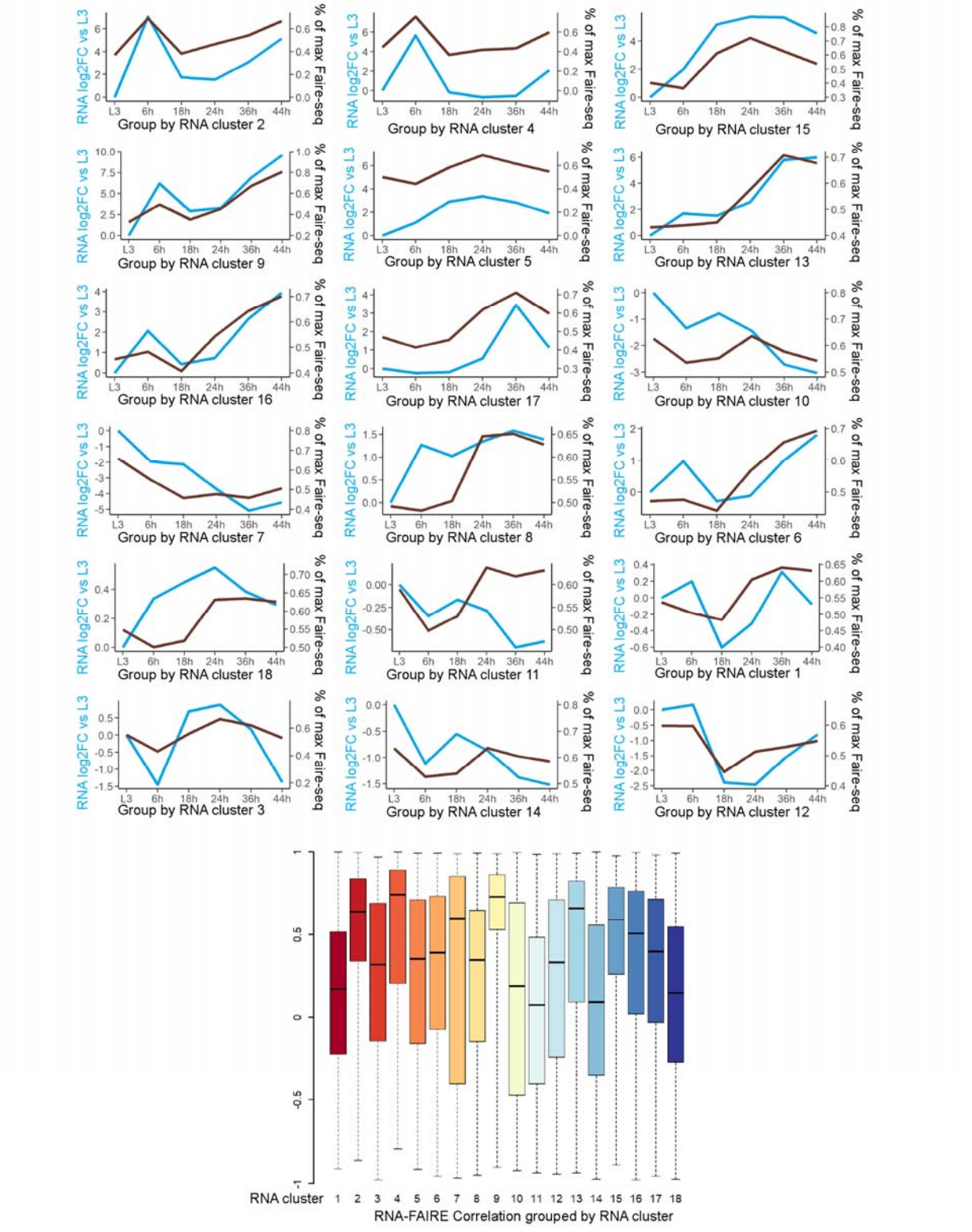

Figure S2.4 Coordination of RNA and Faire changes grouped by RNA cluster. Trajectories of average changes between genes and their corresponding FAIRE peaks over the 6 stages for each of the 18 RNA clusters. Boxplot of the Pearson correlation coefficients between RNA and FAIRE for each RNA cluster is shown.

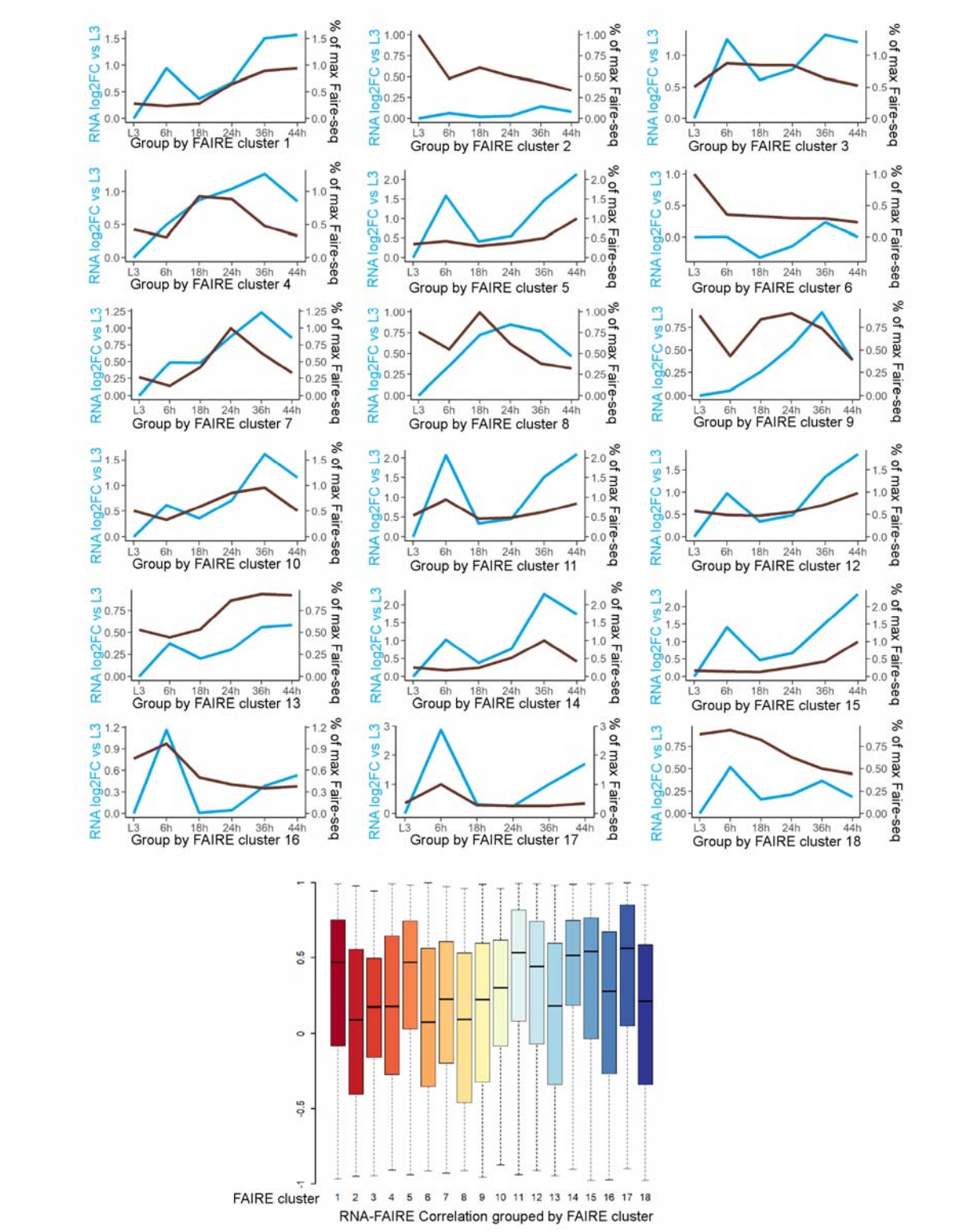

Figure S2.5 Coordination of RNA and Faire changes grouped by FAIRE cluster. Trajectories of average changes between FAIRE peaks and their corresponding genes over the 6 stages for each of the 18 FAIRE clusters. Boxplot of the Pearson correlation coefficients between RNA and FAIRE for each FAIRE cluster is shown.

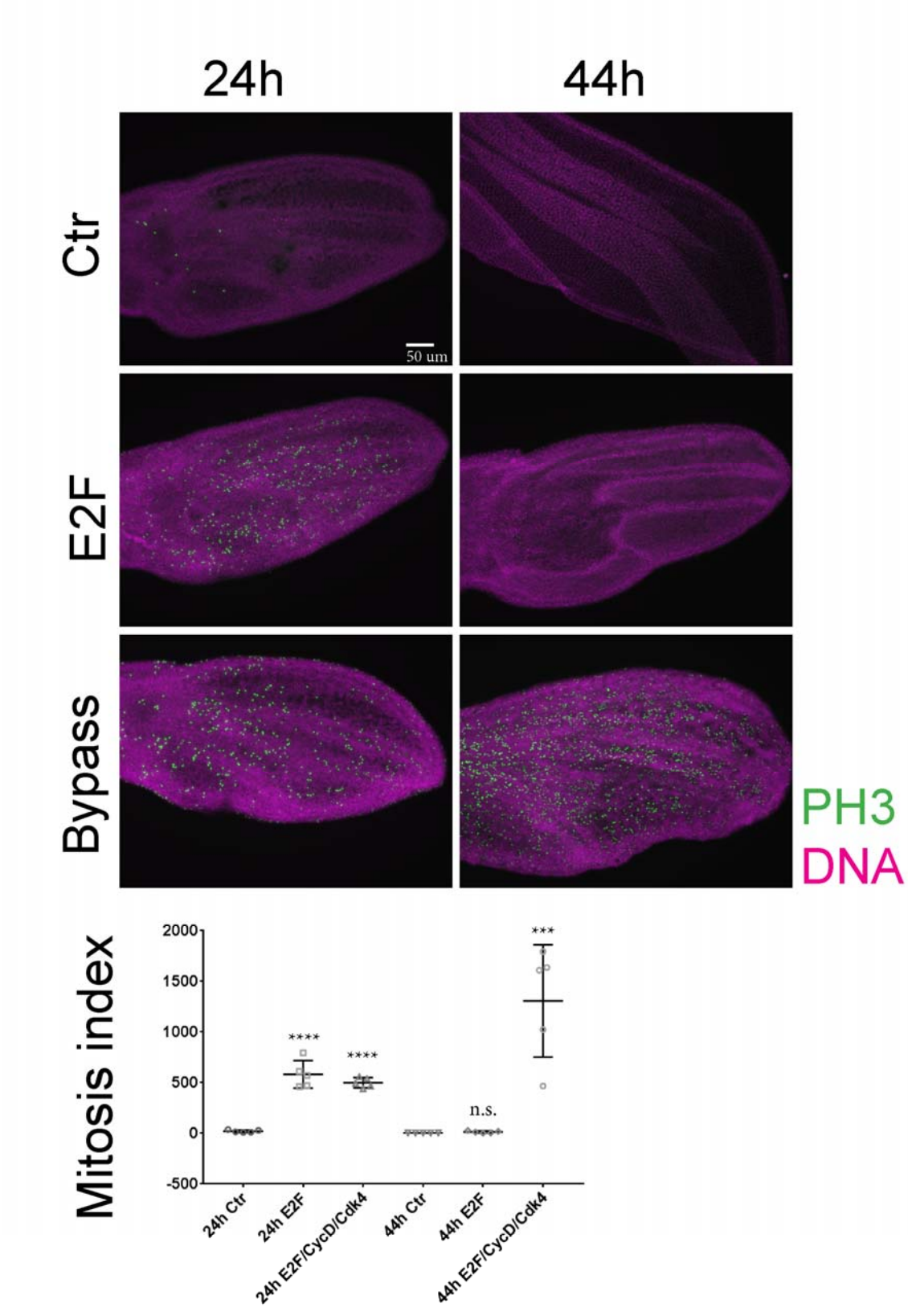
24h
44h
Ctr
E2F
Bypass
50 um
PH3
DNA
Mitosis index
2000
1500
1000
500
0
-500
****
****
n.s.
***
24h Ctr
24h E2F
24h E2F/CycD/Cdk4
44h Ctr
44h E2F
44h E2F/CycD/Cdk4

Figure S2.6 Two stages of G0 exist in differentiating wings. E2F or E2F/CycD/Cdk4 (bypass) was overexpressed in the dorsal layer of wing epithelia under the control of *Apterous*-Gal4/Gal80^{ts} from 12h APF. 24h and 44h wings were immunostained against phospho-histone H3 (ph3). The number of PH3 spots of each wing is counted and 5 wings for each genotype are quantified. P-values were determined by an unpaired t-test; **** <0.0001, ***<0.001.

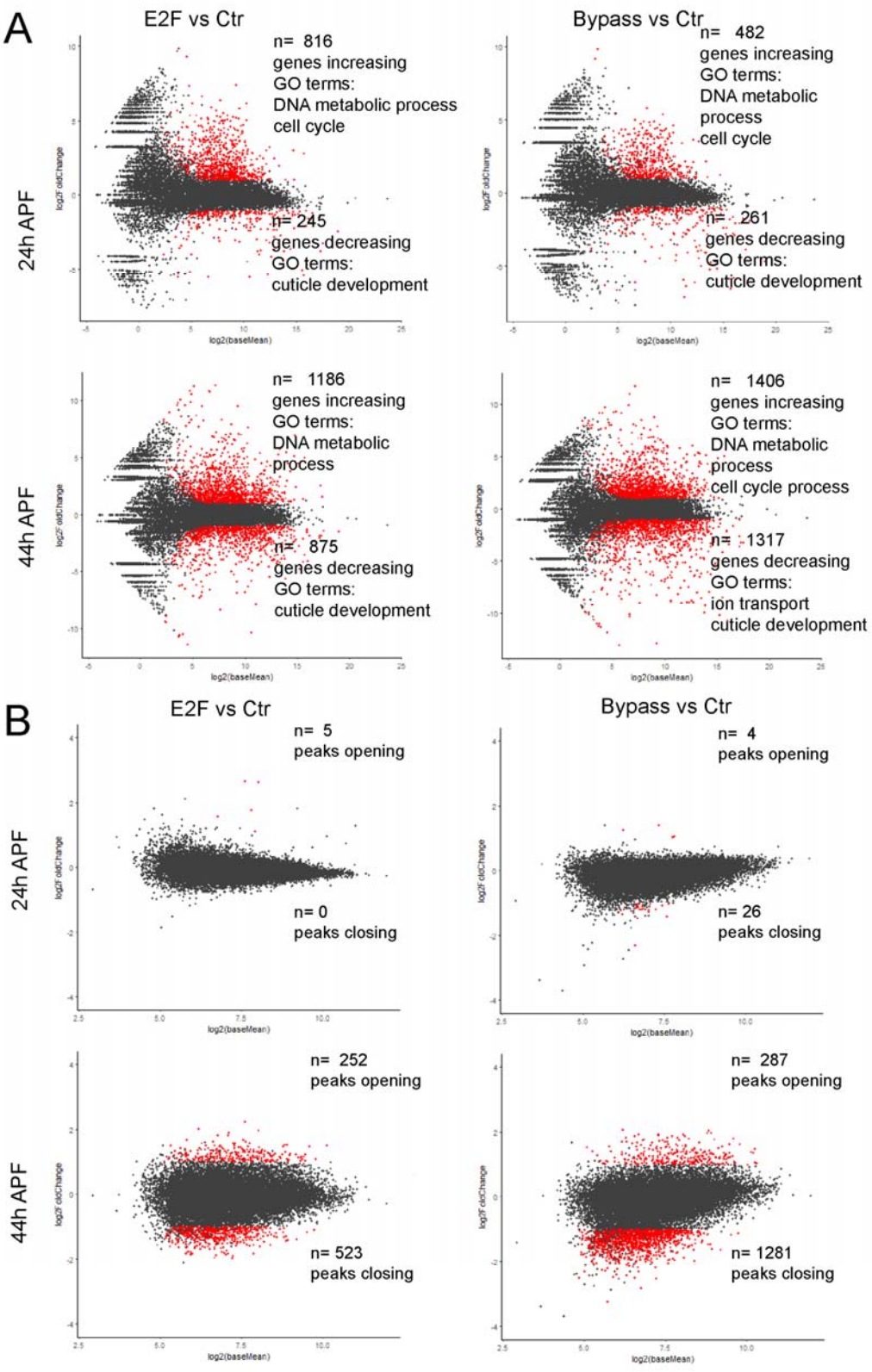
A
E2F vs Ctr
Bypass vs Ctr
24h APF
44h APF
n= 816
genes increasing
GO terms:
DNA metabolic process
cell cycle
n= 245
genes decreasing
GO terms:
cuticle development
n= 482
genes increasing
GO terms:
DNA metabolic
process
cell cycle
n= 261
genes decreasing
GO terms:
cuticle development
n= 1186
genes increasing
GO terms:
DNA metabolic
process
n= 875
genes decreasing
GO terms:
cuticle development
n= 1406
genes increasing
GO terms:
DNA metabolic
process
cell cycle process
n= 1317
genes decreasing
GO terms:
ion transport
cuticle development
log2(baseMean)
B
E2F vs Ctr
Bypass vs Ctr
n= 5
peaks opening
n= 0
peaks closing
n= 4
peaks opening
n= 26
peaks closing
n= 252
peaks opening
n= 523
peaks closing
n= 287
peaks opening
n= 1281
peaks closing

Figure S2.7 RNA and FAIRE changes when G0 is compromised by E2F or E2F/CycD/Cdk4. MA-plots of RNA (A) and FAIRE (B) changes of 24 and 44h wings compared to control. Genes and peaks that are significant in changes with 2-fold difference and adjusted P-value less than 0.05 are labeled in red.

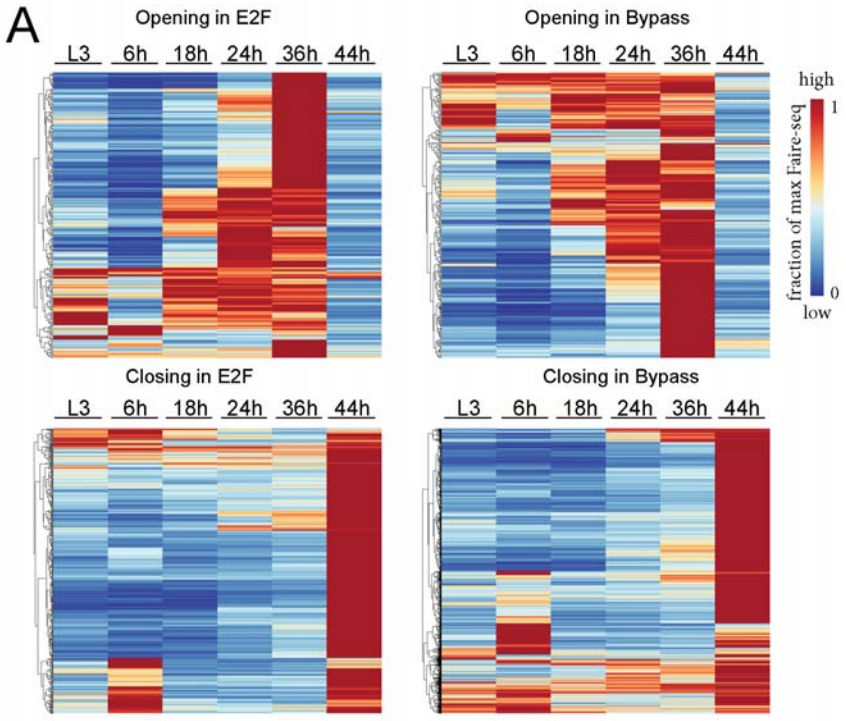

B

Opening in E2F	Opening in Bypass
Adj.P 1.60e-4	Adj.P 5.02e-11
Closing in E2F	**Closing in Bypass**
Adj.P 2.76e-10	Adj.P 1.30e-25

C

Gene	Adjust. P-value
Eip74EF	0.0381
Cyp303a1	0.0271
Spn88Ea	0.0271
TwdlT	0.0351
CG17600	0.0351
pgant2	0.0329
CG17127	0.0351
Cpr47Ec	0.0271
Cpr50Ca	0.0271
CG14257	0.0271
Cda5	0.0351

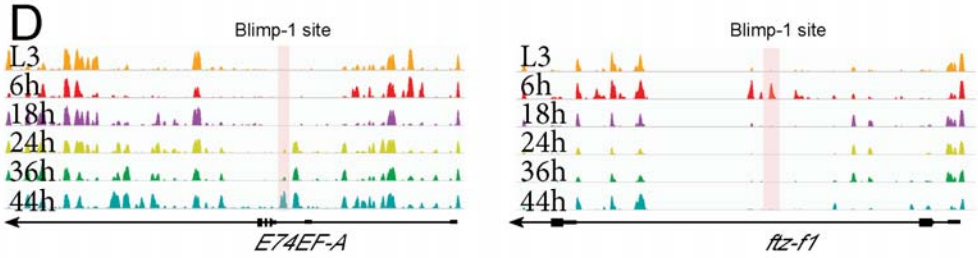

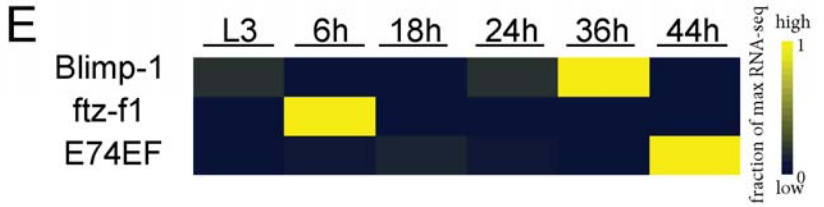

Figure S2.8 Compromising G0 disrupts the temporal dynamics of open chromatin. (A) Heatmap shows the temporal dynamics during normal development for the peaks that are more accessible or less accessible at 44h wings with E2F or E2F/CycD/Cdk4 overexpression, plotted as a fraction of the maximum FAIRE rpkm value. Compromising G0 by E2F or bypass leads to the failure of proper closing of 36h peaks as well as the opening of 44h peaks. (B) Blimp-1 motif is enriched in the dynamic peaks disrupted by E2F or bypass through AME analysis. (C) List of genes containing peaks that fail to open at 44h with high scoring Blimp-1 binding sites. (D) Chromatin accessibility changes at *E74EF* and *ftz-f1* locus with Blimp-2 binding sites shown. (E) Expression changes of *Blimp-1, ftz-f1* and *E74EF* during normal development.

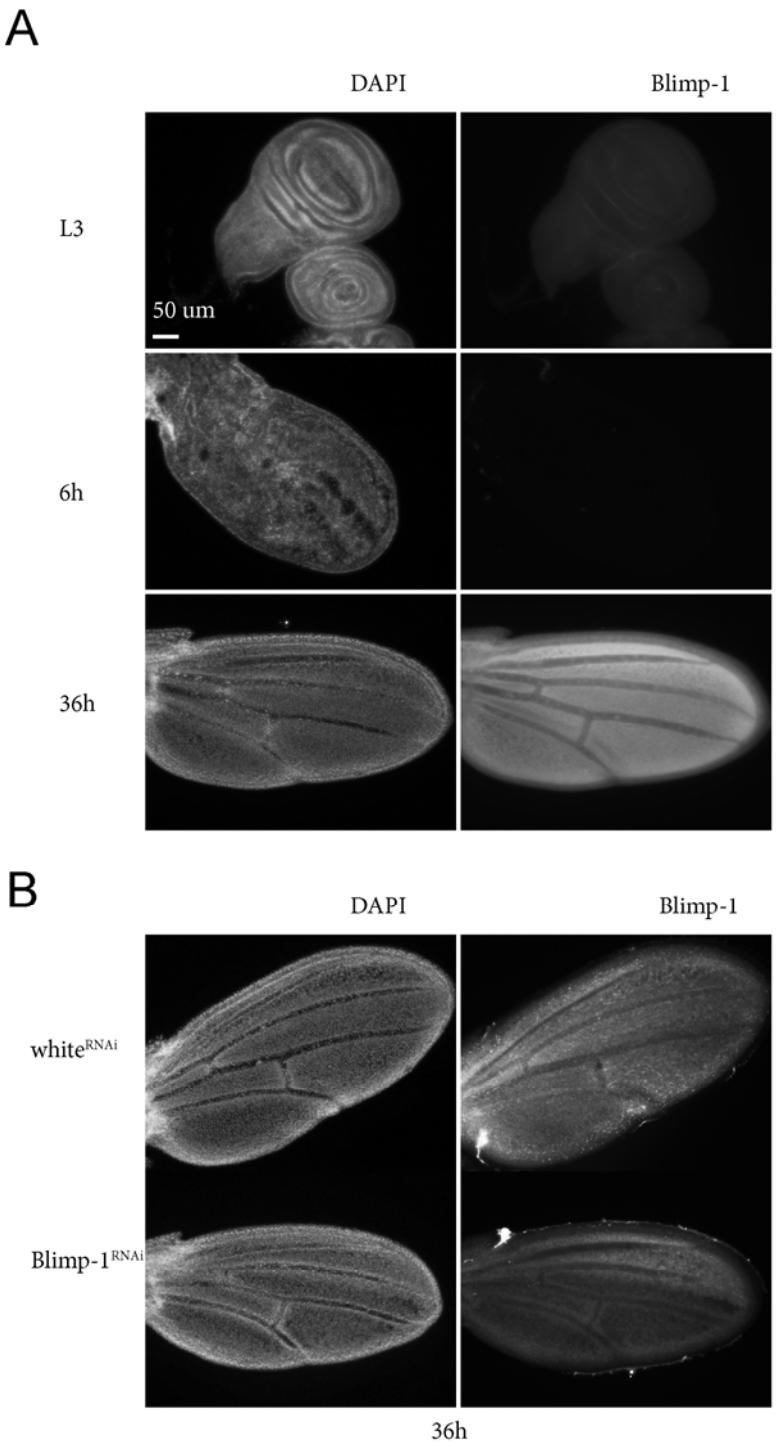

Figure S2.9 Validation of Blimp-1 reagents. (A) Blimp-1 antibody staining in wildtype L3, 6h and 36h wings corresponds to the gene expression changes of *Blimp-1*. (B) Expressing Blimp-^{RNAi} in the posterior wings by *engrailed*-Gal4/Gal80^{ts} from 0h APF reduces the level of Blimp-1 protein at 36h wings.

2.6 Reference

1. Novitch BG, Spicer DB, Kim PS, Cheung WL, Lassar AB. pRb is required for MEF2-dependent gene expression as well as cell-cycle arrest during skeletal muscle differentiation. Curr Biol. 1999;9:449–59.

2. Matus DQ, Lohmer LL, Kelley LC, Schindler AJ, Kohrman AQ, Barkoulas M, et al. Invasive Cell Fate Requires G1 Cell-Cycle Arrest and Histone Deacetylase-Mediated Changes in Gene Expression. Dev Cell. 2015;35:162–74.

3. O'Keefe DD, Thomas SR, Bolin K, Griggs E, Edgar BA, Buttitta LA. Combinatorial control of temporal gene expression in the Drosophila wing by enhancers and core promoters. BMC Genomics. 2012;13:498.

4. van den Heuvel S, Dyson NJ. Conserved functions of the pRB and E2F families. Nat Rev Mol Cell Biol. 2008;9:713–24.

5. Blais A, Dynlacht BD. E2F-associated chromatin modifiers and cell cycle control. Curr Opin Cell Biol. 2007;19:658–62.

6. Buttitta LA, Katzaroff AJ, Perez CL, de la Cruz A, Edgar BA. A double-assurance mechanism controls cell cycle exit upon terminal differentiation in Drosophila. Dev Cell. 2007;12:631–43.

7. Firth LC, Baker NE. Extracellular signals responsible for spatially regulated proliferation in the differentiating Drosophila eye. Dev Cell. 2005;8:541–51.

8. The I, Ruijtenberg S, Bouchet BP, Cristobal A, Prinsen MBW, van Mourik T, et al. Rb and FZR1/Cdh1 determine CDK4/6-cyclin D requirement in C. elegans and human cancer cells. Nat Commun. 2015;6:5906.

9. Buttitta LA, Katzaroff AJ, Edgar BA. A robust cell cycle control mechanism limits E2F-induced proliferation of terminally differentiated cells in vivo. J Cell Biol. 2010;189:981–96.

10. Nagl NG, Wang X, Patsialou A, Van Scoy M, Moran E. Distinct mammalian SWI/SNF chromatin remodeling complexes with opposing roles in cell-cycle control. EMBO J. 2007;26:752–63.

11. Hendricks KB, Shanahan F, Lees E. Role for BRG1 in cell cycle control and tumor suppression. Mol Cell Biol. 2004;24:362–76.

12. The I, Ruijtenberg S, Bouchet BP, Cristobal A, Prinsen MBW, van Mourik T, et al. Rb and FZR1/Cdh1 determine CDK4/6-cyclin D requirement in C. elegans and human cancer cells. Nat Commun. 2015;6:5906.

13. Liu K, Luo Y, Lin F-T, Lin W-C. TopBP1 recruits Brg1/Brm to repress E2F1-induced apoptosis, a novel pRb-independent and E2F1-specific control for cell survival. Genes Dev. 2004;18:673–86.

14. Ruijtenberg S, van den Heuvel S. G1/S Inhibitors and the SWI/SNF Complex

Control Cell-Cycle Exit during Muscle Differentiation. Cell. 2015;162:300–13.

15. Albini S, Coutinho Toto P, Dall'Agnese A, Malecova B, Cenciarelli C, Felsani A, et al. Brahma is required for cell cycle arrest and late muscle gene expression during skeletal myogenesis. EMBO Rep. 2015;16:1037–50.

16. Johnson SA, Milner MJ. Cuticle secretion in Drosophila wing imaginal discs in vitro: parameters of exposure to 20-hydroxy ecdysone. Int J Dev Biol. 1990;34:299–307.

17. Halme A, Cheng M, Hariharan IK. Retinoids regulate a developmental checkpoint for tissue regeneration in Drosophila. Curr Biol. 2010;20:458–63.

18. Schubiger M, Carré C, Antoniewski C, Truman JW. Ligand-dependent de-repression via EcR/USP acts as a gate to coordinate the differentiation of sensory neurons in the Drosophila wing. Development. 2005;132:5239–48.

19. Ashburner M. Puffs, genes, and hormones revisited. Cell. 1990;61:1–3.

20. Thummel CS. Ecdysone-regulated puff genes 2000. Insect Biochem Mol Biol. 2002;32:113–20.

21. Uyehara CM, Nystrom SL, Niederhuber MJ, Leatham-Jensen M, Ma Y, Buttitta LA, et al. Hormone-dependent control of developmental timing through regulation of chromatin accessibility. Genes Dev. 2017;31:862–75.

22. King-Jones K, Thummel CS. Nuclear receptors--a perspective from Drosophila. Nat Rev Genet. 2005;6:311–23.

23. Stoiber M, Celniker S, Cherbas L, Brown B, Cherbas P. Diverse Hormone Response Networks in 41 Independent Drosophila Cell Lines. G3 (Bethesda). 2016;6:683–94.

24. Fristrom D, Liebrich W. The hormonal coordination of cuticulin deposition and morphogenesis in Drosophila imaginal discs in vivo and in vitro. Dev Biol. 1986;114:1–11.

25. Sobala LF, Adler PN. The Gene Expression Program for the Formation of Wing Cuticle in Drosophila. PLoS Genet. 2016;12:e1006100.

26. Taylor J, Adler PN. Cell rearrangement and cell division during the tissue level morphogenesis of evaginating Drosophila imaginal discs. Dev Biol. 2008;313:739–51.

27. Sotillos S, De Celis JF. Interactions between the Notch, EGFR, and decapentaplegic signaling pathways regulate vein differentiation during Drosophila pupal wing development. Dev Dyn. 2005;232:738–52.

28. Guo Y, Flegel K, Kumar J, McKay DJ, Buttitta LA. Ecdysone signaling induces two phases of cell cycle exit in Drosophila cells. Biol Open. 2016;5:1648–61.

29. Buttitta LA, Katzaroff AJ, Edgar BA. A robust cell cycle control mechanism limits E2F-induced proliferation of terminally differentiated cells in vivo. J Cell Biol. 2010;189:981–96.

30. Song L, Zhang Z, Grasfeder LL, Boyle AP, Giresi PG, Lee B-K, et al. Open chromatin defined by DNaseI and FAIRE identifies regulatory elements that shape cell-type identity. Genome Res. 2011;21:1757–67.

31. Thomas S, Li X-Y, Sabo PJ, Sandstrom R, Thurman RE, Canfield TK, et al. Dynamic reprogramming of chromatin accessibility during Drosophila embryo development. Genome Biol. 2011;12:R43.

32. Arnold CD, Gerlach D, Stelzer C, Boryń ŁM, Rath M, Stark A. Genome-wide quantitative enhancer activity maps identified by STARR-seq. Science. 2013;339:1074–7.

33. Zabidi MA, Arnold CD, Schernhuber K, Pagani M, Rath M, Frank O, et al. Enhancer-core-promoter specificity separates developmental and housekeeping gene regulation. Nature. 2015;518:556–9.

34. FitzGerald PC, Sturgill D, Shyakhtenko A, Oliver B, Vinson C. Comparative genomics of Drosophila and human core promoters. Genome Biol. 2006;7:R53.

35. Ohler U, Liao G, Niemann H, Rubin GM. Computational analysis of core promoters in the Drosophila genome. Genome Biol. 2002;3:RESEARCH0087.

36. Gurudatta B V, Yang J, Van Bortle K, Donlin-Asp PG, Corces VG. Dynamic changes in the genomic localization of DNA replication-related element binding factor during the cell cycle. Cell Cycle. 2013;12:1605–15.

37. Williams LH, Fromm G, Gokey NG, Henriques T, Muse GW, Burkholder A, et al. Pausing of RNA polymerase II regulates mammalian developmental potential through control of signaling networks. Mol Cell. 2015;58:311–22.

38. Blais A, van Oevelen CJC, Margueron R, Acosta-Alvear D, Dynlacht BD. Retinoblastoma tumor suppressor protein-dependent methylation of histone H3 lysine 27 is associated with irreversible cell cycle exit. J Cell Biol. 2007;179:1399–412.

39. Sdek P, Zhao P, Wang Y, Huang C-J, Ko CY, Butler PC, et al. Rb and p130 control cell cycle gene silencing to maintain the postmitotic phenotype in cardiac myocytes. J Cell Biol. 2011;194:407–23.

40. Swanhart LM, Sanders AN, Duronio RJ. Normal regulation of Rbf1/E2f1 target genes in Drosophila type 1 protein phosphatase mutants. Dev Dyn. 2007;236:2567–77.

41. Lehman DA, Patterson B, Johnston LA, Balzer T, Britton JS, Saint R, et al. Cis-regulatory elements of the mitotic regulator, string/Cdc25. Development. 1999;126:1793–803.

42. Richardson HE, O'Keefe L V, Reed SI, Saint R. A Drosophila G1-specific cyclin E homolog exhibits different modes of expression during embryogenesis. Development. 1993;119:673–90.

43. Li X, Zhao X, Fang Y, Jiang X, Duong T, Fan C, et al. Generation of destabilized green fluorescent protein as a transcription reporter. J Biol Chem. 1998;273:34970–5.

44. Ma Y, Buttitta L. Chromatin organization changes during the establishment and maintenance of the postmitotic state. Epigenetics Chromatin. 2017;10:53.

45. Schulz KN, Bondra ER, Moshe A, Villalta JE, Lieb JD, Kaplan T, et al. Zelda is differentially required for chromatin accessibility, transcription factor binding, and gene expression in the early Drosophila embryo. Genome Res. 2015;25:1715–26.

46. Pajoro A, Madrigal P, Muiño JM, Matus JT, Jin J, Mecchia MA, et al. Dynamics of chromatin accessibility and gene regulation by MADS-domain transcription factors in flower development. Genome Biol. 2014;15:R41.

47. de la Torre-Ubieta L, Stein JL, Won H, Opland CK, Liang D, Lu D, et al. The Dynamic Landscape of Open Chromatin during Human Cortical Neurogenesis. Cell. 2018;172:289–304.e18.

48. Liang L, Haug JS, Seidel CW, Gibson MC. Functional genomic analysis of the periodic transcriptome in the developing Drosophila wing. Dev Cell. 2014;29:112–27.

49. Champlin DT, Truman JW. Ecdysteroids govern two phases of eye development during metamorphosis of the moth, Manduca sexta. Development. 1998;125:2009–18.

50. Champlin DT, Truman JW. Ecdysteroid control of cell proliferation during optic lobe neurogenesis in the moth Manduca sexta. Development. 1998;125:269–77.

51. Neto M, Naval-Sánchez M, Potier D, Pereira PS, Geerts D, Aerts S, et al. Nuclear receptors connect progenitor transcription factors to cell cycle control. Sci Rep. 2017;7:4845.

52. Jögi A, Vaapil M, Johansson M, Påhlman S. Cancer cell differentiation heterogeneity and aggressive behavior in solid tumors. Ups J Med Sci. 2012;117:217–24.

53. Agawa Y, Sarhan M, Kageyama Y, Akagi K, Takai M, Hashiyama K, et al. Drosophila Blimp-1 is a transient transcriptional repressor that controls timing of the ecdysone-induced developmental pathway. Mol Cell Biol. 2007;27:8739–47.

54. Akagi K, Sarhan M, Sultan A-RS, Nishida H, Koie A, Nakayama T, et al. A biological timer in the fat body comprising Blimp-1, βFtz-f1 and Shade regulates pupation timing in Drosophila melanogaster.

55. Uyehara CM, Nystrom SL, Niederhuber MJ, Leatham-Jensen M, Ma Y, Buttitta LA, et al. Hormone-dependent control of developmental timing through regulation of chromatin accessibility. Genes Dev. 2017;31:862–75.

56. Guo Y, Flegel K, Kumar J, McKay DJ, Buttitta LA. Ecdysone signaling induces two phases of cell cycle exit in *Drosophila* cells. Biol Open. 2016;5:1648–61.

57. McKay DJ, Lieb JD. A common set of DNA regulatory elements shapes Drosophila appendages. Dev Cell. 2013;27:306–18.

58. Langmead B, Salzberg SL. Fast gapped-read alignment with Bowtie 2. Nat Methods. 2012;9:357–9.

59. Zhang Y, Liu T, Meyer CA, Eeckhoute J, Johnson DS, Bernstein BE, et al. Model-based analysis of ChIP-Seq (MACS). Genome Biol. 2008;9:R137.

60. Zhang Y, Lin Y-H, Johnson TD, Rozek LS, Sartor MA. PePr: a peak-calling prioritization pipeline to identify consistent or differential peaks from replicated ChIP-Seq data. Bioinformatics. 2014;30:2568–75.

61. Ramírez F, Ryan DP, Grüning B, Bhardwaj V, Kilpert F, Richter AS, et al. deepTools2: a next generation web server for deep-sequencing data analysis. Nucleic Acids Res. 2016;44:W160-5.

62. Robinson JT, Thorvaldsdóttir H, Winckler W, Guttman M, Lander ES, Getz G, et al. Integrative genomics viewer. Nat Biotechnol. 2011;29:24–6.

63. Zhu LJ, Christensen RG, Kazemian M, Hull CJ, Enuameh MS, Basciotta MD, et al. FlyFactorSurvey: a database of Drosophila transcription factor binding specificities determined using the bacterial one-hybrid system. Nucleic Acids Res. 2011;39 Database issue:D111-7.

64. Bailey TL, Boden M, Buske FA, Frith M, Grant CE, Clementi L, et al. MEME SUITE: tools for motif discovery and searching. Nucleic Acids Res. 2009;37 Web Server issue:W202-8.

65. Zhu LJ, Gazin C, Lawson ND, Pagès H, Lin SM, Lapointe DS, et al. ChIPpeakAnno: a Bioconductor package to annotate ChIP-seq and ChIP-chip data. BMC Bioinformatics. 2010;11:237.

66. Dobin A, Davis CA, Schlesinger F, Drenkow J, Zaleski C, Jha S, et al. STAR: ultrafast universal RNA-seq aligner. Bioinformatics. 2013;29:15–21.

67. Anders S, Pyl PT, Huber W. HTSeq--a Python framework to work with high-throughput sequencing data. Bioinformatics. 2015;31:166–9.

68. Trapnell C, Williams BA, Pertea G, Mortazavi A, Kwan G, van Baren MJ, et al. Transcript assembly and quantification by RNA-Seq reveals unannotated transcripts and isoform switching during cell differentiation. Nat Biotechnol. 2010;28:511–5.

69. Huang DW, Sherman BT, Lempicki RA. Systematic and integrative analysis of large gene lists using DAVID bioinformatics resources. Nat Protoc. 2009;4:44–57.

70. Love MI, Huber W, Anders S. Moderated estimation of fold change and dispersion for RNA-seq data with DESeq2. Genome Biol. 2014;15:550.

Chapter 3. Chromatin Organization Changes During the Establishment and Maintenance of the Postmitotic State[1]

3.1 Abstract

Genome organization changes during development as cells differentiate. Chromatin motion becomes increasingly constrained and heterochromatin clusters as cells become restricted in their developmental potential. These changes coincide with slowing of the cell cycle, which can also influence chromatin organization and dynamics. Terminal differentiation is often coupled with permanent exit from the cell cycle, and existing data suggest a close relationship between a repressive chromatin structure and silencing of the cell cycle in postmitotic cells. Heterochromatin clustering could also contribute to stable gene repression to maintain terminal differentiation or cell cycle exit, but whether clustering is initiated by differentiation, cell cycle changes, or both is unclear. Here we examine the relationship between chromatin organization, terminal differentiation and cell cycle exit. We focused our studies on the Drosophila wing, where epithelial cells transition from active proliferation to a postmitotic state in a temporally controlled manner. We find there are two stages of G0 in this tissue, a flexible G0 period where cells can be induced to re-enter the cell cycle under specific genetic manipulations

[1] This chapter is reprinted from Ma, Y. & Buttitta, L. (2017). Chromatin organization changes during the establishment and maintenance of the postmitotic state. *Epigenetics Chromatin. 2017 Nov 10;10(1):53. doi: 10.1186/s13072-017-0159-8*, with minor modifications.

and a state we call “robust”, where cells become strongly refractory to cell cycle re-entry. Compromising the flexible G0 by driving ectopic expression of cell cycle activators causes a global disruption of the clustering of heterochromatin-associated histone modifications such as H3K27 trimethylation and H3K9 trimethylation, as well as their associated repressors, Polycomb and heterochromatin protein 1(HP1). However, this disruption is reversible. When cells enter a robust G0 state, even in the presence of ectopic cell cycle activity, clustering of heterochromatin associated modifications are restored. If cell cycle exit is bypassed, cells in the wing continue to terminally differentiate, but heterochromatin clustering is severely disrupted. Heterochromatin-dependent gene silencing does not appear to be required for cell cycle exit, as compromising the H3K27 methyltransferase Enhancer of zeste, and/or HP1 cannot prevent the robust cell cycle exit, even in the face of normally oncogenic cell cycle activities. Thus, heterochromatin clustering during terminal differentiation is a consequence of cell cycle exit, rather than differentiation. Compromising heterochromatin-dependent gene silencing does not disrupt cell cycle exit.

3.2 Background

Cellular differentiation is the acquisition of cell-type specific characteristics, driven by changes in gene expression. Changes in gene expression are largely controlled by transcription factors, which can be facilitated or impeded by chromatin modifications, binding site accessibility and chromatin organization. A reciprocal relationship exists between chromatin organization, modification and gene expression, and several studies have shown that chromatin organization and modifications can change during differentiation. For example, during neural differentiation silenced genes move to

repressive compartments in the nucleus [1–3]. In certain contexts of differentiation global nuclear compartments can become dramatically re-organized to facilitate specialized functions [4]. At a more local level, chromatin modifiers can be recruited to specific genes involved in differentiation to facilitate their expression and limit the expression of genes involved in other cell-type programs that must be kept off [5]. Thus dynamic changes in chromatin organization and modification can have critical consequences on proper differentiation during development.

There is also an intimate relationship between the cell cycle and chromatin organization and modifications. Chromatin in actively cycling cells is highly dynamic. During S-phase, new histones are incorporated onto nascent DNA requiring re-establishment of histone modifications [6]. During mitosis, nuclear organization including intra and inter-chromosomal contacts are lost and many chromatin modifiers are ejected from chromatin to facilitate proper chromosome condensation and segregation [7, 8]. In addition the activity of histone modifiers can be regulated in a cell cycle-dependent manner [9–14]. During differentiation cells often transition from rapid proliferation to slower cycling, which can be followed by cell cycle exit or entry into G_0 coordinated with terminal differentiation. Thus the modification and organization of chromatin in the nucleus can be impacted by the differentiation process itself, but also by the changes in cell cycle dynamics during differentiation. For example, chromatin compacts and heterochromatin clusters as cells in the embryo cycle more slowly and become lineage restricted [15]. In *Drosophila* loci within constitutive heterochromatin show increased association in terminally differentiated postmitotic cells [16] and facultative heterochromatin-forming Polycomb bodies cluster as cells differentiate and the cell cycle

slows during embryogenesis [17]. Methods such as inducing developmental arrest have been used in attempt to disentangle the influence of cell cycle changes from differentiation process [16], but these approaches cannot fully uncouple terminal differentiation from the accompanying cell cycle exit and it has remained unclear whether changes in heterochromatin clustering and dynamics are due to differentiation, the accompanying cell cycle changes, or both. The influence of cell cycle changes during differentiation adds a layer of complexity to our understanding of the relationship between chromatin organization and modifications and differentiation.

Here we directly address the relationship between heterochromatin organization, chromatin modification and cell cycle exit using the temporally controlled cell cycle exit in the *Drosophila* wing [18–20]. In our experiments, we take advantage of tools that can effectively uncouple cell cycle exit and differentiation to ask whether heterochromatin clustering is a consequence of cell cycle exit or differentiation. In addition we examine changes in chromatin modifications caused by the delay of cell cycle exit and examine the impact of disrupting heterochromatin-dependent gene silencing on cell cycle exit.

3.3 Methods

3.3.1 Fly stocks and genetics

Disruption of G0 in the posterior wing:

w/y, w, hs-FLP; en-GAL4, UAS-GFP/ UAS-E2F1, UAS-DP; tub-gal80TS/ +

w/y, w, hs-FLP; en-GAL4, UAS-GFP/ UAS-CycD, UAS-Cdk4; tub-gal80TS/ UAS-E2F1, UAS-DP

w/y, w, hs-FLP; en-GAL4, UAS-GFP/ +; tub-gal80TS/ UAS-CycE, UAS-Cdk2

w/y, w, hs-FLP; en-GAL4, UAS-GFP/ UAS-CycD, UAS-Cdk4; tub-gal80TS/ +

w/y, w, hs-FLP; en-GAL4, UAS-GFP/ UAS-CycA; tub-gal80TS/ +

Disruption of G0 in clones:

w/ y, w, hs-FLP; tub>CD2>GAL4, UAS-GFP/ UAS-CycD, UAS-Cdk4; tub-gal80TS/ UAS-E2F1, UAS-DP

Disruption of H3K27me3:

w/y, v; en-GAL4, UAS-GFP/ +; tub-gal80TS/ UAS-E(z)^{RNAi} (Bloomington 33659)

Disruption of HP1:

w/y, v; en-GAL4, UAS-GFP/ +; tub-gal80TS/ UAS-Su(var)205^{RNAi} (Bloomington 33400)

Disruption of HP1 with Y10C:

w/w, Y10C; en-Gal4, UAS-RFP/ +; +/ UAS-Su(var)205^{RNAi} (Bloomington 33400)

All the crosses containing gal80^{TS} were maintained in 18°C to suppress Gal4 in early development. To disrupt G_0 with cell cycle regulators, white prepupae were collected and shifted to 28°C to indicated time points. For *E(z)* knockdown experiments, L3 larva were shifted from 18°C to 28°C to induce *E(z)* RNAi. For *HP1* knockdown, crosses were kept in 28°C after egg laying (AEL). For clonal expression of cell cycle regulators, animals were heat shock in 37°C for 8 minutes during 48-72h AEL, and then kept in 18°C. White prepupae were collected and shifted to 28°C to indicated time points. All timings are adjusted according to the equivalent development at 25°C as described previously [18].

3.3.2 Immunostaining

Imaginal discs or pupal wings were dissected in 1x PBS, and fixed in 4% paraformaldehyde /1x PBS for 30 minutes. Samples were washed twice in 1x PBS, 0.1%

Triton X, 10 min each, and incubated in PAT (1XPBS, 0.1% Triton X-100 and 1% BSA) for 10 mins for larval tissues and 3 x 20 mins for pupal tissues. Samples were then incubated with primary antibodies for 4 hours or 4°C overnight followed by 3 washes and secondary antibodies at room temperature for 4 hours or 4°C overnight. Primary antibodies used in this study include: Anti-phospho-Ser10 histone H3, 1:2000 rabbit (Millipore #06-570) or mouse (Cell Signaling #9706); Anti-GFP, 1:1000 chicken (Life Technologies A10262) or 1:1000 rabbit (Life Technologies A11122); Anti-pH2Av, 1:100 mouse (DSHB, UNC93-5.2.1); Anti-H3K27me3, 1:500 rabbit (Millipore #07-449); Anti-HP1, 1:250 mouse (DSHB, C1A9); Anti-H2Av, 1:500 rabbit (Active Motif #39715); Anti-H3, 1:500 mouse (Cell Signaling #3638); Anti-H3ac, 1:500 rabbit (Millipore #06-599); Anti-H3K4me3, 1:500 rabbit (Millipore #07-473); Anti-H3K9me3, 1:500 rabbit (Millipore #07-523) or (Active Motif #39161) ; Anti-H3K27ac, 1:500 rabbit (Abcam ab4729); Anti-H4ac, 1:500 rabbit (Millipore #06-866); Anti-H4K16ac, 1:500 rabbit (Millipore #07-329); Anti-H4K20me3, 1:500 mouse (Abcam ab78517); Anti-E2F, 1:500 guinea pig (kindly provided by Dr. Terry L. Orr-Weaver); Anti-Ubx, 1:250 mouse (DSHB, FP3.38); Anti-D1, 1:200 guinea pig (kindly provided by Dr. Yukiko Yamashita). DNA was labeled by 1 ug/ml DAPI in 1× PBS, 0.1% Triton X for 10 min. F-actin was stained using 1:100 rhodamine–phalloidin (Invitrogen; R415) in 1x PBS for 4 hours.

3.3.3 Microscopy and Image quantification

Images were taken with a 100x oil objective on a Leica SP5 confocal with a system optimized z-section of 0.13 μm. 3-D reconstructions were performed using the "3D viewer" function in Leica LAS AF software. Images of whole pupal wings in Fig. 3.2 and

3.7 were obtained using a Leica DMI6000B epifluorescence system. All adjustments of brightness or contrast were applied to the entire image in Adobe Photoshop and performed equally with equal threshold values across control and experiment samples.

For integrated intensity quantifications, we used maximum projections of 12 continuous z-sections of confocal images. We developed a toolkit in Matlab (Release 2015b) that automatically segments nuclei and foci within nuclei and integrates the pixel intensities with the help of the Advocacy and Research Support, U.Michigan LSA-IT. To identify nuclei. images were smoothed using a circular averaging filter through the fspecial and imfilter function of Matlab. Next a watershed algorithm was applied to segment nuclei from the background and nuclei were masked using local maxima with an h-maxima transform. Thresholds were manually set and checked for each image to accurately delineate nuclei. GFP positive vs. negative was established using an intensity threshold for the GFP channel. Integrated intensities for all nuclei were exported to Excel. Segmentation and measurement of foci followed a similar process for foci within the defined nuclear regions. In brief, foci were segmented using a watershed algorithm, then further measured for pixel intensity and number, which was used for foci area and intensity measurements.

3.3.4 Fluorescent *in situ* Hybridization (FISH)

Alexa-488 probes against the rDNA Internal Transcribed Spacer (ITS) region and Cy3 probes against AACAC repetitive satellite sequences were kindly provided by Dr. Yukiko Yamashita. For FISH, fixed tissues were treated with 2 mg/ml Rnase A in 1x PBS, 0.1% Triton X at 37°C for 10 min, and rinsed in 2x SSC/1mM EDTA/0.2%Tween 20. Then

tissues were incubated in 2x SSC/1mM EDTA/0.2%Tween 20 solution with increasing formamide concentration from 20%, 40% to 50% for 15 min to 30 min. Finally, tissues were incubated in 100 µl hybridization solution with 50 µl formamide, 20 µl 50% dextran sulfate, 20 µl 2X SSC/1mM EDTA/0.2%Tween 20 and 10 µl of probe at µg/mL for 15 min at 91°C, and left at 37°C overnight. Quantification of size for rDNA loci area was carried out using our customized Matlab toolkit. For the quantification of AACAC satellite to the chromocenter, we used a single 0.13 µm z-section with the strongest FISH signal and measured the relative distance of the center of the FISH signal to the brightest Dapi-stained region and corrected for the total nuclear radius using the Leica LAS AF software.

3.3.5 Flow cytometry

FACS was performed on dissociated wings to measure DNA content on an Attune Cytometer (Life Technologies) as described [21].

3.3.6 RNA interference

Kc167 cells were kindly provided by Dr. K. Cadigan and cultured as described [22]. For RNA interference, cells were placed with concentration of 1 million/ml and starved in serum free medium with 10 ug/ml double-strand RNA (dsRNA) for 4-6 hours, then 10% serum medium was added to the culture and cells were collected for staining 3 days after serum medium addition. dsRNA was synthesized with T7 Megascript Kit (Ambion). T7 primers used in this study:

T7-Wee-fwd, TAATACGACTCACTATAGGGATGACTTTGACAAGGACAC;

T7-Wee-rev, TAATACGACTCACTATAGGATCTAGTCGATTGACGCATT;

T7-Myt1-fwd, TAATACGACTCACTATAGGAATTGCACGACGACAAACAC;

T7-Myt1-rev, TAATACGACTCACTATAGGTGTCCAGATGGATGAGATTC;

T7-Myt1-fwd2, TAATACGACTCACTATAGGACAACAATCTGAACCGAAGC;

T7-Myt1-rev2, TAATACGACTCACTATAGGTGGAGCCATATACCTCGAAT;

T7-GFP-fwd, TAATACGACTCACTATAGGCATGTGGTCTCTCTTTTCGT

T7-GFP-rev, TAATACGACTCACTATAGGGGGCACAAATTTTCTGTCAG

T7-CycB-fwd TAATACGACTCACTATAGGGGCGTTTTTGCGTTCGAATT

T7-CycB-rev, TAATACGACTCACTATAGGCAATTGCAAGTACGTGCGTT

3.3.7 Western Blots

Western Blots were performed on staged fly wings using BioRad TGX precast 4-20% gels and high sensitivity ECL reagents (Thermo) to detect HRP conjugated secondary antibodies [23]. Mouse anti-α-tubulin (1:1000, DSHB, AA4.3) was used as a loading control. Blot signals were detected and quantified with FluorChem M digital system from Protein Simple.

3.4 Results

3.4.1 Heterochromatin clusters as proliferation slows and cells differentiate

The impact of the cell cycle on heterochromatin clustering during cellular differentiation has not been resolved. Specifically, how the transition from a proliferative to a postmitotic state impacts global chromatin organization in *Drosophila* is unclear. To examine this, we immunostained for various chromatin marks and chromatin binding proteins in wild-type *Drosophila* wings at three stages with distinct proliferation

parameters. We examined quickly proliferating second instar larval (L2) wings, slowly proliferative wandering third instar larva (L3) and post-mitotic 28h pupal wings (Fig.3.1A). Cells of the L2 wing region examined have a cell doubling time (CDT) of about 10h, while cells of the same region in L3 wings have a longer CDT of 15h. By 28h after puparium formation (APF) during metamorphosis, cells of the wing blade have entered G0 and are permanently postmitotic [18, 24, 25]. We examined the histone modification H3K27me3 associated with facultative heterochromatin, H3K9me3, HP1 and the AT rich repetitive sequence binding protein D1 associated with constitutive heterochromatin and the euchromatin-associated modification H3K4me3 (Fig. 3.1A). The immunofluorescence (IF) signals for H3K27me3, H3K9me3 and D1 were weakest at the L2 stage, but increased at the L3 and pupal stages and clustered into larger and more intense, distinct foci in the slower cycling tissues (Fig. 3.1A). In *Drosophila* cells, the chromocenter, containing constitutive heterochromatin such as clustered centromeres, can be easily visualized as a DAPI-bright region within the nucleus [26]. We confirmed the co-localization of the chromocenter with D1 staining, which binds centromeric satellite repeats, and also co-localized with the centromeric histone Cenp-A (not shown) [27]. H3K9Me3 and HP1 label heterochromatin foci partially overlapping and adjacent to the DAPI-bright region [28]. H3K27Me3 labels distinct foci throughout the nucleus associated with facultative heterochromatin, and represents Polycomb repressive complex 2 (PRC2) binding and formation of Polycomb group (PcG) clusters or foci [29–31]. By contrast, H3K4Me3 broadly localizes throughout the chromatin, does not form distinct foci, and is excluded from the centromeric and pericentromeric regions (Fig.3.1A).

To automatically detect and measure heterochromatin foci parameters such as intensity and number for a large number of nuclei, we developed a custom MatLab App (described in supplemental methods) that uses DAPI staining to mask individual nuclei followed by foci segmentation and measurement. We measured clustering of heterochromatin foci as a function of the integrated intensity for each focus (the sum of intensities for all pixels in a focus) [17, 31]. This automated approach allowed us to examine the distribution of heterochromatin foci at a single cell level, across hundreds to thousands of nuclei, sampled from multiple wings for each experiment in an unbiased manner. We found that heterochromatin clustering increased as the cell cycle slowed and stopped during L3 and pupal stages (Fig. 3.1B). We noted a dramatic increase in H3K9Me3 and HP1 staining at the L3 stage, which may reflect a developmentally controlled stage-specific increase in this modification/reader pair.

To distinguish whether an increase in heterochromatin clustering is due to changes in the cell cycle, we turned to *Drosophila* cell culture. In *Drosophila* Kc cells, the overall cell doubling time is controlled by the negative and positive regulators of the G2/M transition Wee/Myt and CycB respectively [22]. We sped up the cell cycle by reducing Wee/Myt1 activity via RNAi or slowed the cell cycle using RNAi to *cycB*. Slowing the cell cycle increased the clustering and intensity of H3K27Me3 and H3K9Me3 compared to controls exposed to RNAi to GFP (Fig. 3.1C-D).

The increased clustering of heterochromatin could be due to chromatin condensation and compaction. To examine chromatin condensation we performed Fluorescent *In Situ* Hybridization (FISH) using probes against the internal transcribed spacer region between the 18S RNA and 28S rDNA loci, which are tandemly repeated

on the X, and measured the total rDNA area before and after cell cycle exit in the wing [32, 33]. In proliferating L3 wings the rDNA is extended. The rDNA becomes more compact as cells enter G0 at 24-28h APF and condense further as G0 is maintained at 42h APF (Fig. 3.1E-F). The changes in the rDNA locus suggest chromatin condensation increases in prolonged G0. To verify that compaction is not specific to the rDNA locus on the X, we also performed FISH to the pericentromeric satellite repeat AACAC on chromosome II and measured the distance of the signal to the chromocenter (Fig. 3.1G-H). The distance of the pericentromeric heterochromatin to the chromocenter also decreased suggesting that heterochromatin condensation, coalescence and compaction occurs throughout the nucleus after cell cycle exit.

An increase in chromatin clustering could be correlated with a global reduction in gene expression when cells become postmitotic [34]. To test whether global gene expression is reduced in postmitotic wings we examined an RNAseq timecourse of gene expression from proliferating to postmitotic stages [22]. We found the global gene expression levels to be similar in proliferating and postmitotic tissues (Fig. 3.1I), however since RNAseq reveals steady-state mRNA levels, changes in RNA Pol II could still occur. Transcriptional shutoff upon quiescence in yeast is associated with a repressive chromatin structure and reduced chromatin accessibility [34]. Therefore we also compared the global changes in chromatin accessibility between proliferating and postmitotic wings through Formaldehyde-assisted Identification of Regulatory Elements [FAIRE]-seq [35] (Fig. 3.1J). Consistent with the global gene expression profile, we found no obvious changes in the average level of chromatin accessibility in cycling vs. post mitotic tissue. This suggests that clustering of heterochromatin as cells exit the cell cycle

does not cause global changes in genome accessibility or steady state mRNA levels during differentiation and cell cycle exit.

3.4.2 Compromising heterochromatin-dependent gene silencing does not disrupt cell cycle exit

We have shown that heterochromatin clustering increases with entry into G0. Heterochromatin clustering is associated with increased target gene silencing [31], and has been suggested to repress cell cycle gene expression to facilitate cell cycle exit in mammalian muscle and neurons [36–38]. To test whether heterochromatin-dependent gene silencing promotes cell cycle exit in Drosophila wings, we compromised the H3K27me3 methyltransferase E(z) and/or the H3K9Me3 binding protein HP1. As E(z) and HP1 perform many functions during development, we turned to an inducible system with RNAi to alter gene function after embryogenesis. We used the *engrailed*-Gal4 driver with a temperature sensitive Gal80 (*en*-Gal4/Gal80^{TS}) to turn on UAS-driven expression of dsRNAs to *E(z)* and *HP1* in the posterior wing from the early L1 and L3 stages respectively. We then dissected wings at 24-28h APF and stained for the mitotic marker phosphorylated phospho-Ser-10 histone H3 (PH3) to determine whether cells in the posterior wing delayed or bypassed cell cycle exit. We saw no effect of *E(z)* or *HP1* reduction on cell cycle exit despite a clear loss of H3K27Me3 and HP1 in the posterior wing (Fig. 3.2 A-C). We further confirmed that our knockdowns effectively compromised heterochromatin-dependent gene silencing in the wing, by examining de-repression of the Polycomb target Ultrabithorax (UBX) and the HP1-silenced Y10C GFP reporter (Fig. 3.2 B,D). Recent work has suggested Polycomb (Pc) can repress certain targets

independent of *E(z)* [29]. We therefore also directly inhibited *Pc* by RNAi, but observed no effect on cell cycle exit despite de-repression of UBX in the wing (Supp. Fig. 3.2).

Compromising heterochromatin-dependent gene silencing does not disrupt or delay cell cycle exit on its own, but we wondered whether it may sensitize cells to other perturbations that compromise cell cycle exit. We have previously shown that activation of various cell cycle regulators including the cell cycle transcription factor complex E2F/DP (hereafter referred to as E2F), can cause 1-2 extra cell cycles in the pupa wing between 24-36h APF followed by a delayed entry into G0 at 36 APF (Supp. Fig. 3.3). We refer to the 24-36h APF period as flexible cell cycle exit or "flexible G0" which is followed by a more difficult to disrupt "robust G0" after 36h. We co-expressed E2F with RNAi to E(z) and/or HP1 to examine whether loss of heterochromatin-dependent gene silencing can further delay cell cycle exit in the presence of high E2F activity. However, inhibition of E(z), *HP1* or *E(z)+HP1* together did not further compromise cell cycle exit in the presence of high E2F activity (Fig. 3.2G-O). Altogether our results demonstrate that compromising heterochromatin-dependent gene silencing does not disrupt cell cycle exit in the *Drosophila* wing.

3.4.3 Delaying cell cycle exit disrupts heterochromatin clustering and chromosome compaction

Constitutive and facultative heterochromatin clusters in post-mitotic wings. To examine whether compromising cell cycle exit affects clustering, we used the system described above to express E2F in the posterior pupal wing to drive 1-2 extra cell cycles and delay exit from 24 to 36h APF. We immunostained for the heterochromatin-

associated histone modifications H3K27me3, H3K9me3 and H4K20me3 at 26-28h APF, a timepoint when E2F induces abundant mitoses in the posterior wing (Supp. Fig. 3.3). We compared the clustering of the chromatin marks in the unperturbed anterior to the posterior wing. When cell cycle exit is delayed, all three modifications appear more diffuse throughout the nucleus and heterochromatin clustering is disrupted (Fig. 3.3A-M). To determine whether E2F altered the total abundance of the modified histones, we performed semi-quantitative western blots on 28h pupal wings. With E2F expression, total levels of H3 were increased, consistent with additional S-phases leading to replication-coupled canonical histone production [39, 40]. However the ratio of modified H3 to total H3 was relatively unchanged or even slightly increased when cell cycle exit was delayed (Fig. S3.1). This may be because E2F activity also increases the expression of several PRC2 components (*E(z), esc, Su(z)12*) and *Su(var)3-9)* as well as several other histone modifying enzymes (Table S3.1), a feature conserved with mammalian E2Fs [41]. Thus, delaying cell cycle exit increases new histone production, but the histone modification rate is maintained by a coordinated increase in the expression of the modifying enzymes.

3.4.4 Delaying cell cycle exit disrupts the localization of heterochromatin-associated proteins

To determine whether delaying cell cycle exit also affected the localization of proteins associated with heterochromatin, we examined HP1, D1 and Polycomb using a Pc-GFP fusion protein [17]. We observed a more diffuse localization and a reduction in the clustering of these heterochromatin-associated proteins when cell cycle exit was compromised (Fig. 3.4A-M). This was also accompanied by a reduction in

heterochromatin condensation, as assessed by the distance of the AACAC satellite to the chromocenter (Fig. 3.4 N).

The accumulation of PRC1 components such as Pc into large foci or Pc bodies is important for target gene repression [17, 31]. Since E2F expression disrupts Pc clustering we examined whether increased E2F activity can disrupt the repression of Pc target genes [42–44]. We selected 12 high-confidence Pc target genes predicted not to be direct E2F targets based upon published genome-wide E2F complex binding in *Drosophila* [45]. We examined their expression upon E2F activation in pupal wings at 24 and 36h APF using our previously published array data [46]. We found four Pc targets, *dsx*, *kni*, *twi* and *dve* to be reproducibly de-repressed 1.97-2.12-fold specifically at 24h APF, during the window of time that cell cycle exit is delayed. This suggests that delaying cell cycle exit can partially compromise Pc-dependent gene silencing. E2F activity similarly impacts heterochromatin-dependent gene silencing at the pericentromeric heterochromatin, with the loss of *e2f1* increasing gene silencing by position effect variegation and an increase in E2F activity de-repressing variegated gene expression [47].

In our experiments to delay cell cycle exit E2F is overexpressed for 28h, which includes the final 1-2 normal cell cycles in the pupa wing as well as 1-2 extra cell cycles based upon lineage tracing [18, 46]. We therefore asked whether expression of E2F within only the final cell cycle during terminal differentiation is adequate to disrupt heterochromatin clustering. We used temperature shifts to limit the expression of E2F to a 12h window within the final cell cycle in the pupa and observed a similar disruption of heterochromatin clustering (Fig. S3.4). We also observed similar effects on heterochromatin clustering when cell cycle exit was delayed by expression of other cell

cycle regulators such as CycE/Cdk2 or CycD/Cdk4 (Fig. S3.5). This demonstrates that heterochromatin clustering in differentiating cells can be disrupted by a single extra cell cycle and that this effect is not specific to E2F overexpression.

3.4.5 Histone modifications associated with de-condensation are upregulated upon G0 disruption

Compromising G0 leads to the disruption of heterochromatin clustering and chromatin condensation (Fig. 3.4). H3K27ac and H4K16ac are associated with open chromatin such as active enhancers and origins [48–51] and H4K16ac can suppress the formation of higher order chromatin structure [52]. We therefore examined whether these histone modifications were affected by delaying cell cycle exit with E2F overexpression. Indeed during the delay of cell cycle exit, we observed dramatic increase in the levels of these two histone marks throughout the nucleus (Fig. 3.5A-D). However other histone modifications associated with active chromatin were not affected, such as H3K4me3, pan H3 and H4 acetylation (Fig. 3.5E-J). Thus, an increase of H3K27ac and H4K16ac could contribute to the compromised chromatin condensation and disruption of heterochromatin clustering observed when cell cycle exit is delayed.

3.4.6 Heterochromatin clustering is restored when cells enter a robust G0 state

Delaying cell cycle exit disrupts heterochromatin clustering, however this is reversible. When we examined wings at 42h -46h, a timepoint when cells enter a robust G0 state refractory to E2F activation, heterochromatin clustering is either partially or completely restored (Fig. 3.6). Interestingly, levels of H3K27me3 and HP1 became higher

in robust G0 after cell cycle exit is delayed (Fig. 3.6A, D). This could be due to the E2F-dependent upregulation of *E(z)* and *Su(var)3-9*, which may indicate an expansion of heterochromatin in differentiating cells that enter a robust G0. Consistent with this idea we also observe an increase in the H2A variant H2Av in E2F-expressing cells in robust G0 (Fig. 3.6F) and an upregulation of several components of the NuA4 complex responsible for incorporation of H2Av (Table S3.1). Heterochromatin expansion is associated with senescence, suggesting delaying cell cycle exit with E2F overexpression could induce oncogenic stress or senescence-like features [53, 54]. Consistent with this, ectopic E2F in the wing induced multiple genes associated with senescence in mammals during robust G0 (Table S3.2) and led to a widespread increase in phosphorylated H2Av, a hallmark of E2F-induced replication stress and DNA damage in *Drosophila* (Fig. 3.6E) [55].

3.4.7 Heterochromatin clustering during terminal differentiation is a consequence of cell cycle exit, rather than differentiation.

Heterochromatin clustering becomes restored at the robust G0 phase in the wing as terminal differentiation proceeds. But whether differentiation or cell cycle arrest restores the heterochromatin clustering remains unclear. We previously demonstrated that the robust G0 state in the wing can be bypassed by co-expression of E2F + CycD/Cdk4 [18]. Under these conditions cells in the wing continue cycling past 48h APF, yet physical hallmarks of wing terminal differentiation such as cuticle secretion and wing hair formation proceed after 36h and adult wings form. This condition effectively uncouples cell cycle exit from terminal differentiation in the wing, with actively dividing

cells forming actin-rich wing hairs and developing adult cuticle (Fig. 3.7A-E). We took advantage of this dividing-yet-differentiated context to ask whether heterochromatin clustering requires cell cycle exit. We immunostained 42h wings expressing E2F+CycD/Cdk4 for H3K27Me3, H3K9Me3 and HP1 and found that clustering of facultative and constitutive heterochromatin was dramatically disrupted. We quantified facultative heterochromatin foci and found H3K27Me3 forming fewer, smaller and less intense foci (Fig. 3.7F-K). By contrast, HP1 levels became extremely high, with a diffuse localization throughout the nucleus (Fig. 3.7H, J), similar to the effects of E2F on HP1 at robust G0 (Fig. 3.6). These results demonstrate that heterochromatin clustering is a consequence of cell cycle exit rather than terminal differentiation. In addition, terminal differentiation can proceed despite a visibly significant disruption of heterochromatin organization.

3.5 Discussion

3.5.1 The relationship between heterochromatin clustering and differentiation

A number of studies have documented increased clustering and condensation of heterochromatin as cells differentiate [reviwed in 56]. In this study we reveal a substantial effect of the cell cycling status on heterochromatin clustering independent of differentiation. Heterochromatin clustering increases as the cell cycle slows and cells exit the cell cycle. By delaying or bypassing cell cycle exit in terminally differentiating cells, we show that the highly clustered state of heterochromatin in postmitotic cells is a consequence of cell cycle exit rather than the process of terminal differentiation. Importantly, we show that differentiation still proceeds even when cell cycle exit is

prevented and heterochromatin clustering is severely disrupted (Fig. 3.7). We suggest this is because disrupting heterochromatin clustering has only limited effects on the expression of specific heterochromatin-repressed genes in the context of the *Drosophila* wing (Fig. 3.4) and minimal effects on the terminal differentiation gene expression program. Indeed, we show that cell cycle exit can proceed normally in the *Drosophila* wing even when heterochromatin-dependent gene silencing is directly compromised (Fig. 3.2). Altogether this demonstrates that the increased heterochromatin clustering observed during differentiation is a consequence rather than a cause of cell cycle exit and raises questions regarding the function of increasing very long-range heterochromatin interactions and heterochromatin clustering in differentiation.

3.5.2 What is the function of heterochromatin clustering?

When we delay or bypass cell cycle exit, we visibly disrupt heterochromatin clustering. We find that this leads to very mild effects on the expression of only a small number of Polycomb target genes (Fig. 3.4), and we did not find significant de-repression of genes that are located in or near constitutive heterochromatin [57] (not shown). Our result is consistent with recent work showing that compromising some types of PcG clustering seems to have limited and selective effects on Polycomb target gene silencing [31]. However, the minimal effect of disrupting cell cycle exit on heterochromatin-dependent gene silencing is somewhat unexpected as the E2F1 gene was one of the early-identified modifiers of position-effect variegation (PEV), which is thought to be due to heterochromatin-dependent gene silencing through association with constitutive heterochromatin [47, 58, 59]. This suggests either the PEV assay is highly sensitive to

even mild or selective changes in heterochromatin-dependent gene silencing or that this assay reads out changes in the chromatin state that are different from the silencing of the endogenous genes we examined. Indeed, there are additional possible functions for heterochromatin clustering beyond heterochromatin-dependent gene silencing. For example, heterochromatin clustering could facilitate DNA damage repair in postmitotic cells, which downregulate many DNA repair genes when they exit the cell cycle and become more reliant on error prone NHEJ [reviewed in 60]. Sequestration of heterochromatin may prevent inappropriate interactions and fusions. It has also been proposed that sequestration of heterochromatin could lead to an increased efficiency of gene activation for very highly expressed genes by reducing the availability of possible binding sites for specific transcription factors [56], or could facilitate the formation of transcription factories [61].

A number of other studies also describe changes in the abundance of specific chromatin modifications associated with entry into or exit from G0. For example, H3K9Me3 and H3K27Me3 accumulate in postmitotic, differentiated cardiac muscle [37] while H4K16Ac and H3K27Ac increase in activated B cells exiting G0 [62]. While our data from the *Drosophila* wing suggests clustering of H3K9Me3 and H3K27Me3 domains during cell cycle exit rather than obvious changes in total levels, we do observe a strong up-regulation of H4K16 acetylation when G0 is delayed by E2F activation, a situation similar to cell cycle re-entry from G0. We also observe a decrease in H4K20Me3 when G0 is compromised, similar to what has been reported for quiescent human fibroblasts [63]. While H4K16Ac was not specifically measured in the fibroblast study, H4K20 methylation and H4K16 acetylation are antagonistic marks [64] and H4K16 acetylation

can decompact nucleosomes *in vitro*, although whether this also occurs *in vivo* has been questioned [52, 65]. We suggest some aspects of chromatin remodeling, such as compaction and coalescence of heterochromatin (which may be tied to H4K16/20 dynamics) are shared among different contexts of cell cycle exit/re-entry, while other chromatin changes associated with G0 entry/exit may be more cell type specific.

3.5.3 Why does delaying or bypassing cell cycle exit disrupt heterochromatin clustering in interphase?

Our experiments effectively separate cell cycle exit from terminal differentiation to reveal that heterochromatin clustering is a consequence of cell cycle exit. Furthermore, heterochromatin clustering can be disrupted within a single cell cycle (Fig. S3.4), suggesting progression through one round of S or M-phase is sufficient to disrupt heterochromatin clustering and long-range interactions. The effects we observe are not due to the dilution of chromatin marks by incorporation of new histones in S-phase, since we do not see changes in all histone marks (e.g. H3K4 methylation) or reduced global levels of histone marks in proliferating vs. postmitotic cells (Fig. S3.1). Indeed, when global levels of chromatin marks in actively proliferating fibroblasts were quantified and compared to fibroblasts held in G0 under contact inhibition for 14d, the majority of histone modifications did not exhibit significantly different levels [63]. This is likely because the levels of many histone modifiers are upregulated by positive cell cycle regulators through E2F transcriptional activity (Table S3.1) which effectively coordinates increased histone modification with increased production and incorporation in S-phase.

Overexpression of E2F could have effects on chromatin modifications and

condensation through sequestration or indirect inhibition of RB-family proteins via increased Cyclin/Cdk expression. RB associates with chromatin modifying complexes that promote facultative and constitutive heterochromatin formation [66–68]. RB also impacts chromosome condensation and cohesin levels at pericentromeric heterochromatin [69–71]. However in our experiments during robust exit, E2F levels and transcriptional targets remain high while heterochromatin clustering and chromatin marks are restored (Fig. 3.6). This suggests that even if RB is inhibited by overexpression of E2F, the eventual entry into robust G0 somehow restores heterochromatin organization and chromatin modifications independent of RB.

During mitosis most transcription factors and chromatin modifiers are ejected from chromatin and higher order architecture is lost [7]. This together with mitotic spindle assembly leads to the loss of long-range interactions and interchromosomal associations. These interactions are then restored, even in the presence of high E2F activity once cells engage additional mechanisms to exit the cell cycle during the robust G0 phase [46]. Our findings are in agreement with previous studies showing that the motion of heterochromatin domains and Polycomb bodies become more constrained as the cell cycle slows and cells exit the cell cycle [16, 17]. We suggest that constrained motion combined with increased self-association or polymerization likely leads to the coalescence of heterochromatin after cell cycle exit.

Coalescence of heterochromatin can be driven by heterochromatin-bound proteins that self-associate such as HP1. HP1 has recently been shown to undergo phase separation to form liquid droplets that fuse when interphase becomes longer during *Drosophila* embryogenesis [72]. These droplets have been suggested to form diffusion

barriers to limit heterochromatin access to specific factors such as TFIIB [73]. As the droplets fuse and mature during longer interphases, an immobile HP1 fraction forms. In our experiments to bypass cell cycle exit, we may limit the coalescence and maturation of HP1 droplets without preventing HP1 binding to H3K9me3. This could explain why dramatic effects on HP1 clustering may have minimal effects on gene de-repression. Alternatively, the role for HP1 clustering after cell cycle exit may largely affect silencing of transposons and piRNA clusters, an intriguing possibility to be addressed in future studies [74].

3.6 Conclusions:

Heterochromatin clusters as cell exit the cell cycle and terminally differentiate. Delaying or preventing cell cycle exit disrupts heterochromatin clustering and globally alters chromatin modifications. Heterochromatin clustering during terminal differentiation is a consequence of cell cycle exit, rather than differentiation. Compromising heterochromatin-dependent gene silencing does not disrupt cell cycle exit.

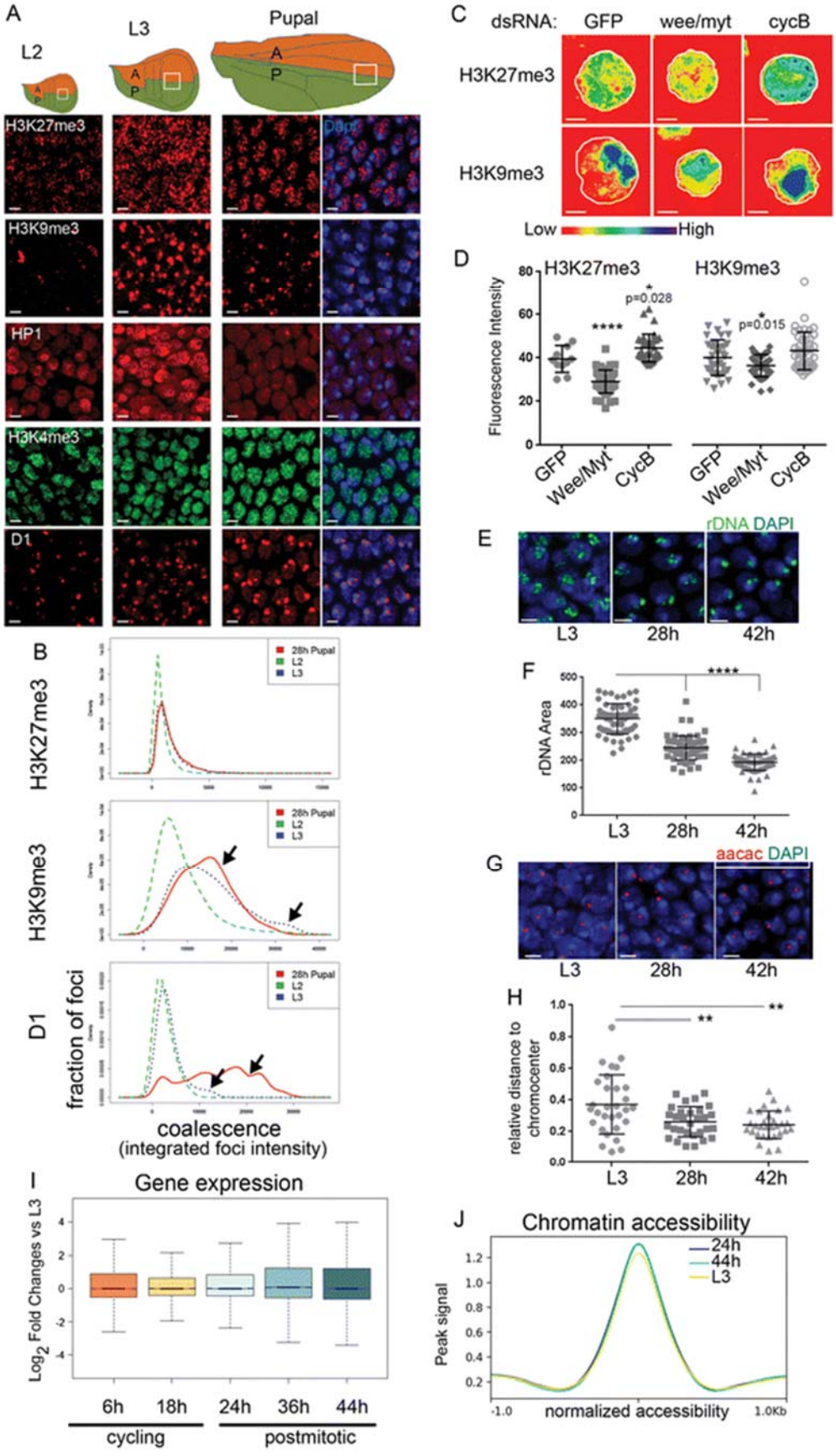
A
L2
L3
Pupal
A
P
H3K27me3
H3K9me3
HP1
H3K4me3
D1
Dapi
B
H3K27me3
H3K9me3
D1
fraction of foci
28h Pupal
L2
L3
coalescence
(integrated foci intensity)
C
dsRNA:
GFP
wee/myt
cycB
H3K27me3
H3K9me3
Low
High
D
H3K27me3
H3K9me3
Fluorescence Intensity
p=0.028
p=0.015
****
GFP
Wee/Myt
CycB
E
rDNA DAPI
L3
28h
42h
F
rDNA Area
****
L3
28h
42h
G
aacac DAPI
L3
28h
42h
H
relative distance to chromocenter
**
**
L3
28h
42h
I
Gene expression
Log2 Fold Changes vs L3
6h
18h
24h
36h
44h
cycling
postmitotic
J
Chromatin accessibility
24h
44h
L3
Peak signal
-1.0
normalized accessibility
1.0Kb

Figure 3.1 Heterochromatin clustering increases as the cell cycle slows and cells differentiate. (A) Wings of the indicated developmental stages were immunostained for the indicated chromatin modifications and chromatin binding proteins. (B) As the cell cycle slows down and cells differentiate, the distribution of heterochromatin-associated foci shift toward larger, brighter foci indicating increased clustering. Coalescence is quantified as the total intensity of individual focus within 129-448 nuclei at each developmental stage. (C,D) KC cells treated with dsRNA against GFP, *wee/myt* and *cycB* were immunostained for the indicated chromatin modifications and fluorescence intensity was quantified. (E,F) Fluorescent in situ hybridization (FISH) against the rDNA ITS region was performed on wings of the indicated stages. rDNA foci coalesce and condense in postmitotic cells. (G, H) FISH against the AACAC pericentromeric satellite repeats was performed on wings of the indicated stages and the distance to the center of the DAPI-bright chromocenter was measured. The distance decreases in postmitotic cells indicating increased condensation of heterochromatin. (I) A box plot of the RNA $\log_2$-fold changes compared to proliferative L3 for each timepoint is shown. (J) A line plot of average FAIRE-seq signal across all accessible chromatin for the indicated stages is shown. The accessibility of regulatory elements are similar in cycling and postmitotic wings. Scale bars=2 um. P-values were determined by an unpaired t-test *<0.05, **<0.01, ***<0.001, ****<0.0001.

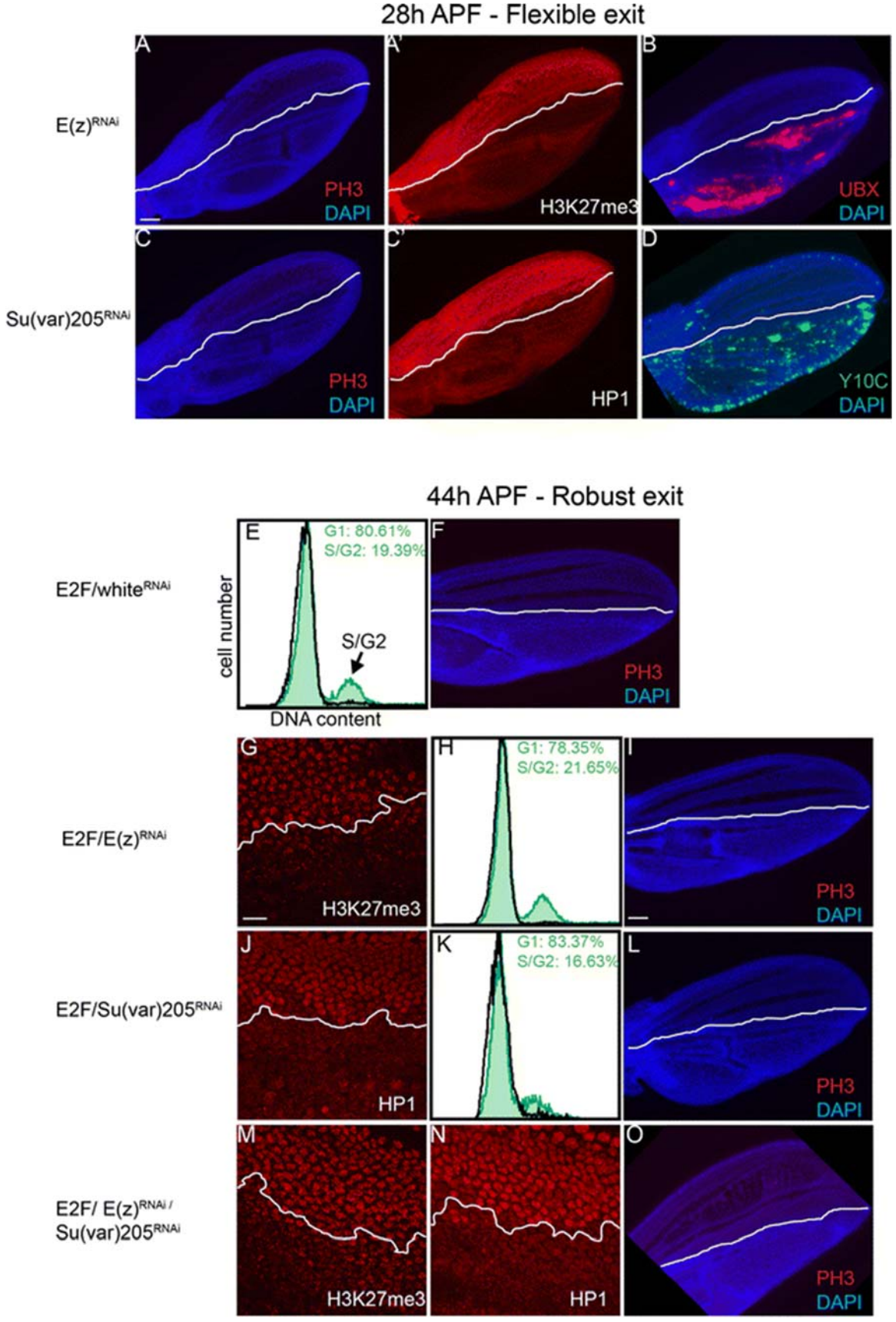
28h APF - Flexible exit
E(z)RNAi
Su(var)205RNAi
A
A'
B
C
C'
D
PH3
DAPI
H3K27me3
UBX
HP1
Y10C
44h APF - Robust exit
E2F/whiteRNAi
E2F/E(z)RNAi
E2F/Su(var)205RNAi
E2F/ E(z)RNAi / Su(var)205RNAi
E
F
G
H
I
J
K
L
M
N
O
G1: 80.61%
S/G2: 19.39%
S/G2
cell number
DNA content
G1: 78.35%
S/G2: 21.65%
G1: 83.37%
S/G2: 16.63%

Figure 3.2 Heterochromatin-dependent gene silencing is not required for cell cycle exit. (A-B) RNAi to *E(z)* was expressed in the posterior wing from the L3 stage until the indicated timepoints in metamorphosis. Postmitotic wings at 26-28h were examined for mitoses as indicated by phospho-Ser10-histone H3, PH3 (A), H3K27me3 (A') and de-repression of Ubx (B). (C) RNAi to *Su(var)205* (the gene encoding HP1) was overexpressed in the posterior wing and postmitotic tissues were immunostained for PH3 and HP1 (C'). These conditions led to loss of HP1 and disrupted heterochromatin-mediated silencing of the Y10C reporter (D). Control RNAi (to the *white* gene), *E(z)* and/or *Su(var)205* was expressed in the posterior wing in combination with E2F from the start of metamorphosis. Postmitotic wings at 42-44h were dissected and examined for H3K27me3 (G, M), HP1 (J, N) and PH3 (F, I, L, O). (E, H, K) Flow cytometry was also performed to measure cells that enter S and G2 phases. Green trace indicates cells from the posterior wing expressing the indicated transgenes. Black trace: control non-expressing anterior wing cells. Reduced heterochromatin gene silencing does not compromise G0 even in the presence of high E2F activity. Scale bars=50 um A-D,F,I,L and O; 10 um G,J,M and N.

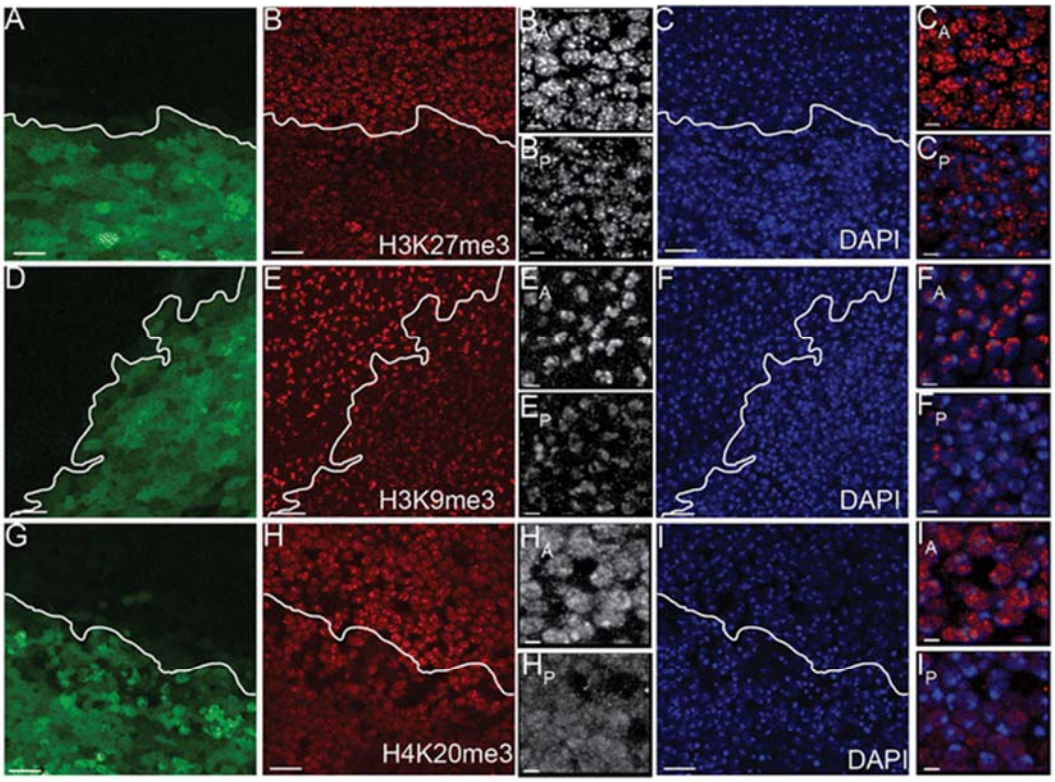
A
B
H3K27me3
C
DAPI
D
E
H3K9me3
F
DAPI
G
H
H4K20me3
I
DAPI

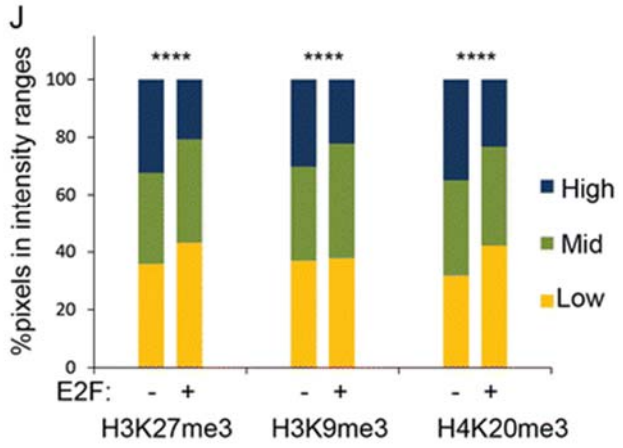
J
%pixels in intensity ranges
****
High
Mid
Low
E2F: - + - + - +
H3K27me3
H3K9me3
H4K20me3

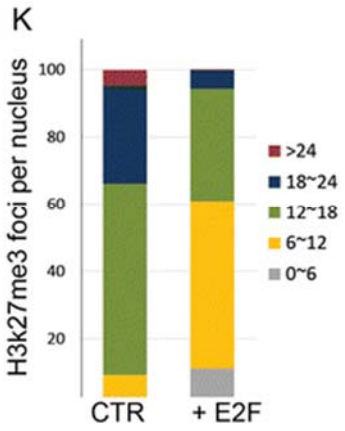
K
H3k27me3 foci per nucleus
>24
18~24
12~18
6~12
0~6
CTR
+ E2F

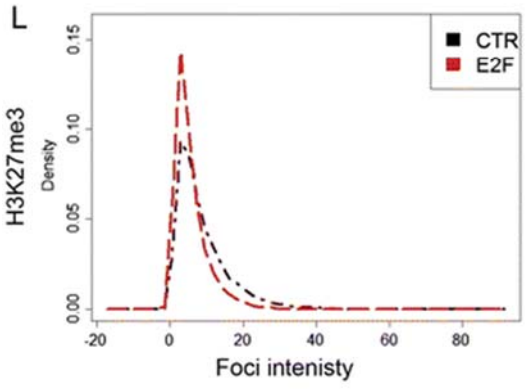
L
H3K27me3
Density
CTR
E2F
Foci intenisty

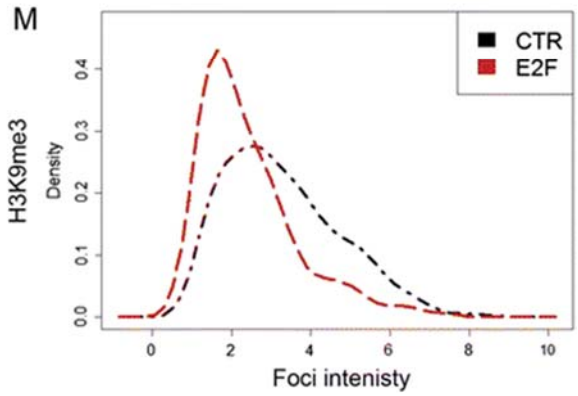
M
H3K9me3
Density
CTR
E2F
Foci intenisty

Figure 3.3 Heterochromatin clustering is disrupted when G0 is compromised. E2F was co-expressed with GFP in the posterior wing (boundary indicated by a white line) from the start of metamorphosis (0h APF) to delay cell cycle exit. At 26-28h wings were dissected and immunostained for the indicated chromatin modifications and DAPI to label nuclei (A-I). (J-M) Fluorescence signal were measured for 485-848 nuclei for each chromatin modification. The distribution of overall fluorescence intensity (J), foci number per nucleus section (K) and individual foci intensity (L, M) all indicate that delaying cell cycle exit disrupts heterochromatin clustering in wing cell nuclei. Scale bars=10 um in A-I except for anterior (A) and posterior (P) zoomed images where the bar = 2 um (e.g. B_A,B_P). P-values were determined by an unpaired t-test. *<0.05, **<0.01, ***<0.001, ****<0.0001.

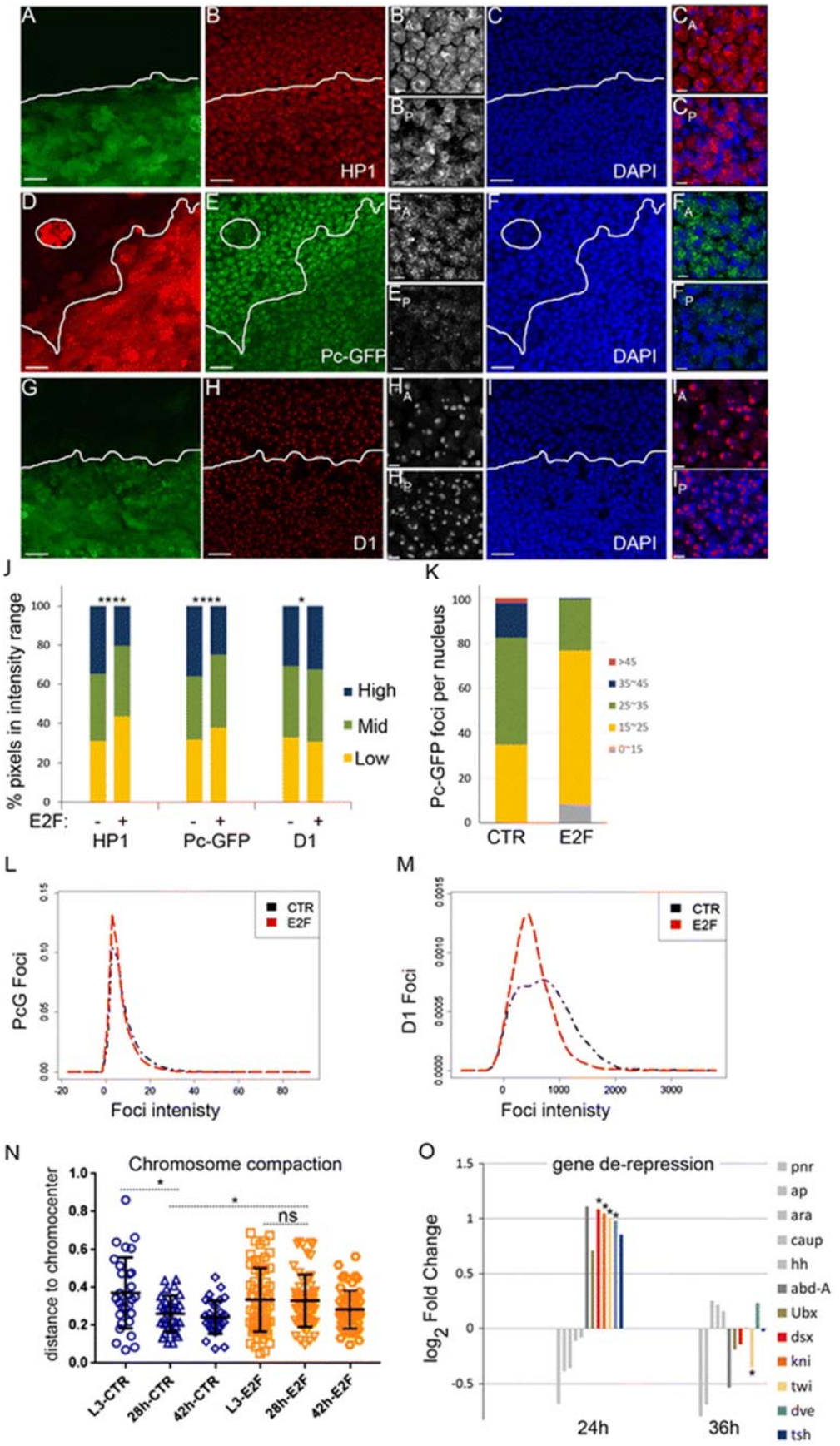
HP1
DAPI
Pc-GFP
DAPI
D1
DAPI
% pixels in intensity range
High
Mid
Low
E2F:
HP1
Pc-GFP
D1
Pc-GFP foci per nucleus
>45
35~45
25~35
15~25
0~15
CTR
E2F
PcG Foci
Foci intenisty
D1 Foci
Foci intenisty
Chromosome compaction
distance to chromocenter
ns
L3-CTR
28h-CTR
42h-CTR
L3-E2F
28h-E2F
42h-E2F
gene de-repression
log2 Fold Change
24h
36h
pnr
ap
ara
caup
hh
abd-A
Ubx
dsx
kni
twi
dve
tsh

Figure 3.4 Compromising G0 disrupts D1, HP1 and Polycomb body clustering and leads to partial de-repression of select PcG targets. E2F was co-expressed with GFP or RFP in the posterior wing to delay cell cycle exit. At 26-28h wings were dissected and immunostained for the indicated heterochromatin binding proteins and DAPI to label nuclei (A-I). (J) Overall fluorescence intensities were measured for 319-1270 nuclei for each chromatin modification. The distribution of individual foci intensity (L, M), foci number per nucleus section (K) all indicate that delaying cell cycle exit disrupts heterochromatin clustering and formation of large Polycomb bodies in wing cell nuclei. (N) Chromosome compaction was measured using the distance of the AACAC repeats to the chromocenter. When cell cycle exit is delayed, chromosome compaction is also compromised. For J, N, P-values were determined by an unpaired t-test. *<0.05, **<0.01, ***<0.001, ****<0.0001. (O) Microarray analysis revealed specific PcG target genes that become temporarily de-repressed in wings expressing E2F at 24h when cell cycle exit is delayed. P-values were determined by Anova *<0.05. Scale bars=10 um in A-I except for anterior (A) and posterior (P) zoomed images where the bar = 2 um (e.g. B_A, B_P).

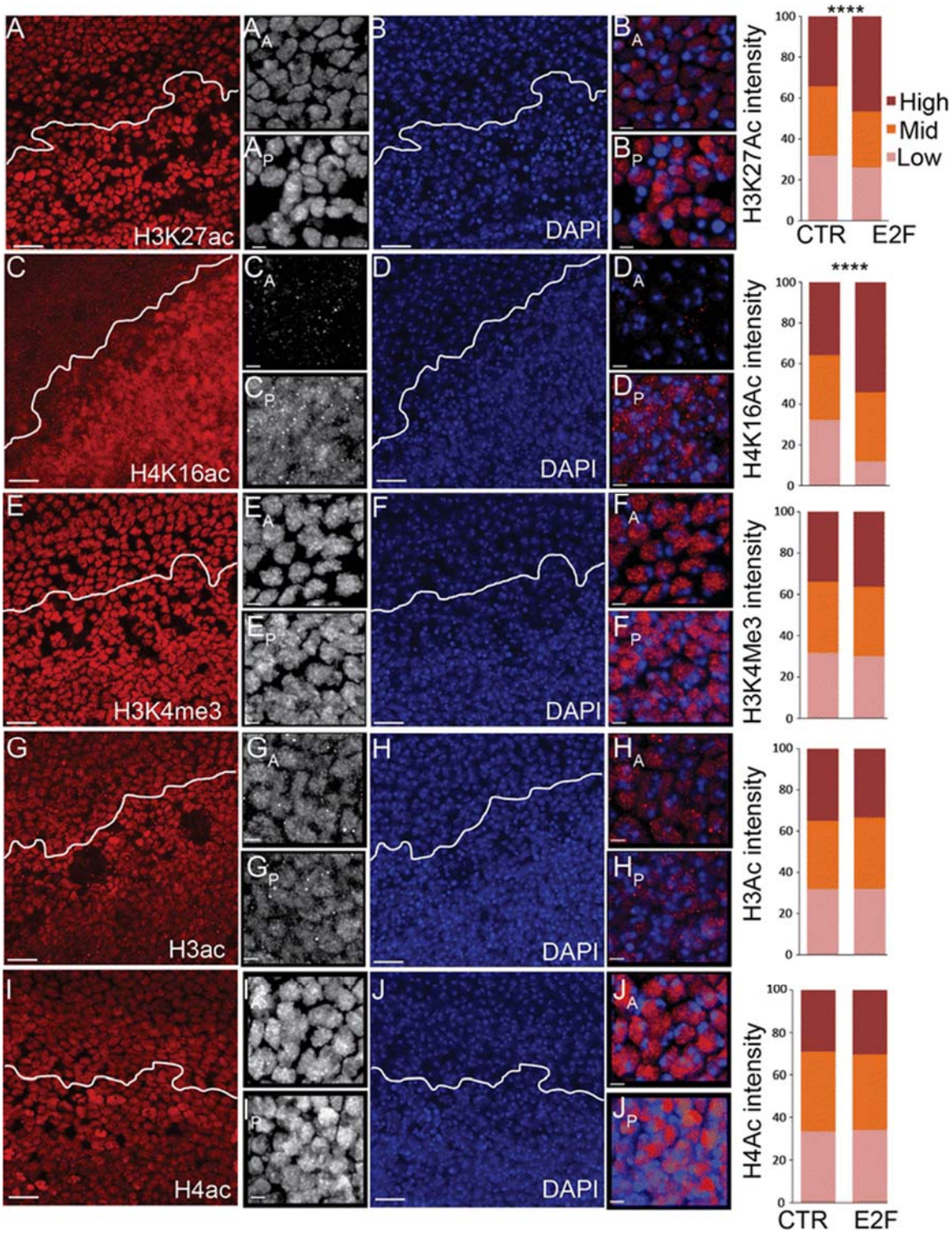
A
H3K27ac
B
DAPI
H3K27Ac intensity
****
High
Mid
Low
CTR
E2F
C
H4K16ac
D
DAPI
H4K16Ac intensity
****
E
H3K4me3
F
DAPI
H3K4Me3 intensity
G
H3ac
H
DAPI
H3Ac intensity
I
H4ac
J
DAPI
H4Ac intensity
CTR
E2F

Figure 3.5 Specific histone modifications associated with gene activation are increased when flexible G0 is compromised. E2F was expressed in the posterior wing to delay cell cycle exit. At 26-28h wings were dissected and immunostained for the indicated histone modifications and DAPI to label nuclei (A-J). The anterior–posterior boundary is indicated by a white line. The distribution of staining intensity in 217-1312 nuclei, binned into three ranges, is shown at right. Compromising flexible G0 specifically increases H3K27ac and H4K16ac. P-values were determined by an unpaired t-test; **** <0.0001. Scale bars=10 um in A-J except for anterior (A) and posterior (P) zoomed images where the bar = 2 um (e.g. B_A,B_P).

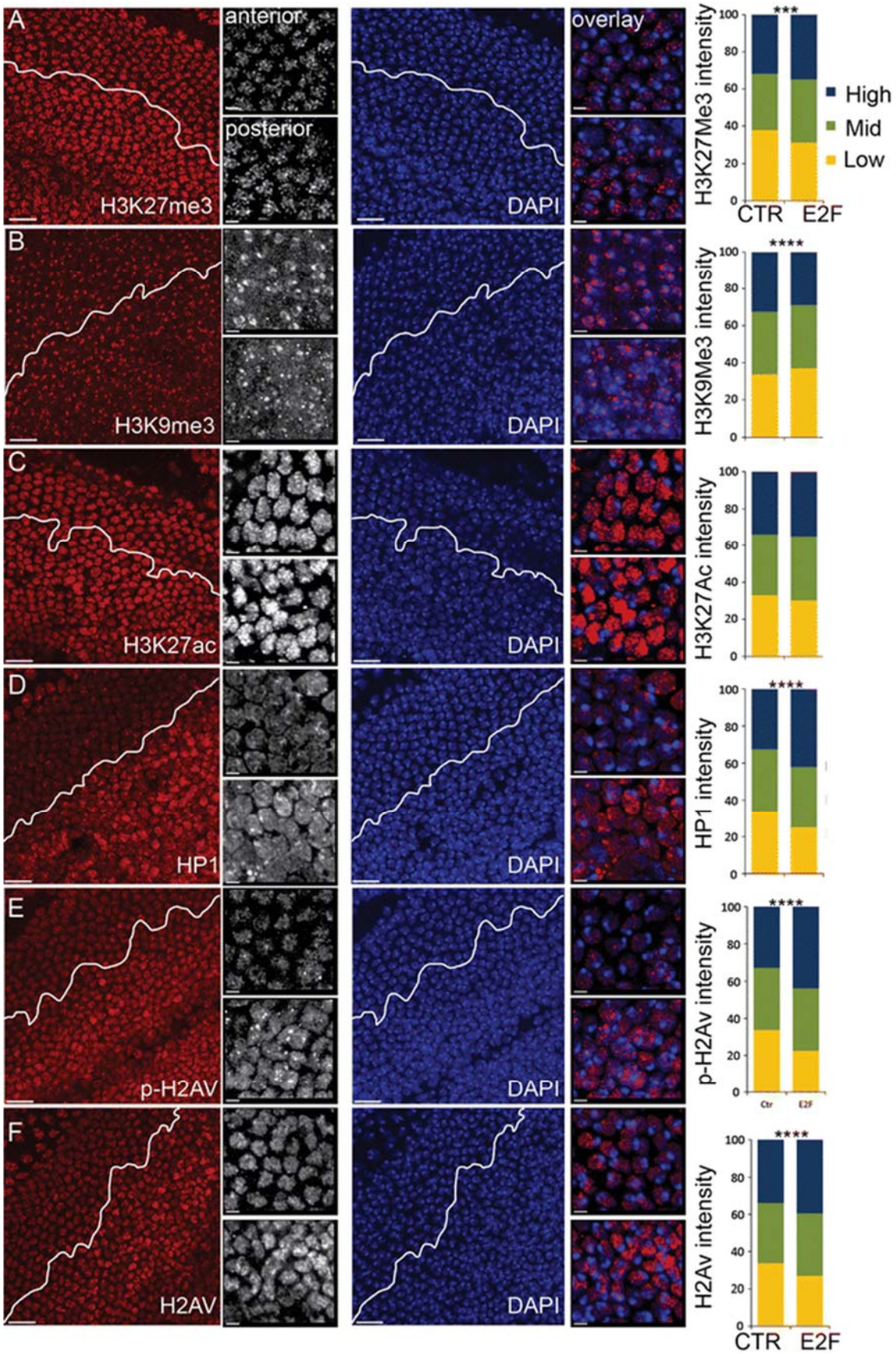
A
anterior
posterior
overlay
H3K27me3
DAPI
H3K27Me3 intensity
***
High
Mid
Low
CTR
E2F
B
H3K9me3
DAPI
H3K9Me3 intensity
****
C
H3K27ac
DAPI
H3K27Ac intensity
D
HP1
DAPI
HP1 intensity
****
E
p-H2AV
DAPI
p-H2Av intensity
****
Ctr
E2F
F
H2AV
DAPI
H2Av intensity
****
CTR
E2F

Figure 3.6 Robust G0 restores heterochromatin clustering and shares features with senescence. E2F was expressed in the posterior wing to delay cell cycle exit. At 42-44h, when cells are in robust G0, wings were dissected and immunostained for the indicated histone modifications or chromatin binding proteins and DAPI to label nuclei (A-F). The distribution of staining intensity in 509-1185 nuclei, binned into three ranges, is shown at right. Robust G0 in the presence of high E2F increases H3K27Me3, HP1 and pH2Av, chromatin marks associated with senescence. P-values were determined by an unpaired t-test; **** <0.0001, ***<0.001. Scale bars=10 um in A-F except for anterior (A) and posterior (P) zoomed images where the bar = 2 um (e.g. B_A,B_P).

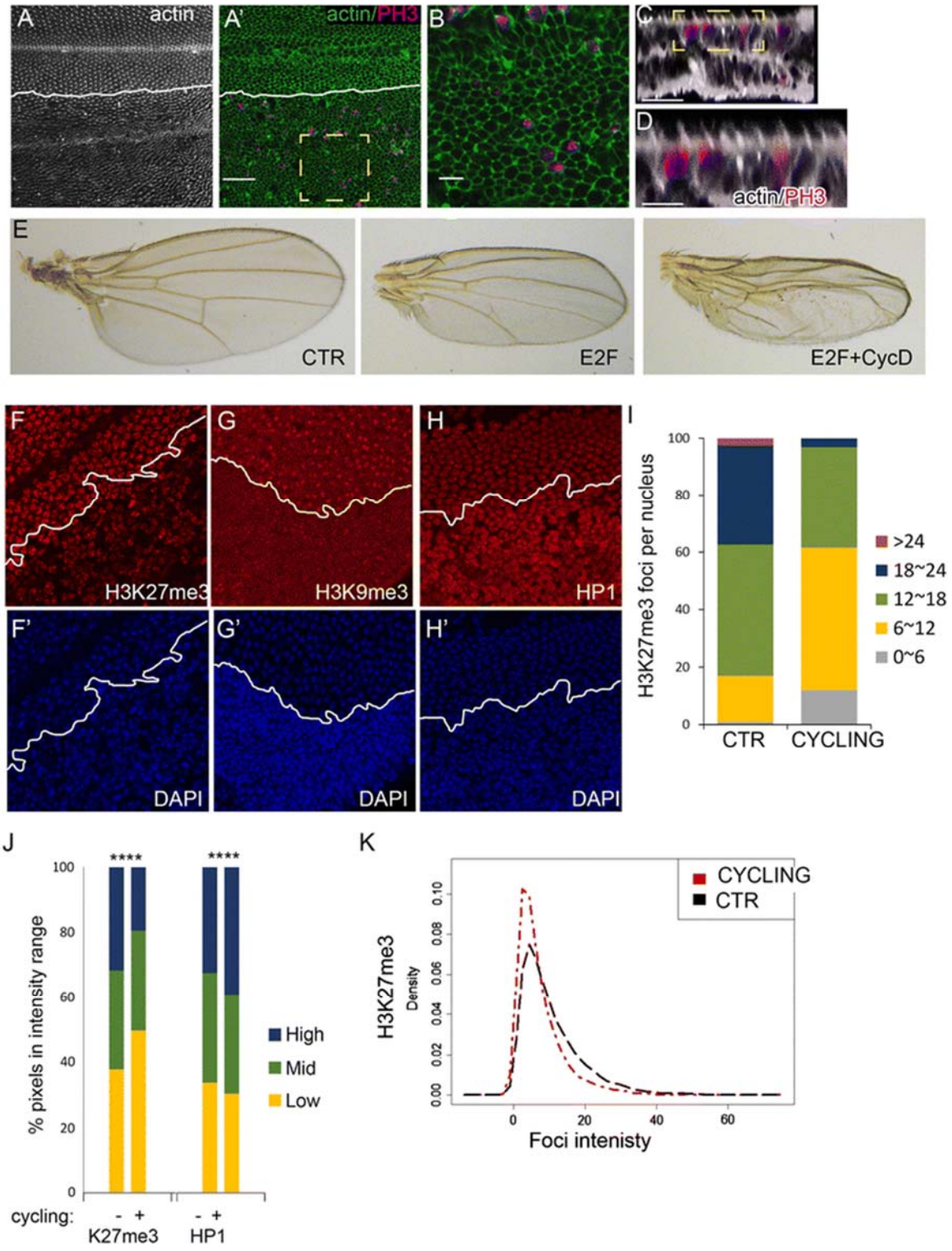
A
actin
A'
actin/PH3
B
C
D
actin/PH3
E
CTR
E2F
E2F+CycD
F
H3K27me3
G
H3K9me3
H
HP1
F'
DAPI
G'
DAPI
H'
DAPI
I
H3K27me3 foci per nucleus
100
80
60
40
20
0
CTR
CYCLING
>24
18~24
12~18
6~12
0~6
J
% pixels in intensity range
100
80
60
40
20
0
****
****
High
Mid
Low
cycling:
- +
- +
K27me3
HP1
K
H3K27me3
Density
0.00
0.02
0.04
0.06
0.08
0.10
0
20
40
60
Foci intenisty
CYCLING
CTR

Figure 3.7 Heterochromatin clustering during terminal differentiation is a consequence of cell cycle exit. CycD, Cdk4 and E2F were co-expressed in the posterior wing to bypass robust cell cycle exit without preventing terminal differentiation. The anterior-posterior boundary is indicated by a white line. (A-D) Pupal wings at 42-44h were dissected stained for actin and PH3 to label mitoses. Mitoses are evident in cells generating wings hairs, a hallmark of wing terminal differentiation (E) and the wings generate intact adult wing cuticle. C and D show optical cross sections (x/z) of wings to reveal PH3 and actin-rich hairs in the same section. (F-K) CycD, Cdk4 and E2F expression in the posterior wing prevents G0 entry and disrupts proper localization of heterochromatin associated histone modifications and HP1. (J) The distribution of staining intensity in 474-1191 nuclei, binned into three ranges is shown. The reduced foci number (I) and intensity (K) indicates compromised clustering of H3K27me3 containing chromatin when entry into G0 is prevented. P-values were determined by an unpaired t-test; ****<0.0001. Scale bars=10 um in A, 5 um in B and 2.5 um in D.

Supplemental Figures

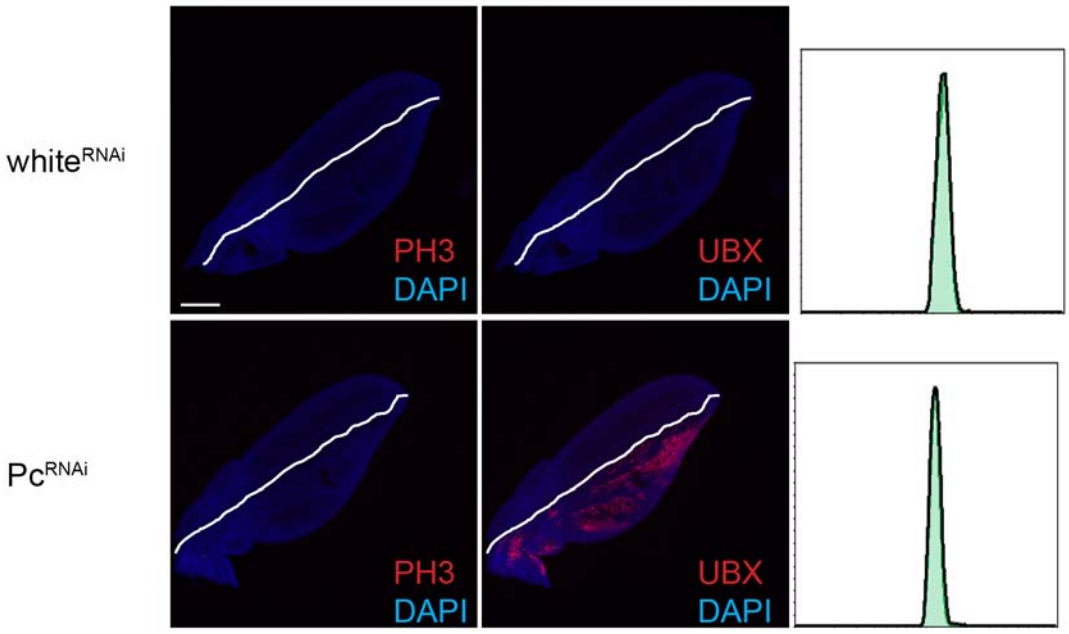

Figure S3.1 Global levels of histone modifications do not dramatically change at cell cycle exit. (A-D) Quantitative western blots were performed on wings of the indicated stages to assess the levels of modified or total histone H3 or HP1. Control (Ctrl) and E2F samples are from 28h postmitotic wings overexpressing GFP or E2F respectively. Total H3K9Me3, H3K27Me3, and HP1 levels do not dramatically change with cell cycle exit, however they increase with E2F expression. Modifications associated with active chromatin, H3K4Me3 and H3K27Ac also do not dramatically change with cell cycle exit, but increase upon E2F expression.

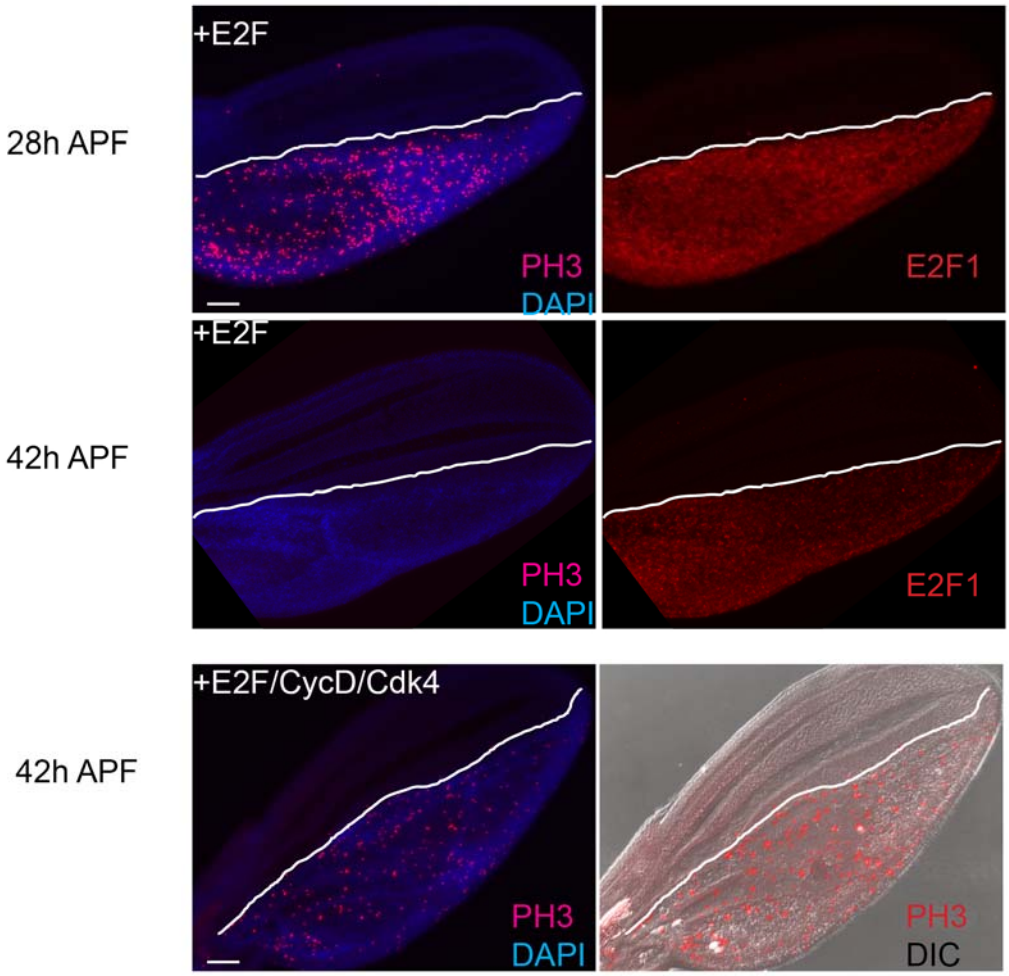

Figure S3.2 Compromising PRC1 does not delay cell cycle exit. RNAi to *Pc* or *white* (as a control) was expressed in the posterior wing from the L3 stage and postmitotic wings at 26-28h were examined for mitoses as indicated by PH3 and effective knockdown of PRC1 function by de-repression of the PRC1 target gene Ubx. Flow cytometry was also performed to measure cells that enter S and G2 phases. Green trace indicates cells from the posterior wing expressing the indicated transgenes. Black trace: control non-expressing anterior wing cells. Compromising PRC1 activity does not delay cell cycle exit. Scale bars=100 um.

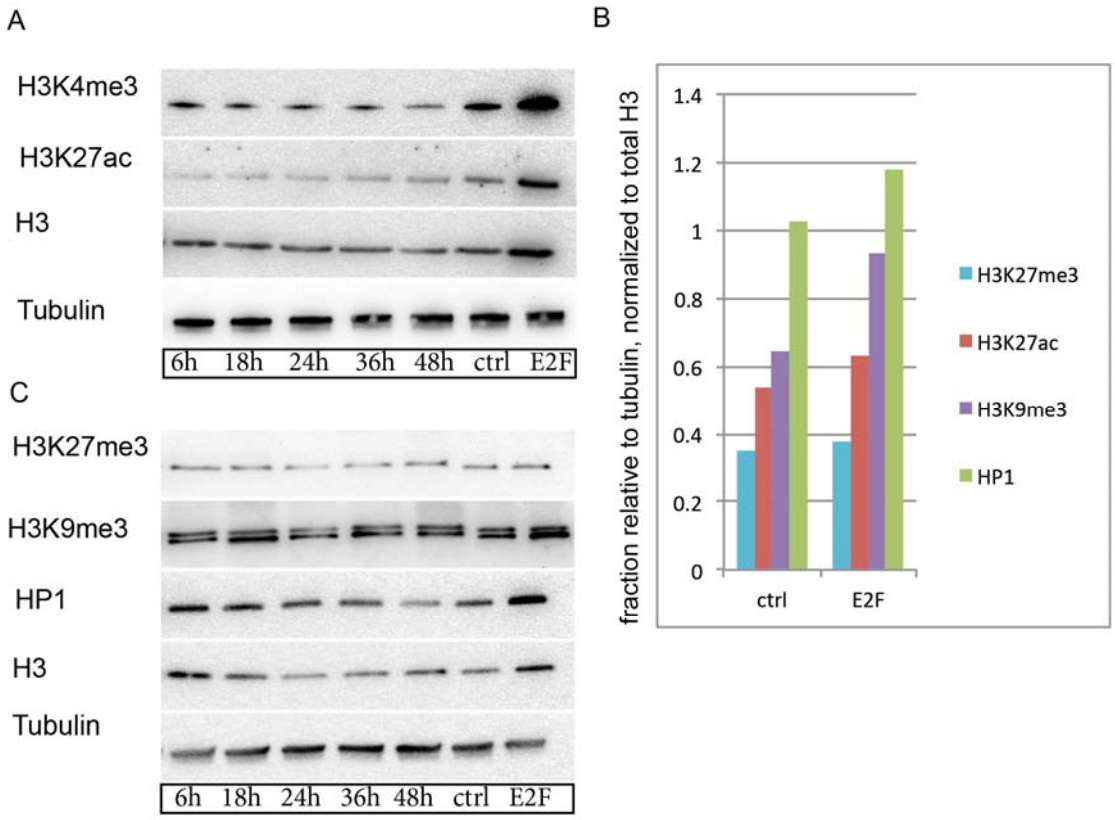

Figure S3.3 Two stages of G0 in differentiating wings. E2F was expressed in the posterior wing to delay cell cycle exit. 28h and 42h APF pupal tissues were dissected and immunostained for PH3 (to label mitoses) and E2F1. The anterior/posterior boundary is specified by the white line. Overexpression of E2F delays entry into G0 until 36h. At 42h cells expressing high E2F1 are postmitotic (in robust G0). CycD/Cdk4+E2F expression in the posterior wing is able to bypass the robust G0 to promote continued cycling, as shown by abundant mitoses (PH3) at 42h. Bar= 50um

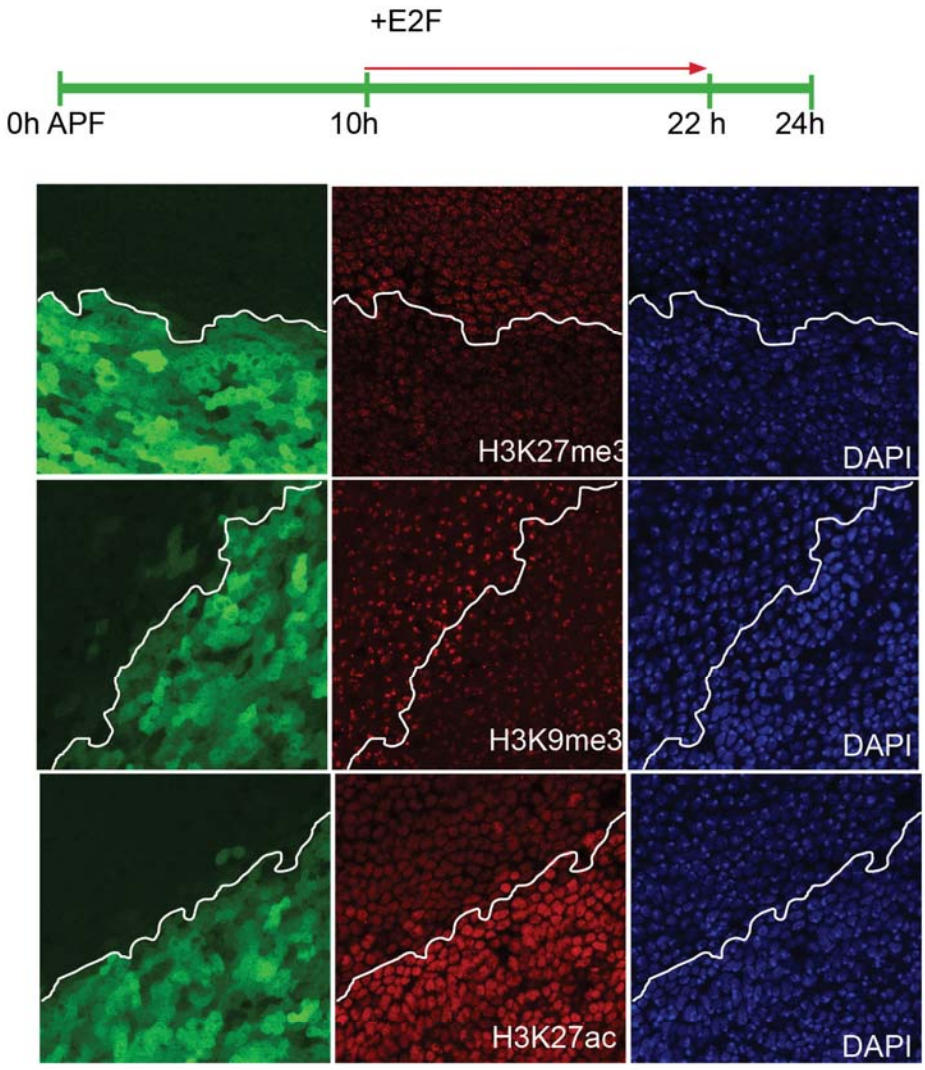
+E2F
0h APF
10h
22 h
24h
H3K27me3
DAPI
H3K9me3
DAPI
H3K27ac
DAPI

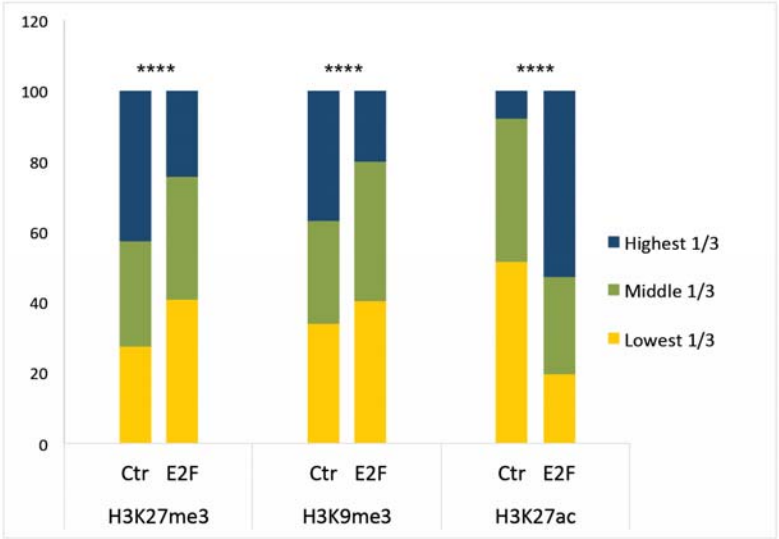
120
100
80
60
40
20
0
****
****
****
Highest 1/3
Middle 1/3
Lowest 1/3
Ctr E2F
H3K27me3
Ctr E2F
H3K9me3
Ctr E2F
H3K27ac

Figure S3.4 Clustering of heterochromatin can be disrupted within one cell cycle. E2F was overexpressed in the posterior wing from 10h APF. 12h later (within approximately one cell cycle) tissues were immunostained for indicated histone modifications. The posterior region is labeled by the expression of GFP and the anterior/posterior boundary is specified by the white line. The distribution of staining intensity in 1112-1339 nuclei, binned into three ranges, is shown at bottom. E2F disrupts heterochromatin clustering within one cell cycle. P-values were determined by an unpaired t-test; **** <0.0001.

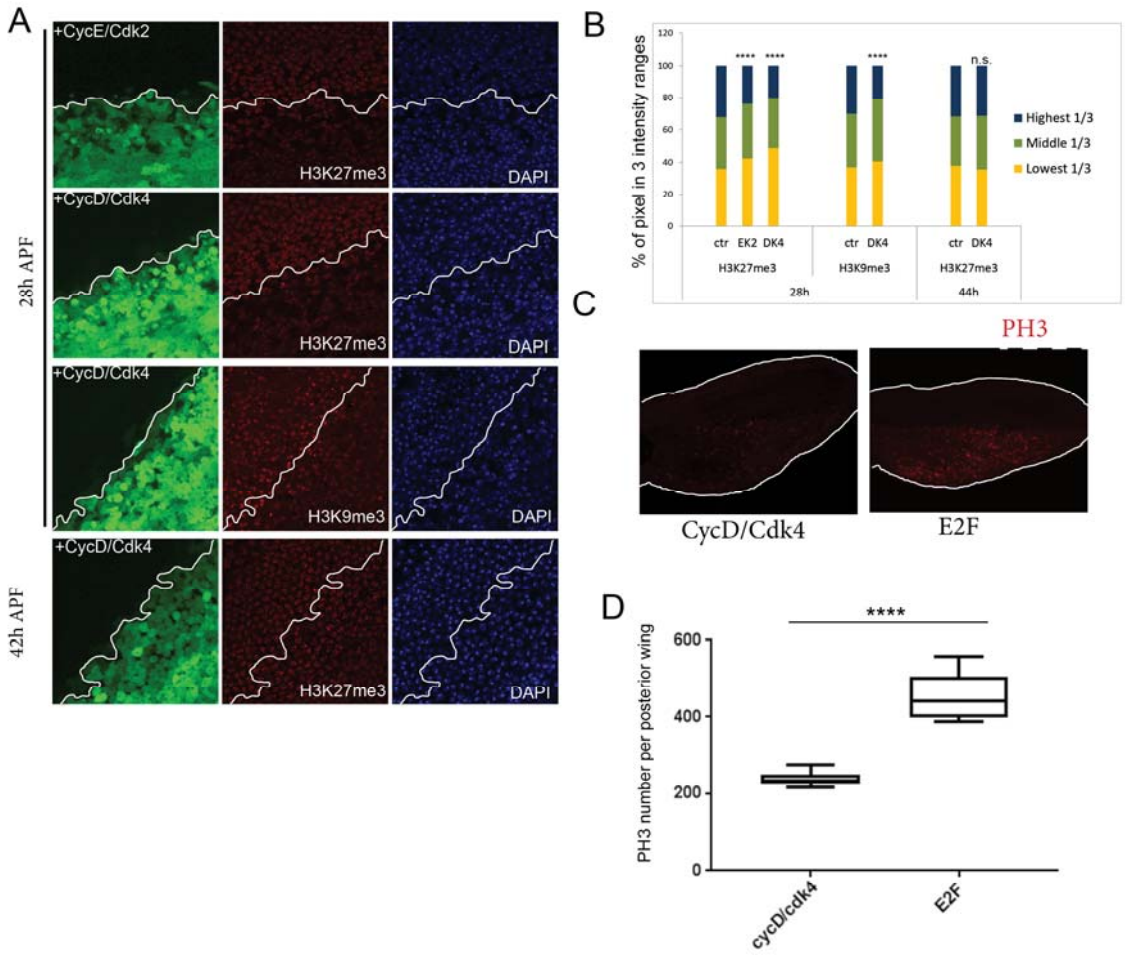

Figure S3.5 Delaying cell cycle exit disrupts heterochromatin (A) CycE/Cdk2 or CycD/Cdk4 complexes were overexpressed in the posterior wing from 0h APF. The anterior/posterior boundary is indicated by the white line. At 28h (flexible G0) or 42h APF (robust G0) pupal tissues were dissected and immunostained for the indicated histone modifications. (B) The distribution of staining intensity from 492-976 nuclei, binned into three ranges, is shown. Wings expressing E2F or CycD/Cdk4 to delay cell cycle exit were stained for mitoses (PH3) and the mitotic index at 27h was quantified for the posterior compartment (C-D). The degree of heterochromatin disruption correlates with the number of cells cycling. P-values were determined by an unpaired t-test; ****P-value <0.0001.

Supplemental Tables

Table S3.1 Chromatin modifiers/organizers/remodelers that are upregulated upon E2F1/DP expression in pupal wings

Gene	Function	log_2FC	Adj. p. value
	Histone Biosynth. /Nucleosome assembly		
Slbp		3.01	<0.001
mxc (NPAT)		0.58	<0.001
Lsm10		2.70	<0.001
Cpsf		1.80	<0.001
Asf1		2.09	<0.001
Hd		3.54	<0.001
Caf1-105		2.87	<0.001
Caf1-180		2.35	<0.001
	CHRAC complex		
Acf1		1.55	<0.001
ISWI		1.07	<0.001
Chrac-14		2.73	<0.001
	NuA4/TINTIN complexes		
Reptin		1.55	<0.001
domino		0.50	<0.001
Mrg15		0.66	<0.001
dMap1		0.58	<0.001
CG2982		1.55	<0.001
	Trithorax/TRR complexes		
Pa1		1.35	0.0039
Mnn1		1.40	<0.001
ash1		0.65	0.0166
Ptip		1.74	<0.001
CG33695 (Bap18)		1.69	<0.001
Trr		0.81	0.0025
	NSL/MSL complex		
Mof	H4K16 acetylase	2.35	<0.001
msl-1		0.68	0.0200
MBD-R2		0.81	<0.001
	DREAM/MMB complex		
mip120		2.51	<0.001
Rbf		2.24	<0.001
lin-52		1.18	0.010
E2f2		0.74	<0.001
	Insulators		
CG9740 (Ibf2)		1.11	<0.001
BEAF-32		1.67	<0.001
Pita		1.53	<0.001
DREF		1.25	<0.001
	NuRD complex		
Mta1-like		0.78	<0.001

rpd3	H3K27 deacetylase	0.91	<0.001
Chd3		4.08	<0.001
	PBAF complex		
Bap170		1.85	<0.001
Polybromo		1.61	<0.001
Bap55		1.10	<0.001
Bap111		0.74	<0.001
	PRC2 complex		
Esc		3.61	<0.001
Su(z)12		0.97	<0.001
Pcl		0.89	<0.001
E(z)	H3K27 methyltransferase	0.88	<0.001
	PhoRC Complex		
phol		0.95	<0.001
sfmbt		0.90	<0.001
	HP1 complexes		
Su(var)3-9	H3K9 methyltransferase	0.95	<0.001
HipHop		3.78	<0.001
cav (HOAP)		2.02	<0.001
Rif1		2.63	<0.001
Mes-4 (NSD)		1.75	<0.001
HP5		1.05	<0.001
Su(var)2-HP2		1.29	<0.001
	Other chromatin regulators		
SuUR		1.75	<0.001
PR-Set-7 (Set8)	H4K20 methylase	1.42	<0.001

Table S3.2 Genes associated with senescence that are upregulated during robust G0 in the presence of ectopic E2F1/DP.

Gene	Possible mammalian ortholog	log_2FC	Adj. p. value
	SASP-phenotype		
Mmp1	Matrix Metalloproteinases	2.52	<0.001
Ast-C	CXCR2 ligand	2.51	<0.001
Dsp1	HMGB1 (SASP regulator)	0.58	<0.002
	NfkB/MapK/TGF-□ signaling		
p38c	MAPKinase	1.38	<0.001
pipe	uronyl 2-sulfotransferase (UST)	0.73	<0.002
Traf4	TRAF4	0.84	<0.001
spitz	TNFRSF1A associated via death domain	1.01	<0.001
cv-2	BMPER	1.17	<0.001
shifted	WIF1	1.15	<0.001
fog	NECAP2	1.36	<0.001
CG4325	TRAIP	0.87	<0.002
frazzled	DCC	0.82	<0.001
	Oxidative Stress		
CG7737	SMOX/KDM1B	0.92	<0.006
CG31937	dehydrogenase/reductase 7	0.68	<0.002
Nmdmc	MTHFD1	0.66	<0.001
CG11200	*DHRSX*	0.85	<0.001
CG5599	DBT	1.09	<0.001
TPC1	Thiamine pyrophosphate carrier 1	1.52	<0.001
Multiple Cytochrome P450 enzymes			
Multiple DNA damage response genes			

3.7 References

1. Peric-Hupkes D, Meuleman W, Pagie L, Bruggeman SWM, Solovei I, Brugman W, et al. Molecular Maps of the Reorganization of Genome-Nuclear Lamina Interactions during Differentiation. Mol Cell. 2010;38:603–13.

2. Kohwi M, Lupton JR, Lai S-L, Miller MR, Doe CQ. Developmentally Regulated Subnuclear Genome Reorganization Restricts Neural Progenitor Competence in Drosophila. Cell. 2013;152:97–108.

3. Clowney EJ, LeGros MA, Mosley CP, Clowney FG, Markenskoff-Papadimitriou EC, Myllys M, et al. Nuclear Aggregation of Olfactory Receptor Genes Governs Their

Monogenic Expression. Cell. 2012;151:724–37.

4. Solovei I, Kreysing M, Lanctôt C, Kösem S, Peichl L, Cremer T, et al. Nuclear Architecture of Rod Photoreceptor Cells Adapts to Vision in Mammalian Evolution. Cell. 2009;137:356–68.

5. Asp P, Blum R, Vethantham V, Parisi F, Micsinai M, Cheng J, et al. Genome-wide remodeling of the epigenetic landscape during myogenic differentiation. Proc Natl Acad Sci. 2011;108:E149–58.

6. Alabert C, Bukowski-Wills J-C, Lee S-B, Kustatscher G, Nakamura K, de Lima Alves F, et al. Nascent chromatin capture proteomics determines chromatin dynamics during DNA replication and identifies unknown fork components. Nat Cell Biol. 2014;16:281–91.

7. Naumova N, Imakaev M, Fudenberg G, Zhan Y, Lajoie BR, Mirny LA, et al. Organization of the Mitotic Chromosome. Science (80-). 2013;342:948–53.

8. Kadauke S, Blobel GA. Mitotic bookmarking by transcription factors. Epigenetics Chromatin. 2013;6:6.

9. Rice JC, Nishioka K, Sarma K, Steward R, Reinberg D, Allis CD. Mitotic-specific methylation of histone H4 Lys 20 follows increased PR-Set7 expression and its localization to mitotic chromosomes. Genes Dev. 2002;16:2225–30.

10. Liu W, Tanasa B, Tyurina O V., Zhou TY, Gassmann R, Liu WT, et al. PHF8 mediates histone H4 lysine 20 demethylation events involved in cell cycle progression. Nature. 2010;466:508–12.

11. Bracken AP, Pasini D, Capra M, Prosperini E, Colli E, Helin K. EZH2 is downstream of the pRB-E2F pathway, essential for proliferation and amplified in cancer. EMBO J. 2003;22:5323–35.

12. Chen S, Bohrer LR, Rai AN, Pan Y, Gan L, Zhou X, et al. Cyclin-dependent kinases regulate epigenetic gene silencing through phosphorylation of EZH2. Nat Cell Biol. 2010;12:1108–14.

13. Kaneko S, Li G, Son J, Xu C-F, Margueron R, Neubert TA, et al. Phosphorylation of the PRC2 component Ezh2 is cell cycle-regulated and up-regulates its binding to ncRNA. Genes Dev. 2010;24:2615–20.

14. Wei Y, Chen Y-H, Li L-Y, Lang J, Yeh S-P, Shi B, et al. CDK1-dependent phosphorylation of EZH2 suppresses methylation of H3K27 and promotes osteogenic differentiation of human mesenchymal stem cells. Nat Cell Biol. 2011;13:87–94.

15. Ahmed K, Dehghani H, Rugg-Gunn P, Fussner E, Rossant J, Bazett-Jones DP. Global Chromatin Architecture Reflects Pluripotency and Lineage Commitment in the Early Mouse Embryo. PLoS One. 2010;5:e10531.

16. Thakar R, Csink AK. Changing chromatin dynamics and nuclear organization during differentiation in Drosophila larval tissue. J Cell Sci. 2005;118:951–60.

17. Cheutin T, Cavalli G. Progressive Polycomb Assembly on H3K27me3 Compartments Generates Polycomb Bodies with Developmentally Regulated Motion. PLoS Genet. 2012;8:e1002465.

18. Buttitta LA, Katzaroff AJ, Perez CL, de la Cruz A, Edgar BA. A double-assurance mechanism controls cell cycle exit upon terminal differentiation in Drosophila. Dev Cell. 2007;12:631–43.

19. Schubiger M, Palka J. Changing spatial patterns of DNA replication in the developing wing of Drosophila. Dev Biol. 1987;123:145–53.

20. Milán M, Campuzano S, García-Bellido A. Cell cycling and patterned cell proliferation in the Drosophila wing during metamorphosis. Proc Natl Acad Sci U S A. 1996;93:11687–92.

21. Flegel K, Sun D, Grushko O, Ma Y, Buttitta L. Live cell cycle analysis of Drosophila tissues using the Attune Acoustic Focusing Cytometer and Vybrant DyeCycle violet DNA stain. J Vis Exp. 2013;:e50239.

22. Guo Y, Flegel K, Kumar J, McKay DJ, Buttitta LA. Ecdysone signaling induces two phases of cell cycle exit in Drosophila cells. Biol Open. 2016;5:1648–61.

23. Sun D, Buttitta L. Protein phosphatase 2A promotes the transition to G0 during terminal differentiation in Drosophila. Development. 2015;142:3033–45.

24. Johnston LA, Sanders AL. Wingless promotes cell survival but constrains growth during Drosophila wing development. Nat Cell Biol. 2003;5:827–33.

25. Reis T, Edgar BA. Negative regulation of dE2F1 by cyclin-dependent kinases controls cell cycle timing. Cell. 2004;117:253–64.

26. Riddle NC, Minoda A, Kharchenko P V, Alekseyenko AA, Schwartz YB, Tolstorukov MY, et al. Plasticity in patterns of histone modifications and chromosomal proteins in Drosophila heterochromatin. Genome Res. 2011;21:147–63.

27. Aulner N, Monod C, Mandicourt G, Jullien D, Cuvier O, Sall A, et al. The AT-hook protein D1 is essential for Drosophila melanogaster development and is implicated in position-effect variegation. Mol Cell Biol. 2002;22:1218–32.

28. Figueiredo MLA, Philip P, Stenberg P, Larsson J. HP1a Recruitment to Promoters Is Independent of H3K9 Methylation in Drosophila melanogaster. PLoS Genet. 2012;8:e1003061.

29. Loubiere V, Delest A, Thomas A, Bonev B, Schuettengruber B, Sati S, et al. Coordinate redeployment of PRC1 proteins suppresses tumor formation during Drosophila development. Nat Genet. 2016;48:1436–42.

30. Gonzalez I, Mateos-Langerak J, Thomas A, Cheutin T, Cavalli G. Identification of Regulators of the Three-Dimensional Polycomb Organization by a Microscopy-Based Genome-wide RNAi Screen. Mol Cell. 2014;54:485–99.

31. Wani AH, Boettiger AN, Schorderet P, Ergun A, Münger C, Sadreyev RI, et al.

Chromatin topology is coupled to Polycomb group protein subnuclear organization. Nat Commun. 2016;7:10291.

32. Lavoie BD, Hogan E, Koshland D. In vivo requirements for rDNA chromosome condensation reveal two cell-cycle-regulated pathways for mitotic chromosome folding. Genes Dev. 2004;18:76–87.

33. Freeman L, Aragon-Alcaide L, Strunnikov A. The condensin complex governs chromosome condensation and mitotic transmission of rDNA. J Cell Biol. 2000;149:811–24.

34. McKnight JN, Boerma JW, Breeden LL, Tsukiyama T. Global Promoter Targeting of a Conserved Lysine Deacetylase for Transcriptional Shutoff during Quiescence Entry. Mol Cell. 2015;59:732–43.

35. Uyehara CM, Nystrom SL, Niederhuber MJ, Leatham-Jensen M, Ma Y, Buttitta LA, et al. Hormone-dependent control of developmental timing through regulation of chromatin accessibility. Genes Dev. 2017;31:862–75.

36. Blais A, van Oevelen CJC, Margueron R, Acosta-Alvear D, Dynlacht BD. Retinoblastoma tumor suppressor protein–dependent methylation of histone H3 lysine 27 is associated with irreversible cell cycle exit. J Cell Biol. 2007;179:1399–412.

37. Sdek P, Zhao P, Wang Y, Huang C, Ko CY, Butler PC, et al. Rb and p130 control cell cycle gene silencing to maintain the postmitotic phenotype in cardiac myocytes. J Cell Biol. 2011;194:407–23.

38. Panteleeva I, Boutillier S, See V, Spiller DG, Rouaux C, Almouzni G, et al. HP1α guides neuronal fate by timing E2F-targeted genes silencing during terminal differentiation. EMBO J. 2007;26:3616–28.

39. Ma T, Van Tine BA, Wei Y, Garrett MD, Nelson D, Adams PD, et al. Cell cycle-regulated phosphorylation of p220(NPAT) by cyclin E/Cdk2 in Cajal bodies promotes histone gene transcription. Genes Dev. 2000;14:2298–313.

40. Zhao J, Kennedy BK, Lawrence BD, Barbie DA, Matera AG, Fletcher JA, et al. NPAT links cyclin E-Cdk2 to the regulation of replication-dependent histone gene transcription. Genes Dev. 2000;14:2283–97.

41. Muller H, Bracken AP, Vernell R, Moroni MC, Christians F, Grassilli E, et al. E2Fs regulate the expression of genes involved in differentiation, development, proliferation, and apoptosis. Genes Dev. 2001;15:267–85.

42. Schwartz YB, Kahn TG, Nix DA, Li X-Y, Bourgon R, Biggin M, et al. Genome-wide analysis of Polycomb targets in Drosophila melanogaster. Nat Genet. 2006;38:700–5.

43. Tolhuis B, Muijrers I, de Wit E, Teunissen H, Talhout W, van Steensel B, et al. Genome-wide profiling of PRC1 and PRC2 Polycomb chromatin binding in Drosophila melanogaster. Nat Genet. 2006;38:694–9.

44. Schuettengruber B, Cavalli G. Recruitment of Polycomb group complexes and their role in the dynamic regulation of cell fate choice. Development. 2009;136:3531–42.

45. Korenjak M, Anderssen E, Ramaswamy S, Whetstine JR, Dyson NJ. RBF Binding to both Canonical E2F Targets and Noncanonical Targets Depends on Functional dE2F/dDP Complexes. Mol Cell Biol. 2012;32:4375–87.

46. Buttitta LA, Katzaroff AJ, Edgar BA. A robust cell cycle control mechanism limits E2F-induced proliferation of terminally differentiated cells in vivo. J Cell Biol. 2010;189:981–96.

47. Seum C, Spierer A, Pauli D, Szidonya J, Reuter G, Spierer P. Position-effect variegation in Drosophila depends on dose of the gene encoding the E2F transcriptional activator and cell cycle regulator. Development. 1996;122:1949–56.

48. Ho JWK, Jung YL, Liu T, Alver BH, Lee S, Ikegami K, et al. Comparative analysis of metazoan chromatin organization. Nature. 2014;512:449–52.

49. Schwaiger M, Stadler MB, Bell O, Kohler H, Oakeley EJ, Schubeler D. Chromatin state marks cell-type- and gender-specific replication of the Drosophila genome. Genes Dev. 2009;23:589–601.

50. Liu J, McConnell K, Dixon M, Calvi BR. Analysis of model replication origins in Drosophila reveals new aspects of the chromatin landscape and its relationship to origin activity and the prereplicative complex. Mol Biol Cell. 2012;23:200–12.

51. Shlyueva D, Stampfel G, Stark A. Transcriptional enhancers: from properties to genome-wide predictions. Nat Rev Genet. 2014;15:272–86.

52. Shogren-Knaak M, Ishii H, Sun J-M, Pazin MJ, Davie JR, Peterson CL. Histone H4-K16 Acetylation Controls Chromatin Structure and Protein Interactions. Science (80-). 2006;311:844–7.

53. Di Micco R, Sulli G, Dobreva M, Liontos M, Botrugno OA, Gargiulo G, et al. Interplay between oncogene-induced DNA damage response and heterochromatin in senescence and cancer. Nat Cell Biol. 2011;13:292–302.

54. Narita M, Nũnez S, Heard E, Narita M, Lin AW, Hearn SA, et al. Rb-mediated heterochromatin formation and silencing of E2F target genes during cellular senescence. Cell. 2003;113:703–16.

55. Davidson JM, Duronio RJ. S Phase–Coupled E2f1 Destruction Ensures Homeostasis in Proliferating Tissues. PLoS Genet. 2012;8:e1002831.

56. Meister P, Mango SE, Gasser SM. Locking the genome: nuclear organization and cell fate. Curr Opin Genet Dev. 2011;21:167–74.

57. Smith CD, Shu S, Mungall CJ, Karpen GH. The Release 5.1 Annotation of Drosophila melanogaster Heterochromatin. Science (80-). 2007;316:1586–91.

58. Harmon B, Sedat J. Cell-by-Cell Dissection of Gene Expression and Chromosomal Interactions Reveals Consequences of Nuclear Reorganization. PLoS Biol. 2005;3:e67.

59. Csink AK, Henikoff S. Genetic modification of heterochromatic association and nuclear organization in Drosophila. Nature. 1996;381:529–31.

60. Iyama T, Wilson DM. DNA repair mechanisms in dividing and non-dividing cells. DNA Repair (Amst). 2013;12:620–36.

61. Van Bortle K, Corces VG. Nuclear Organization and Genome Function. Annu Rev Cell Dev Biol. 2012;28:163–87.

62. Kieffer-Kwon K-R, Nimura K, Rao SSP, Xu J, Jung S, Pekowska A, et al. Myc Regulates Chromatin Decompaction and Nuclear Architecture during B Cell Activation. Mol Cell. 2017;67:566–578.e10.

63. Evertts AG, Manning AL, Wang X, Dyson NJ, Garcia BA, Coller HA. H4K20 methylation regulates quiescence and chromatin compaction. Mol Biol Cell. 2013;24:3025–37.

64. Nishioka K, Rice JC, Sarma K, Erdjument-Bromage H, Werner J, Wang Y, et al. PR-Set7 is a nucleosome-specific methyltransferase that modifies lysine 20 of histone H4 and is associated with silent chromatin. Mol Cell. 2002;9:1201–13.

65. Taylor GCA, Eskeland R, Hekimoglu-Balkan B, Pradeepa MM, Bickmore WA. H4K16 acetylation marks active genes and enhancers of embryonic stem cells, but does not alter chromatin compaction. Genome Res. 2013;23:2053–65.

66. Ishak CA, Marshall AE, Passos DT, White CR, Kim SJ, Cecchini MJ, et al. An RB-EZH2 Complex Mediates Silencing of Repetitive DNA Sequences. Mol Cell. 2016;64:1074–87.

67. Gonzalo S, Blasco MA. Role of Rb Family in the Epigenetic Definition of Chromatin. Cell Cycle. 2005;4:752–5.

68. Isaac CE, Francis SM, Martens AL, Julian LM, Seifried LA, Erdmann N, et al. The Retinoblastoma Protein Regulates Pericentric Heterochromatin. Mol Cell Biol. 2006;26:3659–71.

69. Longworth MS, Herr A, Ji J-Y, Dyson NJ. RBF1 promotes chromatin condensation through a conserved interaction with the Condensin II protein dCAP-D3. Genes Dev. 2008;22:1011–24.

70. Manning AL, Longworth MS, Dyson NJ. Loss of pRB causes centromere dysfunction and chromosomal instability. Genes Dev. 2010;24:1364–76.

71. Longworth MS, Dyson NJ. pRb, a local chromatin organizer with global possibilities. Chromosoma. 2010;119:1–11.

72. Strom AR, Emelyanov A V., Mir M, Fyodorov D V., Darzacq X, Karpen GH. Phase separation drives heterochromatin domain formation. Nature. 2017;547:241–5.

73. Larson AG, Elnatan D, Keenen MM, Trnka MJ, Johnston JB, Burlingame AL, et al. Liquid droplet formation by HP1α suggests a role for phase separation in heterochromatin. Nature. 2017;547:236–40.

74. Penke TJR, McKay DJ, Strahl BD, Matera AG, Duronio RJ. Direct interrogation of the role of H3K9 in metazoan heterochromatin function. Genes Dev. 2016;30:1866–80.

Chapter 4. Discussion and Future Directions

Cell cycle exit, or G0, is tightly controlled during terminal differentiation to ensure proper organogenesis. When and how to initiate entry into G0 is a critical decision a cell must make during development. Two strategies have been identified to establish G0: directly constraining Cyclin-dependent kinases activities and transcriptionally repressing cell cycle gene expression. Multiple regulators can be employed to constrain Cdk activity, for example, upregulating Cyclin-dependent kinase inhibitors to directly repress Cdks function, utilizing degradation machinery APC/C^{Cdh1} to control the protein level of Cdks and CKIs, or removing the activating phosphorylation on Cdks through Protein Phosphatase 2A (PP2A) [1–7].

Transcriptional repression of cell cycle gene is largely exerted through the repressive DREAM complex. Multiple chromatin modifiers or remodelers have been implicated as co-repressors in silencing cell cycle genes through associating with the RB component of DREAM complex, suggesting a potential role for chromatin structure in promoting G0 [8, 9]. However, it is still unclear how chromatin changes in G0 during terminal differentiation. Taking advantage of the temporally coordinated cell cycle exit during *Drosophila* wing terminal differentiation, I investigated the relationship between cell cycle exit, terminal differentiation and chromatin structure.

4.1 Dominant control on the accessibility of complex cell cycle gene enhancers by differentiation program

Components of the nucleosome remodeling complex SWI/SNF have been shown to associate with RB, silence cell cycle genes and promote G0 entry, potentially through regulating chromatin accessibility by moving or displacing nucleosomes [10–14]. However, how chromatin accessibility changes during cell cycle exit is still unclear. I comprehensively examined the genome-wide transcriptome and chromatin accessibility landscape and found that during wing differentiation, chromatin accessibility and gene expression changes are coordinated with the transition from a proliferating to postmitotic state. Most importantly, distal enhancers of complex cell cycle genes such as *stg* and *cycE* lose their accessibility along with gene silencing and remain closed in the prolonged G0 state. Surprisingly, these enhancers still close even when G0 is bypassed through ectopic E2F/CycD/Cdk4 activities, revealing that the accessibility of complex cell cycle genes is dominantly controlled by differentiation program and independent of cell cycling status. However, the expression level of *cycE* and *stg*, although still higher than wildtype control, is lower than flexible stage when the enhancers are accessible, suggesting that the opening of distal enhancers is required for maximal gene activation. It is worth to mention that E2F/CycD/Cdk4 manipulation is able to activate both simple cell cycle genes and complex cell cycle genes more strongly compared to E2F alone. One potential reason is that the extra CycD/Cdk4 activities phosphorylate RBF, and disrupt the assembly of dREAM complex at the proximal promoter around TSS [9]. In sum, my work indicates a robust reinforcement of cell cycle gene regulation by differentiation program at the

chromatin level and elicits future investigations to identify the responsible transcription factors and nucleosome remodeling complex.

4.2 Identifying nucleosome remodeling complex that regulates the accessibility of cell cycle gene enhancers

In chapter 2, I investigated the enhancers of complex cell cycle genes and discovered that they are closed in late, robust G0, under developmental control. The loss of enhancer accessibility is potentially the molecular mechanism underlying the proliferation barrier in robust G0 and failure to close those enhancers could potentially result in ectopic cell cycle gene expression. The accessibility of enhancers is regulated through coordinated activities of nucleosome remodeling complexes as well as transcriptional factors that recognize the enhancers in the first place.

SWI/SNF components have been shown to regulate cell cycle gene expression and G0 in mammalian and *C. elegans* muscle cells [10–12, 14, 15]. However, whether SWI/SNF is the nucleosome remodeling complex that governs cell cycle gene enhancers in *Drosophila* wing is unclear. I undertook a targeted RNAi-based screen to identify nucleosome remodeling factors that may be involved in closing cell cycle gene enhancers and promoting G0. In this screen I used a sensitized background in the fly pupal eye where ectopic overexpression of CycE (using GMR-Gal4/UAS) during the final cell cycle leads to 1-2 extra rounds of division in the eye. The extra rounds of division in this genetic background lead to visibly larger eyes that can be further enhanced when cell cycle genes are de-repressed (Fig.4.1). I tested 23 chromatin remodeling and chromatin-associated

genes via UAS-RNAi in this screen and confirmed only three hits with multiple RNAis or alleles, Mi-2, Brahma and Osa. Of these three hits, Mi-2 RNAi manifested the most dramatic phenotype. Further characterizations showed that inhibition of Mi-2 alone is sufficient to delay cell cycle exit in the fly wing and eye. In addition, Chip-seq data from Modencode shows an enrichment of Mi-2 binding at the cell cycle genes *stg*, *cycE* in *Drosophila* S2 cells, indicating a promising role of Mi-2 in regulating cell cycle gene enhancers (Fig. 4.2). To further investigate a potential role for Mi-2 in promoting cell cycle exit at the pupal stages, we will first determine the genomic localization of Mi-2 in pupal wings. We will perform ChIP on Mi-2 in pupal wings at stages of proliferation, early, flexible G0 and late, robust G0 stages. To facilitate performing ChIP on pupal wings, we will use the *Apterous* (*Ap*)-Gal4 driver combined with Gal80TS to drive UAS-dependent expression of a wild-type Flag-tagged Mi-2 (Mi-2WT) and a dominant negative Mi-2 which lacks ATPase activity (Mi-2DN) kindly provided by Dr. Alexander Brehm [16]. To resolve whether Mi-2 plays an important role in chromatin remodeling at cell cycle exit, we will perform FAIRE-seq on dissected pupal wings expressing Mi-2WT or Mi-2DN during flexible and robust G0. In parallel we will also perform RNAseq on the same samples, so that we can correlate any changes in accessibility with changes in gene expression. We envision that the ChIP assays with Mi-2WT will reveal the normal distribution of Mi-2 during cell cycle exit, while Mi-2DN should reveal any aberrant Mi-2 binding that occurs in the absence of nucleosome remodeling under conditions. We expect that the FAIRE experiments will reveal changes in regulatory element accessibility during cell cycle exit that require Mi-2 function.

4.3 Identifying the transcription factors recognizing cell cycle gene enhancers

For a nucleosome remodeling complex to exert its remodeling function, it needs to be recruited to specific chromatin locations by transcription factors. To identify the transcription factors that recognize enhancers of cell cycle genes *cycE* and *stg* and recruit Mi-2, we computationally predicted potential transcription factors via sequence analysis using the Jaspar database and FlyFactor Survey followed by Evo-Printer. We found conserved potential ecdysone receptor (EcR) binding sites in both *cycE* and *stg* regulatory regions (Fig. 4.2). Importantly, the predicted binding sites were further verified through EcR ChIP-seq data in pupa from Modencode. EcR was recently shown to recruit the chromatin remodeler Mi-2 to mediate target gene repression through nucleosome remodeling [17]. Thus, it is likely that EcR is the transcription factor that developmental program utilizes to regulate complex cell cycle genes such as *stg*, potentially through Mi-2 mediated nucleosome remodeling. We will confirm the predicted binding sites using targeted mutagenesis and transcriptional assays of reporters in S2 cells. This will then be followed by genetic manipulations of EcR and mutagenized reporter assays in flies. With *cycE* and *stg* transcriptional reporters with mutated binding sites we will directly test by ChIP to see whether the loss of binding sites prevents Mi-2 recruitment.

4.4 Relationship between cell cycle and terminal differentiation

The state of G0 is thought to be essential for terminal differentiation [18]. However, there has been some discrepancies on whether terminal differentiation is dependent on G0. In some cases, such as mouse muscle cells and *C. elegans* anchor and muscle cells

[5, 19, 20], disrupting G0 prevents terminal differentiation. In other reports such as fly photoreceptor neurons and wings, mouse horizontal interneurons, terminal differentiation proceeds when G0 entry is inhibited [6, 21–23]. To elaborate the detailed effects of G0 disruption on terminal differentiation, I genetically delayed or disrupted G0 and examined the alterations of differentiation program at both chromatin level and transcription level genomewidely. My work shows that disrupting cell cycle exit delays the temporal activation and chromatin dynamics of a subset of ecdysone-induced transcription factors during wing development, leading to delays in the activation of a portion of the wing terminal differentiation genes. My work reveals that wing differentiation program is only partially dependent on G0 and this is mediated through specific transcriptional factors that are sensitive to G0. Notably, a temporary delay of cell cycle exit through E2F overexpression is sufficient to delay differentiation program, which could be due to either ectopic cell cycling status from 24h to 36h or continuous E2F transcriptional activities, both of which should cease by 24h APF during normal development. This observation suggests that there might be a potential “sensor” that monitors cell cycle related activities and signals to the downstream differentiation program. Mechanistically identifying this “sensor” will be pivotal to further dissect the relationship between proliferation and terminal differentiation.

4.5 Identifying the development sensor that monitors cell cycle activities

As discussed earlier, the differentiation program is able to “sense” ectopic cell cycle activities and correspond accordingly by delaying differentiation gene activation. We reasoned that this “sensor” should be part of the differentiation core pathway and is one

of the early genes that respond to G0 disruption. Because the ecdysone pathway plays a central role in governing differentiation program, we examined the expression of genes involved in the ecdysone pathway after activating E2F or E2F/CycD/Cdk4 by 12hr (Fig. 4.3). Only a handful of genes are disrupted by either E2F or E2F/CycD/Cdk4 and the only common target is woc. woc is a zinc finger protein and is responsible for ecdysone biogenesis [24, 25]. Homozygous woc mutant larva exhibit a deficiency in ecdysone production and fails to pupariate [25]. woc is highly expressed at L3 coinciding with a high pulse of ecdysone, and interestingly, become silenced at 24h when cell cycle exit occurs. These observations imply a potential role for woc in linking cell cycle and temporal cascade of ecdysone target gene expression. Notably, woc remains highly expressed in the 44h postmitotic wing with E2F overexpression, suggesting that woc might be directly responding to E2F transcriptional activity. To investigate if woc is the molecular “sensor” that monitors ectopic cell cycle activity, we will genetically manipulate the level of woc through knockdown by RNAi and overexpression using publicly available stocks.

4.6 Dispensable role of heterochromatin mediated gene silencing in G0

Heterochromatin associated modifications H3K27me3 and H3K9me3 have been shown to be enriched at silenced cell cycle genes in differentiated tissues [26–28]. A common model posits that upon cell cycle exit, repressive modifications H3K27me3 or H3K9me3 recruits repressive heterochromatin binding proteins such as the Polycomb complexes PRC1 and 2 or Heterochromatin Protein 1 (HP1) to silence cell cycle gene expression and promote cell cycle exit. I rigorously tested this model through compromising H3K27me3 methyltransferase E(z), PRC1 core component Pc and HP1

and found that heterochromatin mediated gene silencing is dispensable for the establishment of G0 [22].

4.7 Heterochromatin clustering as a consequence of cell cycle exit

Chromatin organization can change during terminal differentiation. Terminal differentiation is associated with a cessation of proliferation, which could also impact chromatin organization. In my thesis work I directly dissect the relationship between heterochromatin organization, cell cycle exit and differentiation using genetic tools that effectively uncouple cell cycle exit and differentiation. My work reveals that heterochromatin clustering during terminal differentiation is a consequence of cell cycle exit, rather than differentiation. Importantly, heterochromatin clustering can be substantially disrupted by progression through one round of S or M-phase, suggesting that long-range interactions have to be reestablished in interphase during every cycle. In addition, simply disrupting heterochromatin clustering without directly compromising heterochromatin associated modifications has minimal effect on gene repression and differentiation, eliciting future investigations on the biological functions of heterochromatin clustering in differentiation.

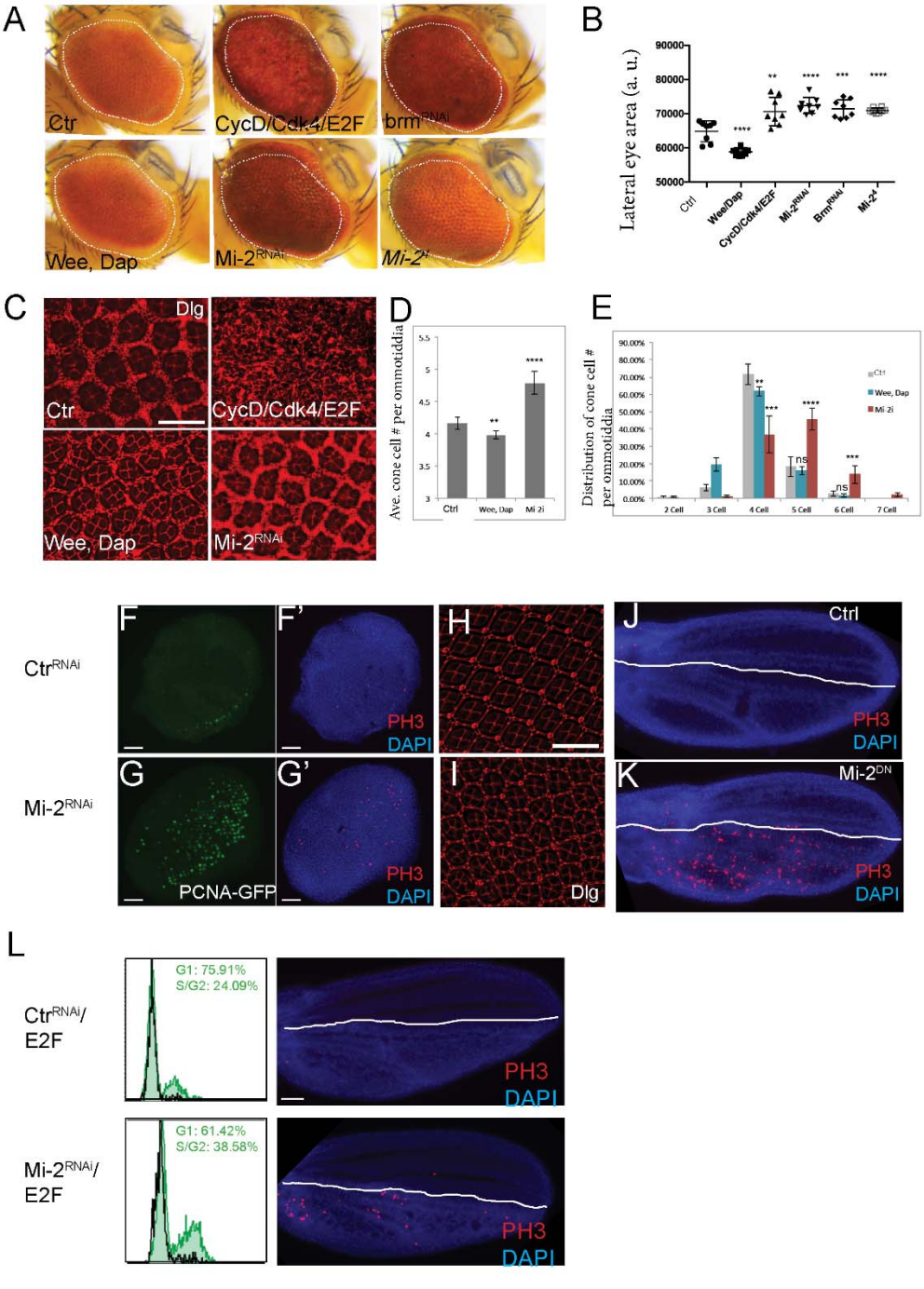
A
Ctr
CycD/Cdk4/E2F
brm^RNAi
Wee, Dap
Mi-2^RNAi
Mi-2^1
B
Lateral eye area (a. u.)
90000
80000
70000
60000
50000
Ctrl
Wee/Dap
CycD/Cdk4/E2F
Mi-2^RNAi
Brm^RNAi
Mi-2^1
C
Dlg
Ctr
CycD/Cdk4/E2F
Wee, Dap
Mi-2^RNAi
D
Ave. cone cell # per ommotiddia
5.5
5
4.5
4
3.5
3
Ctrl
Wee, Dap
Mi 2i
E
Distribution of cone cell # per ommotiddia
90.00%
80.00%
70.00%
60.00%
50.00%
40.00%
30.00%
20.00%
10.00%
0.00%
Ctrl
Wee, Dap
Mi 2i
2 Cell
3 Cell
4 Cell
5 Cell
6 Cell
7 Cell
Ctr^RNAi
Mi-2^RNAi
F
F'
H
J
Ctrl
PH3
DAPI
G
G'
I
K
Mi-2^DN
PCNA-GFP
Dlg
L
Ctr^RNAi/
E2F
G1: 75.91%
S/G2: 24.09%
Mi-2^RNAi/
E2F
G1: 61.42%
S/G2: 38.58%

Figure 4.1 Mi-2 promotes cell cycle exit during development. (A) GMR-Gal4, UAS-CycE, GMR-P35/UAS was used to drive expression of the indicated transgenes in the eye during the final cell cycle. (B) Lateral surface area of adult fly eyes was measured and compared. (C) 44-45h APF pupal eyes were stained for Discs large (Dlg) to visualize cell-cell boundary. The average number of cone cells per ommotidial structure was quantified (D), as well as the distribution of different cone cell number per ommotidial structure (E). Compromising Mi-2 in the CycE hyperactive background leads to extra cone cells. Mi-2^{RNAi} and control ^{RNAi} were expressed in the eye under GMR-Gal4, PCNA-GFP/UAS. 23h APF pupa were dissected and stained for GFP and PH3 (F, G), and 44-45h APF for Dlg (J, K). UAS-Mi-2^{DN} and control were expressed in the posterior wing under *Ents* (H, I) and 28h wings were dissected for PH3 staining. Compromising Mi-2 function alone is able to disrupt G0. Mi-2^{RNAi} and control ^{RNAi} were further expressed in combination with E2F under *Ents* and *Apterous*, 42h APF pupal wings were dissected and subjected to PH3 staining and FACS analysis (L). The increase in S/G2 content and extra PH3 suggests that compromising Mi-2 induce a proportion of cells stay in cycling during the robust stage. Bar: (A) 100um; (C, J) 25 um; (F, L) 50 um.

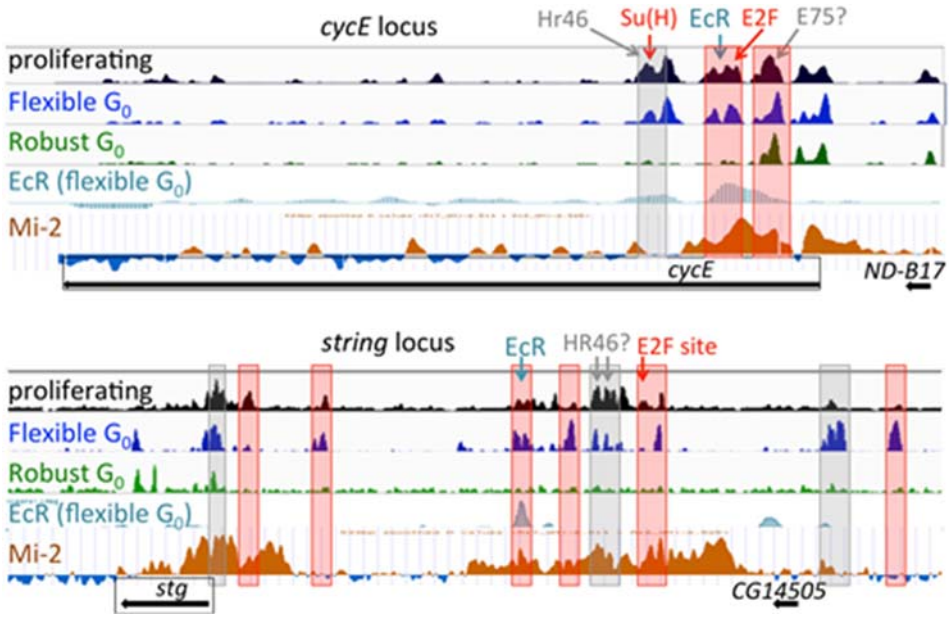

Figure 4.2 Regulatory element accessibility changes at *cycE* and *stg* during cell cycle exit. FAIRE-seq signal in *cycE*, *stg* genome regions during proliferation, Flexible G0 and Robust G0. Grey shaded boxes indicate known enhancers. Red boxes indicate new putative enhancers. Red arrows indicate validated binding sites for HR46, SuH and E2F transcription factors. Question marks indicate potential binding sites identified by MEME. Gold peaks indicate Mi-2 binding and turquoise peaks indicate EcR binding (from ChIP-seq data by Modencode).

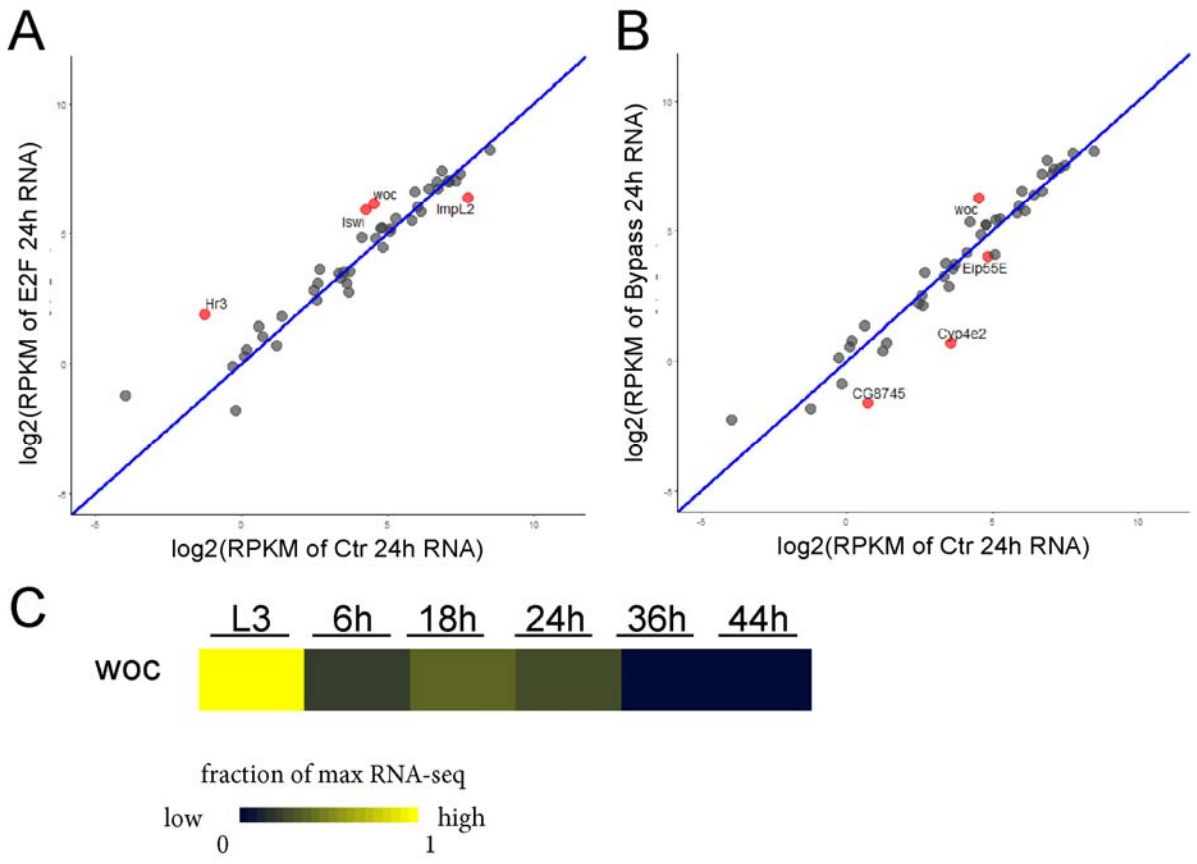

Figure 4.3 *woc* is activated upon G0 disruption. Comparison of gene expression from ecdysone pathway between E2F (A) or E2F/CycD/Cdk4 (Bypass) (B) vs Ctr at 24h wings, plotted as log2(RPKM). woc is induced in both E2F and E2F/CycD/Cdk4 overexpression wings. (C) woc is silenced after cell cycle exit during normal development.

4.8 Reference

1. Spencer SL, Cappell SD, Tsai F-C, Overton KW, Wang CL, Meyer T. The proliferation-quiescence decision is controlled by a bifurcation in CDK2 activity at mitotic exit. Cell. 2013;155:369–83.

2. Coller HA, Sang L, Roberts JM. A new description of cellular quiescence. PLoS Biol. 2006;4:e83.

3. Susaki E, Nakayama K, Nakayama KI. Cyclin D2 translocates p27 out of the nucleus and promotes its degradation at the G0-G1 transition. Mol Cell Biol. 2007;27:4626–40.

4. Coats S, Flanagan WM, Nourse J, Roberts JM. Requirement of p27Kip1 for restriction point control of the fibroblast cell cycle. Science. 1996;272:877–80.

5. The I, Ruijtenberg S, Bouchet BP, Cristobal A, Prinsen MBW, van Mourik T, et al. Rb and FZR1/Cdh1 determine CDK4/6-cyclin D requirement in C. elegans and human cancer cells. Nat Commun. 2015;6:5906.

6. Buttitta LA, Katzaroff AJ, Edgar BA. A robust cell cycle control mechanism limits E2F-induced proliferation of terminally differentiated cells in vivo. J Cell Biol. 2010;189:981–96.

7. Sun D, Buttitta L. Protein phosphatase 2A promotes the transition to G0 during terminal differentiation in Drosophila. Development. 2015;142:3033–45.

8. Blais A, Dynlacht BD. E2F-associated chromatin modifiers and cell cycle control. Curr Opin Cell Biol. 2007;19:658–62.

9. Sadasivam S, DeCaprio JA. The DREAM complex: master coordinator of cell cycle-dependent gene expression. Nat Rev Cancer. 2013;13:585–95.

10. Nagl NG, Wang X, Patsialou A, Van Scoy M, Moran E. Distinct mammalian SWI/SNF chromatin remodeling complexes with opposing roles in cell-cycle control. EMBO J. 2007;26:752–63.

11. Hendricks KB, Shanahan F, Lees E. Role for BRG1 in cell cycle control and tumor suppression. Mol Cell Biol. 2004;24:362–76.

12. Liu K, Luo Y, Lin F-T, Lin W-C. TopBP1 recruits Brg1/Brm to repress E2F1-induced apoptosis, a novel pRb-independent and E2F1-specific control for cell survival. Genes Dev. 2004;18:673–86.

13. Ruijtenberg S, van den Heuvel S. G1/S Inhibitors and the SWI/SNF Complex Control Cell-Cycle Exit during Muscle Differentiation. Cell. 2015;162:300–13.

14. Albini S, Coutinho Toto P, Dall'Agnese A, Malecova B, Cenciarelli C, Felsani A, et al. Brahma is required for cell cycle arrest and late muscle gene expression during skeletal myogenesis. EMBO Rep. 2015;16:1037–50.

15. Ruijtenberg S, van den Heuvel S. G1/S Inhibitors and the SWI/SNF Complex Control Cell-Cycle Exit during Muscle Differentiation. Cell. 2015;162:300–13.

16. Murawska M, Hassler M, Renkawitz-Pohl R, Ladurner A, Brehm A. Stress-induced PARP activation mediates recruitment of Drosophila Mi-2 to promote heat shock gene expression. PLoS Genet. 2011;7:e1002206.

17. Kreher J, Kovač K, Bouazoune K, Mačinković I, Ernst AL, Engelen E, et al. EcR recruits dMi-2 and increases efficiency of dMi-2-mediated remodelling to constrain transcription of hormone-regulated genes. Nat Commun. 2017;8:14806.

18. Ruijtenberg S, van den Heuvel S. Coordinating cell proliferation and differentiation: Antagonism between cell cycle regulators and cell type-specific gene expression. Cell Cycle. 2016;15:196–212.

19. Novitch BG, Spicer DB, Kim PS, Cheung WL, Lassar AB. pRb is required for MEF2-dependent gene expression as well as cell-cycle arrest during skeletal muscle differentiation. Curr Biol. 1999;9:449–59.

20. Matus DQ, Lohmer LL, Kelley LC, Schindler AJ, Kohrman AQ, Barkoulas M, et al. Invasive Cell Fate Requires G1 Cell-Cycle Arrest and Histone Deacetylase-Mediated Changes in Gene Expression. Dev Cell. 2015;35:162–74.

21. Buttitta LA, Katzaroff AJ, Perez CL, de la Cruz A, Edgar BA. A double-assurance mechanism controls cell cycle exit upon terminal differentiation in Drosophila. Dev Cell. 2007;12:631–43.

22. Ma Y, Buttitta L. Chromatin organization changes during the establishment and maintenance of the postmitotic state. Epigenetics Chromatin. 2017;10:53.

23. Ajioka I, Martins RAP, Bayazitov IT, Donovan S, Johnson DA, Frase S, et al. Differentiated horizontal interneurons clonally expand to form metastatic retinoblastoma in mice. Cell. 2007;131:378–90.

24. Raffa GD, Cenci G, Siriaco G, Goldberg ML, Gatti M. The putative Drosophila transcription factor woc is required to prevent telomeric fusions. Mol Cell. 2005;20:821–31.

25. Wismar J, Habtemichael N, Warren JT, Dai JD, Gilbert LI, Gateff E. The mutation without children(rgl) causes ecdysteroid deficiency in third-instar larvae of Drosophila melanogaster. Dev Biol. 2000;226:1–17.

26. Blais A, van Oevelen CJC, Margueron R, Acosta-Alvear D, Dynlacht BD. Retinoblastoma tumor suppressor protein-dependent methylation of histone H3 lysine 27 is associated with irreversible cell cycle exit. J Cell Biol. 2007;179:1399–412.

27. Sdek P, Zhao P, Wang Y, Huang C-J, Ko CY, Butler PC, et al. Rb and p130 control cell cycle gene silencing to maintain the postmitotic phenotype in cardiac myocytes. J Cell Biol. 2011;194:407–23.

28. Ait-Si-Ali S, Guasconi V, Fritsch L, Yahi H, Sekhri R, Naguibneva I, et al. A Suv39h-dependent mechanism for silencing S-phase genes in differentiating but not in cycling cells. EMBO J. 2004;23:605–15.